พฤติกรรมการดัดของจุดต่อไม้ที่มีการจัดเรียงตัวของสลักเกลียวแบบต่าง ๆ

นายอลิ อวาลูดิน

วิทยานิพนธ์นี้เป็นส่วนหนึ่งของการศึกษาตามหลักสูตรปริญญาวิศวกรรมศาสตรมหาบัณฑิต
สาขาวิศวกรรมโยธา ภาควิชาวิศวกรรมโยธา
คณะวิศวกรรมศาสตร์ จุฬาลงกรณ์มหาวิทยาลัย
ปีการศึกษา 2547
ISBN 974-17-6449-9

FLEXURAL BEHAVIOR OF TIMBER CONNECTION WITH VARIOUS MULTIPLE-BOLT CONFIGURATIONS

Mr. Ali Awaludin

A Thesis Submitted in Partial Fulfillment of the Requirements
for the Degree of Master of Engineering in Civil Engineering
Department of Civil Engineering
Faculty of Engineering
Chulalongkorn University
Academic Year 2004
ISBN 974-17-6449-9

Thesis Title	FLEXURAL BEHAVIOR OF TIMBER CONNECTION WITH VARIOUS MULTIPLE-BOLT CONFIGURATIONS
By	ALI AWALUDIN
Field of Study	CIVIL ENGINEERING
Thesis Advisor	WATANACHAI SMITTAKORN, Ph.D.

Accepted by the Faculty of Engineering, Chulalongkorn University in Partial Fulfillment of Requirements for the Master's Degree

…….. Dean of the Faculty of Engineering
(Professor Direk Lavansiri, Ph.D.)

THESIS COMMITTEE

……. Chairman
(Professor Ekasit Limsuwan, Ph.D.)

…….. Thesis Advisor
(Watanachai Smittakorn, Ph.D.)

…….. Member
(Professor Takuro Hirai, D.Agr.)

…….. Member
(Anat Ruangrassamee, Ph.D.)

อลิ อวาลูดิน : พฤติกรรมการดัดของจุดต่อไม้ที่มีการจัดเรียงตัวของสลักเกลียวแบบต่าง ๆ. (FLEXURAL BEHAVIOR OF TIMBER CONNECTION WITH VARIOUS MULTIPLE-BOLT CONFIGURATIONS) อาจารย์ที่ปรึกษา : ดร.วัฒนชัย สมิทธากร, 106หน้า. ISBN 974-17-6449-9.

งานวิจัยนี้มีวัตถุประสงค์เพื่อศึกษาพฤติกรรมของจุดต่อไม้ภายใต้โมเมนต์ดัด โดยจะพิจารณาถึงผลของการจัดเรียงตัวของสลักเกลียวที่มีต่อกำลังต้านทานโมเมนต์ดัด เส้นโค้งโมเมนต์-การหมุนตัว และลักษณะการวิบัติของรอยต่อ ทั้งนี้จะมีการทดสอบพฤติกรรมของจุดต่อทั้งประเภทเหล็กกับไม้ และไม้กับไม้ที่มีการจัดเรียงสลักเกลียว 4 แบบ ลักษณะการวิบัติที่ต้องการศึกษาคือการวิบัติที่แผ่นหลัก ชิ้นตัวอย่างที่เลือกใช้ประกอบด้วยไม้เต็ง (shorea obtusa) หนา 1.5 นิ้ว และแผ่นเหล็กหนา 4 มิลลิเมตร การทำนายกำลังต้านทานโมเมนต์ดัดของจุดต่อจะอาศัยสมมติฐานของแผ่นแข็ง

ผลการทดสอบจุดต่อที่ใช้สลักเกลียวเดี่ยว พบว่าทิศทางของแรงกระทำมีผลอย่างมากต่อกำลังต้านทานและโมดูลัสเคลื่อนตัวยืดหยุ่นของจุดต่อ โดยค่าทั้งสองจะลดลงเมื่อมุมระหว่างแรงที่กระทำกับแนวเสี้ยนเพิ่มขึ้น ในที่นี้จะประยุกต์ใช้สูตรของแฮนคินสันสำหรับคำนวนค่ากำลังต้านทาน และโมดูลัสเคลื่อนตัวยืดหยุ่นเมื่อแรงกระทำในมุมต่างๆ กัน ในส่วนของการทดสอบจุดต่อที่ใช้สลักเกลียวกลุ่ม จุดต่อประเภทเหล็กกับไม้จะมีกำลังต้านทานโมเมนต์ดัดน้อยกว่าค่าจากการทำนาย โดยค่าสัดส่วนของกำลังจากการทดสอบต่อค่ากำลังจากการทำนายมีค่ามากที่สุดเท่ากับ 0.77 ในขณะที่ค่าสัดส่วนดังกล่าวสำหรับจุดต่อประเภทไม้กับไม้มีค่าระหว่าง 0.80 ถึง 1.23 ทั้งนี้เนื่องจากแผ่นประกับที่เป็นไม้จะยอมให้มีการถ่ายแรงระหว่างสลักเกลียวแต่ละตัวได้มากกว่า ส่งผลให้จุดต่อประเภทไม้กับไม้มีกำลังต้านทานโมเมนต์ดัดได้มากกว่าจุดต่อประเภทเหล็กกับไม้

การจัดเรียงตัวของสลักเกลียวจะมีผลต่อพฤติกรรมของจุดต่อทั้งประเภทเหล็กกับไม้ และไม้กับไม้ในทำนองเดียวกัน จุดต่อที่มีระยะระหว่างสลักเกลียวในแนวเสี้ยนที่มาก จะมีกำลังต้านทานโมเมนต์ดัดได้มาก มีความเหนียวสูง มีสติฟเนสสูง และมีการหมุนตัวได้มาก ทั้งนี้จุดต่อประเภทไม้กับไม้จะยอมให้มีการหมุนตัวได้มากกว่าจุดต่อประเภทเหล็กกับไม้ เพราะว่าจุดต่อไม้กับไม้มีการยึดรั้งที่น้อยกว่า นอกจากนี้ เส้นโค้งโมเมนต์-การหมุนจากการทำนายจะให้ค่าใกล้เคียงกับผลการทดสอบเฉพาะในช่วงอีลาสติกเท่านั้น การทำนายในช่วงพลาสติกพบว่ามีความคลาดเคลื่อนมาก เนื่องจากการใช้สมมติฐานของแผ่นแข็ง และพฤติกรรมที่ไม่แน่นอนของไม้ เช่น การแตกปริ เป็นต้น

ภาควิชา.....วิศวกรรมโยธา..... ลายมือชื่อนิสิต.....
สาขาวิชา.....วิศวกรรมโครงสร้าง..... ลายมือชื่ออาจารย์ที่ปรึกษา.....
ปีการศึกษา 2547

4670645021 : MAJOR CIVIL ENGINEERING
KEY WORD : BOLTS CONFIGURATION / MOMENT RESISTANCE / MOMENT-ROTATION CURVE

ALI AWALUDIN: FLEXURAL BEHAVIOR OF TIMBER CONNECTION WITH VARIOUS MULTIPLE-BOLT CONFIGURATIONS. THESIS ADVISOR: WATANACHAI SMITTAKORN, Ph.D. [106] pp. ISBN 974-17-6449-9.

The goal of this research is to investigate the behavior of timber connection subjected to bending moment. The effects of multiple-bolt configuration on maximum moment resistance, moment-rotation curve, and failure mode of connection are the focus of this study. Four types of bolt configurations are examined for both steel to wood and wood to wood connections. Failure in the main member is expected to be the failure mode of the connections. Wood specimens of shorea obtusa of 1.5-inch thickness and steel plate of 4-mm thickness are used. The maximum moment resistance of connections is predicted by applying the rigid plate assumption.

Results from single bolt connection tests have shown that loading angle drastically affects the lateral load resistance and elastic slip modulus of bolted connections. Lateral load resistance and elastic slip modulus decrease as the loading angle increases. Hankinson formula can be applied to find the lateral load resistance and elastic slip modulus in inclined angles to wood grain. In multiple-bolt connections, all steel to wood connections yield less moment capacity than theoretical prediction; the highest ratio between experimental and theoretical maximum moment resistance is 0.77. In wood to wood connections, the ratio between experimental and theoretical maximum moment resistance varies from 0.80 to 1.23. Wooden plates as side members in wood to wood connection allow more load redistribution among bolts. Therefore, wood to wood connection shows more capacity than steel to wood connection significantly.

Bolt configuration affects the steel to wood and wood to wood connections in similar manner. Bolt configuration which has long distance along the grain between bolts yields high moment capacity, high ductility, high stiffness, and high joint rotation. Wood to wood connection has higher joint rotation than steel to wood connection because wood to wood connection behaves with lower degree of restraints. Predicted moment-rotation curves have good agreement with experimental results only in elastic range. In plastic range, predicted moment-rotation curves show some discrepancies because of the rigid plate assumption and uncertain behavior such as wood splitting.

Department of Civil Engineering
Field of Study Civil Engineering
Academic Year 2004

Student's Signature ----------
Advisor's signature ----------

ACKNWOLEDGEMENTS

First of all I would like to thank Dr Watanachai Smittakorn, my advisor, for all the help, support, and advice that he has provided through this journey known as graduate school. I would like to express my gratitude to my committee members Prof. Dr. Ekasit Limsuwan, Prof. Dr. Takuro Hirai, and Dr. Anat Ruangrassamee for their support and counsel in this research. I would like also to express my gratitude to Dr. A.J.M. Leijten of TU-DELFT for all valuable references that he has shared. I would like to express my sincere gratitude to AUN/SEED-Net for granting me a two-year scholarship and providing fund to this research. I believe that without this financial support, my experience of studying in graduate school of Chulalongkorn University will just only be a dream.

I would like to thank the technician staff of Material Testing Laboratory of Civil Engineering, Chulalongkorn University, for their help in preparing the test. I especially would like to thank Mr. Surichet Luang Aram and Mr. Pirote Anantasethikul whose technical support made this research possible. I would like to express my appreciation to Somboon Shaingchin, Chanwut Charuchaimontri, and Warit Prathaksithorn for helping me with laborious task of specimen testing.

Most of all I would like to thank my wife Visi Asriningtyas and my daughter Euis Alina Kusumaningtyas for being there for me through it all.

CONTENTS

Page

CONTENTS (Cont.)

LIST OF TABLES

LIST OF FIGURES

LIST OF FIGURES (Cont.)

LIST OF SYMBOLS

C_g	Center of fastener group
D	Diameter of bolt
F	Lateral load resistance of single bolt connection
F_e	Dowel bearing strength of wood
F_{es}	Dowel bearing strength of side member
F_{em}	Dowel bearing strength of main member
F_{yb}	Yield stress of bolt
G	Specific gravity
k_e, k_{ser}	Elastic slip modulus
k_p, k_u	Plastic slip modulus
M	Moment resistance
M_{yb}	Fastener yield moment
R_e	Ratio of F_{em} to F_{es}
ds, s	Fastener slip
n	Number of bolt
m	Power of sine and cosine terms in Hankinson's formula
r	Distance of fastener to center of group
t_1	Thickness of side member (wood lumber)
t_2, l	Thickness of main member (wood lumber)
t_s	Thickness of steel plate

LIST OF SYMBOLS (Cont.)

w	Moisture content
α	Loading orientation to wood grain
ϕ , θ	Joint rotation

CHAPTER 1

INTRODUCTION

1.1 Background

Joints are often said to be the weakest part of most engineering wood structures. According to the study by Smith *at al* (1998), the assessment of timber building damage after extreme wind and earthquake often pointed out to inadequate connection as the primary cause. Jointing method which has better performance and higher strength has become an interesting issue to study. Jointing with adhesive materials and with mechanical fasteners are examples of jointing methods. Connection with mechanical fasteners, widely called mechanical connection, is usually more ductile than that of connection with adhesive materials. However, mechanical connections have some disadvantages such as the minimum required-distance among fasteners, the cross-section reduction of wood member, and non-uniform stress distribution on wood around fastener. As a result, the strength of connection is reduced.

Bolts are commonly used as fasteners in timber connection. They have the advantage of being easily installed and inspected. They are also economical, and are capable of transmitting high load. The use of a large number of small-diameter bolts results in a more ductile response than a small number of a large diameter bolts (Tucker *et al*. 2000). Bolts can be used in single-shear (two-member) connection or double-shear (three-member) connection. The connection strength of bolted connection is determined by some parameters such as bending yield strength of bolt, the bearing or shear strength of wood member, and the geometry of connection itself.

Moment-resisting connections are mostly used to join members of arches and rigid frames. The bending moment is counter balanced by the product of lateral load in each fasteners and the distance to the center of fastener group. Most fasteners in the group resist lateral load in inclined angles to wood grain. These inclined angles may vary from one fastener to another. Therefore, the moment capacity of connection is greatly affected by the fastener configuration.

A guidance to study the moment resistance of wood to wood connection can be found in EUROCODE 5 (Frangi *et al*. 2003; Blass *et al*. 1995). Some simplifications were applied in this code. However a question may arise whether this simplification is in conservative side for general multiple-fastener configuration. The answer to this question can be explained by studying the flexural parameters of connection such as moment capacity, stiffness, and rotation ductility.

The means to compute the moment capacity of steel to wood connection is not available both in EUROCODE 5 (1995) and in NDS for Timber Construction of U.S (1997). The use of steel plate in timber connection is expected to improve the performance of timber connection. Based on Trayer's work (1932), the strength of steel to wood connection, subjected to tension parallel to grain, is 20% higher than that of wood to wood connection. But this improvement whether can be applied or not to general case of fastener configuration considering elastic and plastic range is remained to discover. If steel to wood connection is subjected to bending moment, will its moment resistance be 20% higher than that of wood to wood connection? The answer to this question is still remained to discover.

To obtain accurate prediction on moment capacity of bolted connection, deep understanding on the behavior of connection is required. This necessity leads to more research on moment-resisting connection. This research will discover not only the

strength of connection itself, but also will deeply investigate the behavior of connection both in elastic range and in plastic range. Several types of multiple-bolt configurations of wood to wood and steel to wood connection will be examined.

1.2 Objectives

The overall goal of this research is to study the flexural behavior of moment resisting connection with some multiple-bolt configurations. The specific objectives are as follows:

1. To examine the relationship between the lateral load resistance of single bolt connection and the angle to wood grain.
2. To investigate the behavior of bolted-connection subjected to bending moment in wood to wood and steel to wood connections.
3. To find out the effect of configuration of multiple-bolt to moment resisting capacity.
4. To compare experimental results with theoretical predictions and/or some other available results.

1.3 Scope

Some constraints will be considered as to limit the scope of this research, so that investigation could be done deeply and some recommendations could be obtained. These constraints are as follows:

1. All connection specimens are double-shear connections (three-member connection).
2. Bending moment is the only applied load in connection.

3. Yield mode of connection under investigation is I_m (failure in main member), since this yield mode is quite often found in multiple-bolt connection.

4. Steel plate used in steel to wood connection is considered as thin plate. Therefore, its probable yield mode can be compared with the I_m yield mode given by NDS of U.S. (1997) or yield mode *h* of EUROCODE 5 (1995) of wood to wood connection.

CHAPTER 2

LITERATURE RIVIEW

2.1 Wood Properties

Wood is a natural material obtained from tree trunk. Tree species are divided into two groups: *hardwoods* and *softwoods*. The hardwoods have broad leaves and lose their leaves in fall or during winter. The softwoods are the coniferous species and have needlelike leaves which, except for a couple of species, remain on the tree throughout the year. The terms hardwood and softwood are slightly related to the actual hardness of the wood; hardwoods species are actually harder than softwoods.

Wood properties differ from species to species. The micro-structure of timber is formed by cellular elements, arranged differently according to species, with a general orientation parallel to the stem axis (Ceccotti 1993). Wood is considered as an orthotropic material for having independent properties in three orthogonal axes: longitudinal, radial, and tangential (Somayaji 1995). Mechanical properties vary greatly among these directions.

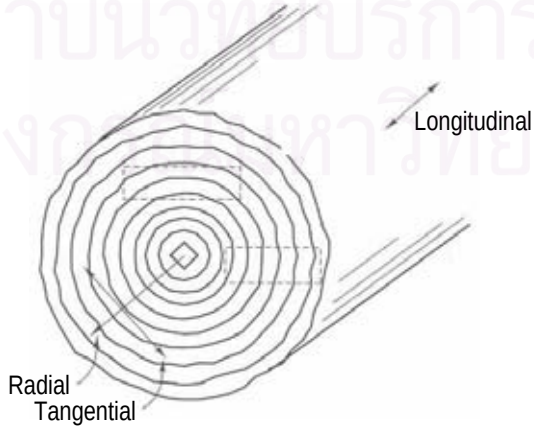

Figure 2.1 Three orthogonal axes of tree trunk (Somayaji 1995)

According to Faherty *et al* (1997), the moisture content in the green wood varies from as little as 30 percent to about 200 percent. Moisture in green wood is partly adsorbed in the cell walls and partly present in the cell cavities. As wood dries, the cell walls do not give off moisture until the cell cavities are empty. This condition in which the cell walls are fully saturated and the cell cavities are empty is known as the *fiber saturation point*. The fiber saturation point for most species is in the range of 25 to 30%. Below the fiber saturation point, there will be dramatic changes in most physical and mechanical properties. Above the fiber saturation point, most properties are approximately constant.

Any piece of wood will give off or take on moisture content from the surrounding atmosphere until the moisture in the wood has come to balance with that in the atmosphere. The moisture in the wood at the point of balance is called the *equilibrium moisture content* (EMC). The EMC is closely related to the relative humidity and the temperature of the surrounding atmosphere. Thus the EMC in an arid atmosphere will be different from that along the coast.

When timber dries below the fiber saturation point, it shrinks perpendicular to grain whereas the shrinkage along the grain is small and may be ignored. The shrinkage can be up to about 7% of the cross-sectional dimension (Faherty *et al*. 1997). Therefore, wood should be installed at a moisture content closes to the equilibrium moisture content likely to be achieved in service condition. Hindered shrinkage deformation in service can, for example in connection, cause tension perpendicular to the grain and hence potential failure (Hoffmeyer 1995).

The mechanical properties of wood depend significantly on moisture content. An increase in moisture content produces lower strength and modulus of elasticity. This effect is partially explained by the cell wall swelling, whereby less cell wall

material per unit area is available. More importantly, water, when penetrating the cell wall, weakens the Hydrogen bonds that responsible for holding the cell wall together (Hoffmeyer 1995).

Density is the most important physical properties of timber since it is the wood substance in the fibers that imparts strength and stiffness. Most mechanical properties of timber are positively correlated to density. Wood of high density is stronger than wood of low density. Woods of high density typically shrink and swell more, with changes in moisture content, than woods of low density.

As a natural material, wood is never perfect; grain variations, knots, cracks, and other growth characteristics are always present. While swirling figures may enhance the appearance and value of decorative members, they reduce the performance of structural members. Therefore, even though these characteristics are natural consequences of the growth and seasoning of wood, they are considered as defects.

2.2 Bolted Connection

Mechanical connections are constructed using two general fastener types: dowel and bearing. Dowel Type fasteners such as nails, screws and bolts, transmit either lateral or withdrawal loads. Lateral loads are transmitted by bearing stress developed between the fastener and the members of connection. Withdrawal loads are loads parallel to the fastener axis transmitted through friction or bearing to the connected materials. Bearing type connections transmit lateral load only. Bearing type fasteners, such as shear plate and split ring connection, transmit shear force through bearing of the connected materials. Each connection must be designed to transmit

forces adequately and provide satisfactory performance for the life of the structure without causing splitting, cracking, or excessive deformation of the wood members.

The first attempt to discover design values for bolted timber joints was conducted by Trayer (1932). Trayer's work focused on developing load-slip curve that can be used to find three important values: the proportional limit load, yield load, and ultimate load. Trayer's conclusion is derived as an empirical fit of experimental results. This is due to the complexity of the interaction of a bolt in orthotropic non-homogenous material (Gatesco 1998). Some of the major conclusions reached by Trayer are: (1) the l/D ratio is the governing parameter, where l is the length of bolt in main member and D is the bolt diameter, (2) connection with steel side plates achieves 20% higher capacity than connection with wood side members for parallel-to-grain loading, and (3) connection with steel side plates and connection with wood side members loaded perpendicular to grain have equal capacities.

Yield model for bolted timber connection was developed by Johansen (1949). The bearing capacity of connection is attained when either the compressive strength of wood beneath the bolt is exceeded or simultaneously the timber under the bolt becomes plastic and one or more plastic hinges formed in the bolt. The bearing capacity which has plastic hinge of fastener will show ductility failure (Tucker *et al*. 2000). McLain *et al* (1983) considered the end fixity due to heads, nuts, and washers of fastener in Johansen's work. Some yield modes of Johansen's work should be taken out when the end fixity is considered.

Soltis *et al* (1986) conducted experimental work on double-shear wood joint with larger bolt diameters (12.7 mm, 25.4 mm, and 38.1 mm). Result of this experiment supports the Trayer's conclusion that parameter l/D is still the governing parameter of connection strength. According to Gatesco (1998), the simplified-model

used by Johansen may be accurate enough for the practical determination of the bearing capacity. Besides the geometric characteristic of the joint, two mechanical parameters govern this model: the embedding strength of wood beneath the bolt, and the bending yield strength of bolt. Experiment done by Gatesco (1998) on strength and local deformability of wood beneath bolted connectors showed that the relationship between the applied load and the displacement shows a nearly elastic perfectly plastic behavior for the case of load parallel to grain and tri-linear path in the case of load perpendicular to grain.

Analysis of bolted wood-joint can also be done by using beam on elastic foundation theory (Foschi 1974; Smith 1983). In this analysis, bolt and wood member of bolted wood-joint referred as the beam and the elastic foundation respectively. Since not only the ultimate lateral load resistance can be obtained but also the whole response (load-slip curve) of the connection, this theory is quite versatile. To get a better analysis, an elastic-plastic foundation model of bolted wood-joint has been developed by Foschi (1974). The plastic part was a linear line with lower tangent than the elastic part. Dolan (1989), White (1995), Blass (1994), and Frenette (1997) make use the Foschi's model in finite element analysis of bolted wood-connection.

A stepwise linear approximation was introduced by Hirai (1983, 1985) to overcome the difficulty of using beam on elastic foundation theory when nonlinear response of bolted wood-joint with steel side-member was considered. Half of wood cross-section was divided into several layers (four, five, six, and eight layers). The relationship between the bearing stress and embedment, and the bending moment and curvature in each layer were approximated by stepwise linear lines. Result of this study showed that there was no remarkable differences were observed among the different number of layers. Moreover, the elastic plastic bending of bolt with the

assumption of perfect plasticity yield closer result with the experiment than that of elastic plastic bending of bolt with constant strain hardening.

Study on load distribution of each fastener and the yield mode in connection with multiple-fastener has been done by many researchers (Blass 1995; Wilkinson 1986; Zahn 1992). According to Blass (1995), even if the load is acting on the centroid of connection, the load distribution between fasteners is not uniform. Wilkinson (1986) stated that the ultimate load distribution in connection with multiple fasteners is complex. Any one of the bolts may be the major carrier. Also, any bolt hole may be misdrilled causing that bolt to transmit almost no loads. Therefore, the ultimate load of connection will not be the same as the sum of the single fastener loads.

The different initial gap of each fastener will lead to non-uniform load distribution among fasteners (Hirai *et al*. 1998). Fastener with small lead-hole clearance will fail first. It becomes in capable of retaining its original lateral resistance. Zahn (1992) derived a formula to obtain the maximum possible effective number of fastener in a serial row of multiple-fastener connection. Due to the low shear strength of wood, the failure mode of connection with multiple fasteners is often caused by wood splitting rather than that of single fastener connection (Taylor 2002). Therefore, all codes require minimum distance among fasteners for each type of fasteners to prevent wood splitting.

Study to improve the performance of timber connection was conducted by Leijten (1988). The idea of Leijten's work is to strengthen the embedding strength of wood, especially at shear plane. In his work, wood to wood connection (double-shear connection) was examined and thin steel plate 1.5 mm, 3 mm and glass fiber were used as reinforcement materials. These materials were glued into the wood surface at

two shear planes. The result showed that significant improvement on ductility was obtained from glass fiber reinforced-connection. While in steel plate reinforced-connection, ductility, stiffness, and capacity were also increased considerably. Blass *et al* (----) used punched metal plate fastener on shear plane as local reinforcement. The addition of this reinforcement has increased the connection capacity by preventing preliminary splitting of timber members and providing a high embedding strength.

2.3 Lateral Load Resistance of Wood to Wood Connection

Connection yield load is calculated based on the connection yield mode. The connection load formula both of National Design and Specification (NDS) for Timber Construction in the U.S. (ASCE, 1997) and EUROCODE 5 (1995) are derived from European Yield Mode (EYM) which is first developed by Johansen (1949). Johansen (1949) assumed that both fastener and wood member are ideally rigid-plastic materials. The Johansen's equation is used to predict the capacity of single bolt connection at limit state. Variables that govern the capacity of connection are dimension and bending yield strength of fastener, dowel bearing strength of wood and geometry of the connection.

Because wood is an orthotropic material, the strengths in different directions are not the same. For strength with angle α to wood, Hankinson formula in Equation (2.1) can be used as an approximation. Here $F_{//}$ and $F_{\perp}$ are the strengths in directions parallel to grain and perpendicular to grain respectively. The value of m in Hankinson formula equal to 2.0 is used by NDS for analyzing the lateral load resistance of single-fastener connection.

$$F_{\alpha} = \frac{F_{//} F_{\perp}}{F_{//} \sin^{m} \alpha + F_{\perp} \cos^{m} \alpha} \qquad \text{.....} \quad (2.1)$$

According to Soltis and Wilkinson (American Society of Civil Engineer, ASCE, 1997), the capacity of single bolt depends on the bearing strength of wood, the bending strength and the slenderness ratio of bolt. The slenderness ratio of bolt is the length of bolt in main member divided by the bolt diameter. For bolted-connection with low slenderness ratio, the bolt is relatively stiff and the full bearing strength of wood is developed. As the slenderness increases bolt stiffness is reduced and bending will occur before full bearing strength is achieved, reducing the capacity of connection.

Yield modes of wood to wood connection in NDS and EUROCODE 5 are shown in Figure 2.2. Both standards have the same yield modes but different on naming. Yield modes in Figure 2.2(a) and 2.2(b) are the results of wood fiber crushing in side members and main member, respectively. Yield mode in Figure 2.2(c) is the result of bolt yielding in one plastic hinge, and yield mode in Figure 2.2(d) is the result of bolt yielding in more than one plastic hinges. Connection strength or lateral load resistance of single bolt connection and the corresponding yield mode are presented in Table 2.1 and Table 2.2 given by NDS and EUROCODE 5, respectively.

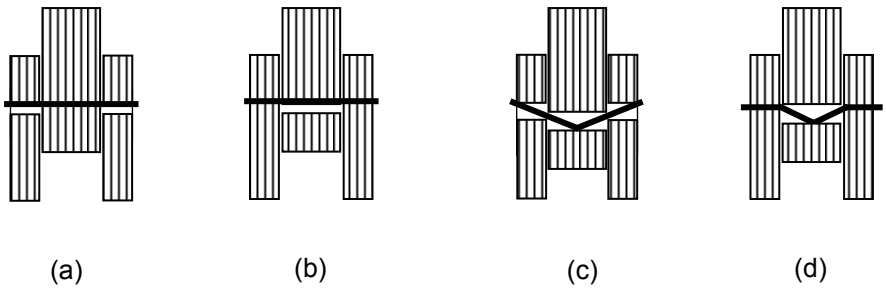

Figure 2.2 Failure modes of wood to wood connection

Table 2.1 Lateral load resistance of wood to wood bolted connection

(NDS for Timber Construction of U.S., ASCE 1997)

Figure	Yield mode	Lateral load resistance (F)
2.2(a)	I_s	$\frac{Dt_1F_{es}}{2K_\alpha}$
2.2(b)	I_m	$\frac{Dt_2F_{em}}{4K_\alpha}$
2.2(c)	III_s	$\frac{k_3Dt_1F_{em}}{1.6(2+R_e)K_\alpha}$ Where $k_3 = -1+\sqrt{\frac{2(1+R_e)}{R_e}+\frac{2F_{yb}(2+R_e)D^2}{3F_{em}t_1^2}}$
2.2(d)	IV	$\frac{D^2}{1.6K_\alpha}\sqrt{\frac{2F_{em}F_{yb}}{3(1+R_e)}}$

Where

t_1, t_2 = thickness of side member and main member, respectively

F_{es}, F_{em} = design value of embedding strength of side member and main member, respectively

R_e = ratio of F_{em} to F_{es}

F_{yb} = design value of fastener yield stress

D = diameter of bolt

α = angle of load to wood grain

$K_\alpha = 1 + \frac{\alpha}{360}$

Table 2.2 Lateral load resistance of wood to wood bolted connection

(EUROCODE 5, 1995)

Figure	Yield mode	Lateral load resistance (F)
2.2(a)	*g*	$2F_{es}t_1D$
2.2(b)	*h*	$F_{em}t_2D$
2.2(c)	*j*	$\frac{2F_{es}t_1D}{2+R_e}\left[\sqrt{2R_e(1+R_e)+\frac{5R_e(2+R_e)M_{yb}}{F_{es}Dt_1^{\,2}}}-R_e\right]$
2.2(d)	*k*	$2.3k_{cal}\sqrt{\frac{2R_e}{1+R_e}}\sqrt{2M_{yb}F_{es}D}$

Where

M_{yb} = the fastener yield moment

k_{cal} = the factor to account axial forces which develop in the fastener

(k_{cal} = 1.2 for bolted connection).

2.4 Lateral Load Resistance of Steel to Wood Connection

Formula of lateral load resistance of steel to wood connection can be found in EUROCODE 5 (1995). The steel plate is divided into two types: thin steel plate and thick steel plate. Steel plate is considered to be thin steel plate if its thickness (t_s) is less than a half of bolt diameter ($t_s \le D/2$), and if its thickness is larger than diameter of bolt ($t_s \ge D$), the steel plate is considered as thick steel plate. The yield

modes of steel to wood connection for thin steel plate and thick steel plate are shown in Figure 2.3. The lateral load resistance that corresponds to each yield mode is given in Table 2.3.

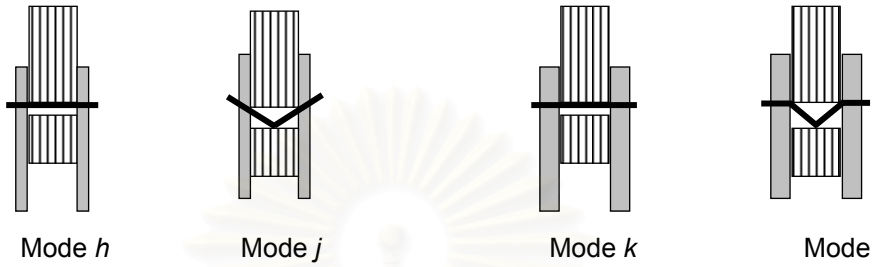

(a). Thin steel plate (b). Thick steel plate

Figure 2.3 Yield mode of steel to wood connection

Table 2.3 Lateral load resistance of steel to wood bolted connection (EUROCODE 5, 1995)

Yield mode	Lateral load resistance (F)
h	$F_{em}t_2D$
j	$2.3k_{cal}\sqrt{2M_{yb}F_{em}D}$
k	$F_{em}t_2D$
l	$4.6k_{cal}\sqrt{M_{yb}f_{em}D}$

2.5 Moment Resisting Connection

In moment-resisting wood joint, due to multiple-fastener geometry, lateral resistance of each fastener will have different angle to wood grain. Since the wood strength is also controlled by load angle to grain, each fastener in multiple-fastener joint will show different load-slip curve. Racher (1995a) proposed the equation to analyze the lateral resistance of fastener with the assumption that wood is an

orthotropic material. Center of rotation will coincide with center of fastener group throughout the loading.

Rigid plate assumption in steel to wood connection is conservative because in large load level, any increase in load will be accompanied by additional large deformation (Faherty *et al*. 1999). This ductile behavior would allow all fasteners in connection to attain high level of stress. In bent fastener, besides bending moment, there will be axial force along the fastener axis that can increase the connection strength (Hirai 1990; Hilson 1995). The true load distribution is highly indeterminate. However, satisfactory results can be obtained by the assumption that deformations of the steel plate are small (rigid-plate assumption).

Mechanical connections are always considered as semi-rigid connection and their strength are strongly dependent on the wood density (Ceccotti 1993). Slip occurs in wood connection, both initial slip (free) and elastic slip, according to the type of fasteners. Initial slip is due to the closing gaps between connection elements; elastic slip derives from the deformation of fastener and their further embedding into wood. Initial slip will not recover during unloading phase. At lower load levels the shear connection exhibits a linier-elastic load-slip relationship. By increasing the load, the shear connection begins to deform plastically and a non-linear structural behavior is occurred. After reaching the maximum load-carrying capacity, the shear connection, depending on its ductility, continues to deform plastically at decreasing load level (Frangi *et al*. 2003).

The load-slip curve usually shows a typical *elastic-plastic* relationship. For design purpose, k_{ser} and k_u are considered for the serviceability and for the ultimate limit state, respectively. In EUROCODE 5 (1995), slip modulus in serviceability state (k_{ser}) is the average value between slip modulus of parallel to grain ($k_{//}$) and slip

modulus of perpendicular to grain ($k_{\perp}$), whereas slip modulus in limit state (k_u) is taken as two third of slip modulus in serviceability state (k_{ser}). In bolted connection with multiple fasteners, the load distribution is not uniform even though the load is applied at center of fastener group. When the most stressed fastener deforms plastically, its stiffness decreases comparing to the stiffness of other fasteners in the joint. Since stiffer fasteners attract more loads (Blass *et al*. 1995), the rigid plate assumption allows for moment redistribution.

For a moment-resisting connection subjected to applied bending moment M as shown in Figure 2.4(a), fastener i will resist lateral load $F_{\alpha i}$ with angle α_i to wood grain. The applied bending moment will be counter balanced by couple moment of lateral force of fastener. Equilibrium state between the applied bending moment (external force) and couple moment created by lateral force of fastener (internal force) can be written as in Equation (2), where n is the number of fasteners.

$$M = \sum_{i=1}^{n} F_{\alpha i} r_i \quad \text{..... (2.2)}$$

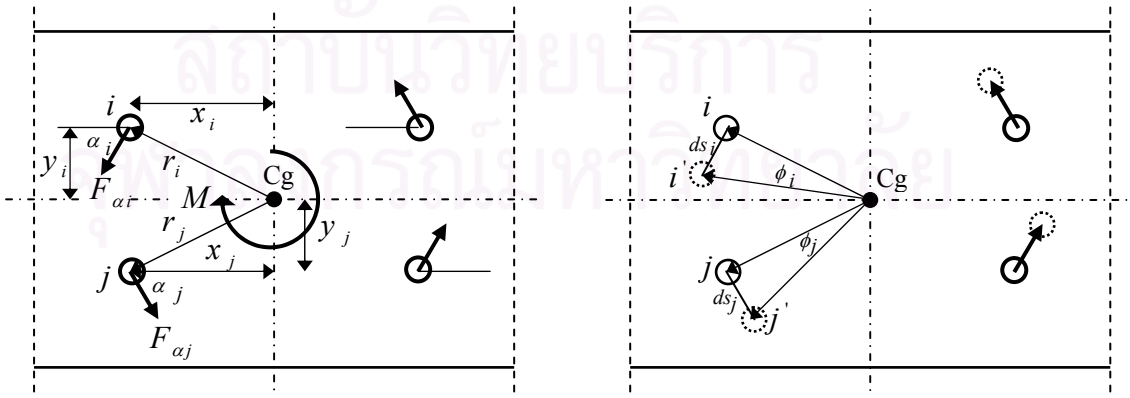

(a) (b)

Figure 2.4 Moment-resisting connection, (a) Acting forces, and (b) Joint rotation

During applying bending moment, each fastener will displace to a new configuration as shown in Figure 2.4(b) (dotted-line); Fastener i will displace by angle of rotation ϕ_i to its new configuration. Rigid plate assumption makes all fasteners displace to its new configuration by the same amount of angle of rotation ϕ ($\phi_i = \phi_j = \ldots = \phi$). For small angle of rotation, then fastener slip can be written as in Equation (2.3a) and Equation (2.3b). Constitutive equation to relate fastener slip and lateral load of fastener can be derived as in Equation (2.4).

$$ds_i = r_i\phi;\ ds_j = r_j\phi \quad \text{..... (2.3a)}$$

$$\frac{ds_i}{r_i} = \frac{ds_j}{r_j} \quad \text{..... (2.3b)}$$

$$F_{\alpha i} = k_{\alpha i} ds_i;\ F_{\alpha j} = k_{\alpha j} ds_j \quad \text{..... (2.4)}$$

Substitution Equation (2.3a) and (2.4) into (2.2) yields:

$$F_{\alpha i} = \frac{k_{\alpha i} r_i}{\sum_{l=1}^{n} k_{\alpha l} r_l^2} M \quad \text{..... (2.5)}$$

Where:

$F_{\alpha i}$ = lateral load of fastener i with angle α to wood grain

ds_i = fastener displacement corresponding to lateral load $F_{\alpha i}$

r_i = distance of fastener i to centre of bolt group = $\sqrt{x_i^2 + y_i^2}$

ϕ = rotation of joint

$k_{\alpha i}$ = slip modulus of fastener i with angle α to wood grain

The value of $k_{\alpha i}$ in Equation (2.5) can be approximated by Hankinson formula as shown in Equation (2.6).

$$k_{\alpha} = \frac{k_{//} k_{\perp}}{k_{//} \sin^{m} \alpha + k_{\perp} \cos^{m} \alpha} \qquad \text{..... (2.6)}$$

In EUROCODE 5 (1995), Equation (2.5) is simplified by replacing slip modulus fastener $k_{\alpha i}$ with k_{ser} for elastic range and with k_u for plastic range. Where k_{ser} is the average value between slip modulus parallel and perpendicular to grain as shown in Equation (2.7), while k_u is approximated as two third of k_{ser}. As a result, the lateral load of fastener in moment-resisting connection can be calculated by Equation (2.9) and (2.10) for elastic and plastic range, respectively.

$$k_{ser} = \frac{k_{//} + k_{\perp}}{2} \qquad \text{..... (2.7)}$$

$$k_u = \frac{2}{3} k_{ser} \qquad \text{..... (2.8)}$$

$$F_{ei} = \frac{k_{ser} r_i}{\sum_{l=1}^{n} k_{ser} r_l^2} M_e = \frac{r_i}{\sum_{l=1}^{n} r_l^2} M_e \qquad \text{..... (2.9)}$$

$$F_{ui} = \frac{k_u r_i}{\sum_{l=1}^{n} k_u r_l^2} M_u = \frac{r_i}{\sum_{l=1}^{n} r_l^2} M_u \qquad \text{..... (2.10)}$$

In Equation (2.9) and (2.10), the slip modulus of each fastener ($k_{\alpha i}$) is disappeared when k_{ser} is applied. Therefore, the lateral load of a fastener depends only on its distance from center of fastener group. Equation (2.9) and (2.10) are used

widely in isotropic materials such as steel structures. In timber connection, however, those equations may no be applicable since the strength properties of wood are greatly affected by the wood grain orientation. In moment-resisting connection, the configuration of fastener will affect the capacity connection significantly. Therefore, for general configuration of multiple-fastener, the slip modulus ($k_{\alpha i}$) should be considered in order to get more accurate analysis.

In this research, lateral load of fastener i is derived from Equation (2.5). Whereas $k_{\alpha i}$ is slip modulus from test result of single bolt connection. Since wood member and steel plate are much stiffer than the joint itself, joint rotation will rotate fasteners with the same angle of rotation at both main member and side members. Although small slip will occur due to imperfect rigid plate assumption, this slip is negligible at elastic range. Finally, Equation (2.5) can be applied both in wood to wood and steel to wood connection.

In plastic range, however, rigid plate assumption could not be applied any longer. The actual behavior of connection will involve many variables and will be more complicated. These variables are failure mode, fastener slip, and ductility of connection. Wood to wood connections will behave differently than that of steel to wood connection. In wood to wood connection, after wood member becomes plastic, its stiffness will decrease and will exhibit a large slip. Meanwhile, in steel to wood connection, steel plate will be in elastic state since the steel plate is much stiffer than wood member. Thus, steel plate still effectively transfers the load to all fasteners and holds the lateral load of all fasteners within the tangential line to Cg.

CHAPTER 3

EXPERIMENT METHODS

To study the flexural behavior of timber connection, several timber connections were tested under bending moment. Four wood to wood connections and four steel to wood connections were prepared in this study. Four multiple-bolt configurations were applied in each type of connections. The moment capacity, rotation ductility, and failure mode of connection was investigated up to collapse condition.

Besides multiple-bolt connection test, test of timber connection with single bolt subjected to a compression load was carried out. The loading orientation to wood grain of compression load was varied into several angles, so that the effect of loading orientation on connection strength could be studied. Furthermore, the test result of single bolt connection would be used as a basis to analyze the multiple-bolt connection.

The strength of bolted connection is greatly depending on the geometric of connection and the strength properties of bolt and wood. In order to analyze the strength of bolted connection, it is a necessary to determine these influencing parameters before. Procedure and test set-up of determining these influencing parameters are explained in this chapter. The test results of these influencing parameters were used to determine the specimens of single bolt connection and multiple-bolt connection. Finally, procedure and test set-up of single bolt connection and multiple-bolt connection are described in this chapter.

3.1 Three-point Bending Test of Bolt

The purpose of this test was to determine the bending yield stress of bolt (F_{yb}) which will be used in the analysis of lateral load resistance of bolted connection. Standard hexagonal-bolt of 12.7 mm diameter was used in this test to obtain I_m failure mode in both wood to wood connection and steel to wood connection. Preliminary analysis according to EUROCODE 5 (1995) of four possible yield modes is shown in Appendix 2.

Bending yield stress test was applied on two of 12.7 mm diameter bolts. Test set up of this experiment is shown in Figure 3.1, which is identical with the test of bending yield stress of Nail (ASTM F1575 – 03). A three-point bending with central point load was applied with a span of 147 mm (11.5 times bolt diameter). The test was run at a constant displacement rate of 6.6 mm/min. Magnitude of point load was recorded automatically by Testing Machine, and flexural displacement at mid-span was acquired by LVDT.

The yield load of EUROCODE 5 was determined as the maximum applied load. Meanwhile, the yield load of NDS was determined from the load-displacement curve as the intersection point between the curve and the offset line of 5% of bolt diameter. The bending yield stress then can be calculated using Equation (3.1).

$$F_{yb} = \frac{M_{yb}}{S_p} = \frac{3P_y s_{bp}}{2D^3} \quad \text{..... (3.1)}$$

Where:

M_{yb} = bending moment in bolt,

S_p = plastic section modulus for bolt,

P_y = yield load,

s_{bp} = spacing of bearing points,

D = diameter of bolt.

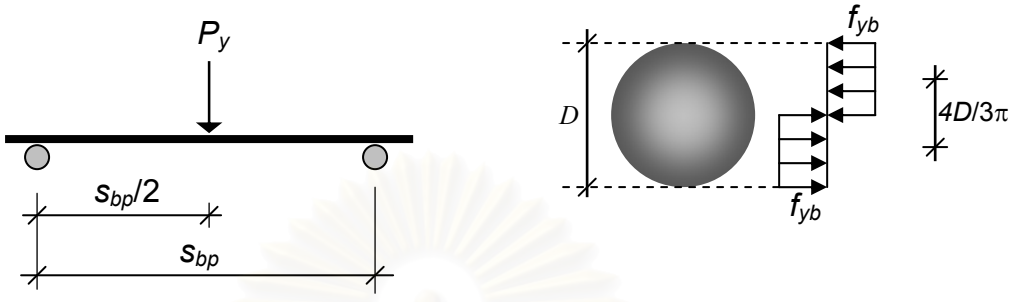

Figure 3.1 Bending yield test of bolt and stress distribution in bolt section

3.2 Moisture Content and Specific Gravity of Wood Measurements

Since moisture content and specific gravity are most important variable affecting the properties of wood, these two physical properties of wood were measured. Moisture content is the amount of water contained (free water and bound water) in the wood, usually expressed as a percentage of the mass of the oven-dry wood. The specific gravity of wood gives an excellent measurement of the amount of wood substance present in a sample. Thus, it may serve as a valuable parameter of the strength characteristic of a specimen. The moisture content and specific gravity specimens shall be fully representative of the material from which they taken and shall also be free from knots.

Wood specimen (shorea obtusa) was used in this experiment. This wood has been used for structural members in Thailand. Shorea obtusa is a hard wood with 1.05 of average specific gravity (Chovichien 1999). Method A in ASTM D4442 – 92 (Primary oven-dry method) and ASTM D2395 – 02 were used as references in preparing the specimen and in conducting the test of moisture content measurement

and specific gravity measurement, respectively. Moisture content and specific gravity measurements were done simultaneously on the same wood specimen. Moisture content and specific gravity can be calculated by Equation (3.2) and (3.3), respectively. Green weight and oven-dry weight were obtained by measuring the weight of specimen before and after drying process in an oven, respectively. Oven-dry specimen could be obtained by drying the green wood specimen in an oven at 105°C for almost twenty four hours or until its weight is constant.

$$w = \frac{w_1 - w_2}{w_2} 100\% \qquad \text{..... (3.2)}$$

$$G = \frac{w_2}{v} \qquad \text{..... (3.3)}$$

Where: v is oven-dry volume, w_1 and w_2 are green weight and oven-dry weight of wood specimen.

3.3 Test of Dowel Bearing Strength of Wood (F_e)

This test provides the basis for determining the compression behavior of wood member beneath a laterally loaded fastener where the thickness of the wood member and the diameter of fastener are such that minimal bending of the fastener occurs during testing (ASTM D5764 – 97a, 2002). The localized wood crushing beneath fastener provides a material property that is used in theoretical models for connection where wood crushing or fastener bending, or both occur.

Dowel bearing strength of wood was evaluated on directions of parallel and perpendicular to wood grain. The dimension of wood specimen is shown in Figure 3.2. The dowel bearing strength of experiment will be compared with estimation values of NDS of U.S (1997) obtained from Equation (3.4) for parallel to grain and Equation (3.5) for perpendicular to grain and also will be compared with estimation

values of EUROCODE 5 (1995) obtained from Equation (3.6) for parallel to grain and Equation (3.7) for perpendicular to grain. Dowel bearing strength found in these following equations is in unit N/mm^2.

$$F_{e//} = 77.25G \quad \text{..... (3.4)}$$

$$F_{e\perp} = 212G^{1.45}D^{-0.5} \quad \text{..... (3.5)}$$

$$F_{e//} = 0.082(1-0.01D)\rho \quad \text{..... (3.6)}$$

$$F_{e\perp} = \frac{F_{e//}}{0.9+0.015D} \quad \text{..... (3.7)}$$

Where: G is the specific gravity, D is diameter of bolt in mm, and ρ is wood density in kg/m^3.

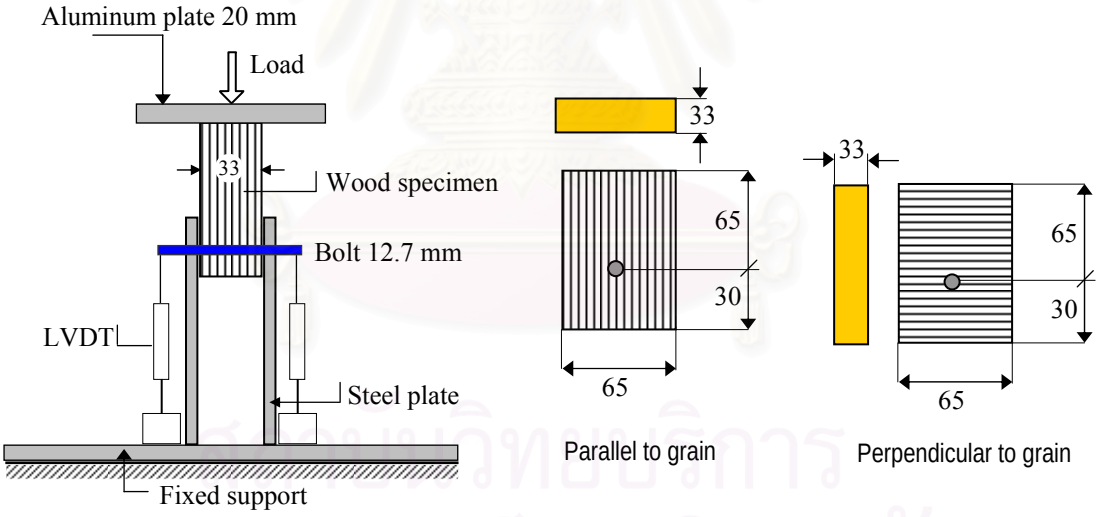

Figure 3.2 Dowel bearing strength test of wood member

Test set up of this experiment is shown in Figure 3.2. A full-hole test configuration was conducted with a hole-diameter of 13 mm. The test was run at a constant displacement rate of 1.2 mm/min so that the maximum load can be reached

in 1 to 10 minutes. The magnitude of compression load was recorded automatically by hand made 10 tons load-cell, and bolt slip was acquired by two LVDTs. The dowel bearing strength of EUROCODE 5 (1995) was determined as the maximum compression load. While, the dowel bearing strength of NDS (1997) was determined from the load-displacement curve as the intersection point between the curve and the 5% of diameter offset line.

3.4 Single Bolt Connection Test

The goal of this test was to examine the lateral load resistance of single bolt connection in various loading orientation to wood grain. The angle of loading orientation to wood grain varies in five loading to grain orientations: 0° (parallel to grain), 30°, 45°, 60°, and 90° (perpendicular to grain). Yield mode I_m (crushing of main member) was expected as the failure mode of connections both wood to wood connections and steel to wood connections.

Wood of 3/2" x 8" was used as main member in both wood to wood connections and steel to wood connections. Steel plate of 4 mm thickness was used as side members in steel to wood connections. This steel to wood connection can be classified as thin plate of steel to wood connection. Wood lumbers of 3/2" x 8" were used as side members in wood to wood connections. Moisture content wood lumber has to be laid at EMC condition (about 14 to 17 percent) to simulate the actual moisture content of service condition.

Connection geometric was designed according to NDS of U.S. (1997). The test was run at a constant displacement rate of 0.5 mm/min up to the failure condition. Code that was used in this test is ASTM D5652-95. Test set-up is shown in Figure 3.3. Three replicate specimens were prepared in each angle of loading orientation to

wood grain. Fastener slip and slip modulus were observed besides the lateral load resistance. The effect of loading orientation to wood grain on the lateral load resistance and slip modulus of experiment was evaluated by Hankinson formula.

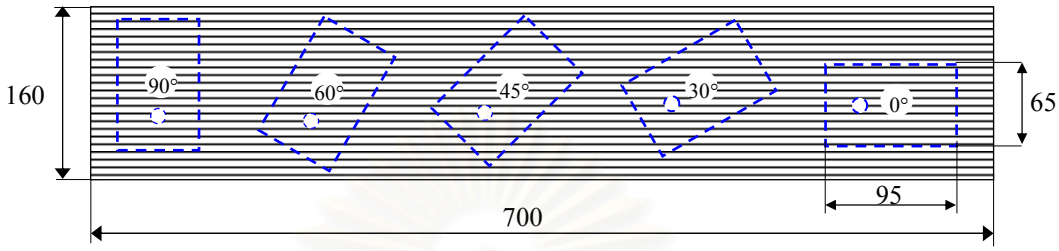

(a) Wood specimens of different angle to grain

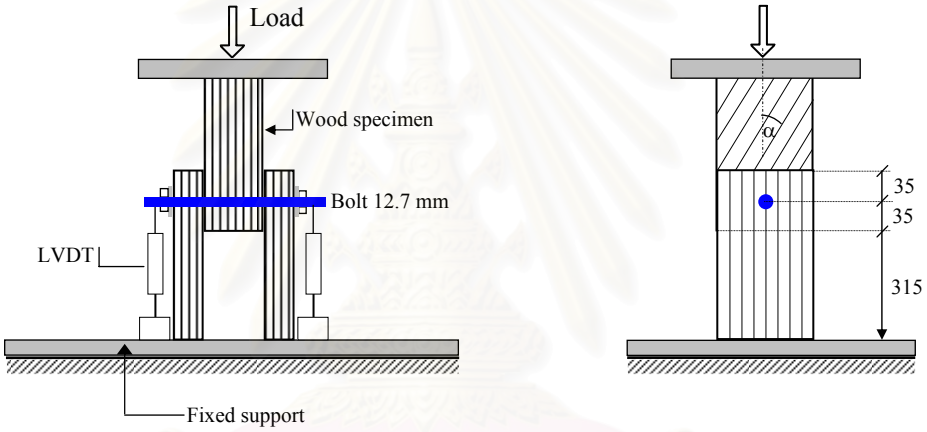

(b) Test set-up of wood to wood connection

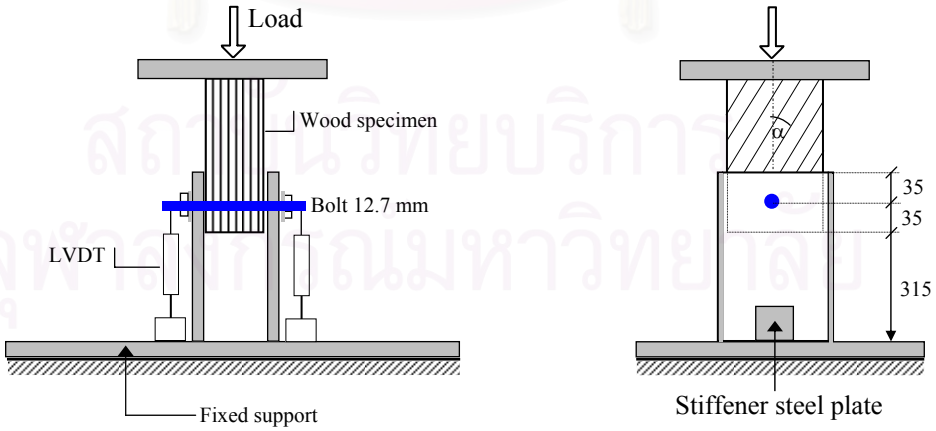

(c) Test set-up of steel to wood connection

Figure 3.3 Wood specimen and test set-up of single bolt connection

3.5 Multiple-Bolt Connection Test

The goal of this test is to investigate the flexural behavior of multiple-bolt connection which subjected to bending moment. Four wood to wood connections and four steel to wood connections were tested in this test. Some flexural parameters such as moment capacity, joint rotation, connection ductility, and failure mode of connection were observed during the test.

Multiple-bolt connections are tested under pure bending using the test set-up as shown in Figure 3.4. Self-weight connection (wood member and fastener) is assumed to be zero, so that applied external load in the connection (mid-span zone) will only be bending moment. The span length of beams intended primarily for evaluation of flexural properties shall be such that the shear span is relatively long. Beam of uniform rectangular cross section having *a/h* (shear-span depth ratio) from 5:1 to 12:1 is recommended by ASTM D198 – 02. The dimension of Multiple-bolt connections was chosen to produce beam with *a/h* ratio of 5:1. Some multiple-bolt configurations of connection that are shown in Figure 3.5 were chosen because they are commonly used in practice. Geometric requirement of connection to anticipate the wood splitting phenomenon is designed with EUROCODE 5 (1995).

The test was run at a constant rate to achieve the maximum load in about 10 minutes. Applied load was generated with a hydraulic jack and its magnitude was measured with hand-made 10 tons load cell. The joint rotation was measured by four LVDTs (LVDT 1 until LVDT 4). The test is stopped when the specimens have shown brittle failure due to wood splitting or load decrease significantly after the maximum load reached. Experimental moment resistance of connection is calculated by static analysis based on the applied load. Joint rotation is approximated by Equation (3.8). Where δ_1 and δ_2 are the slips of two observation points as shown in Figure 3.6.

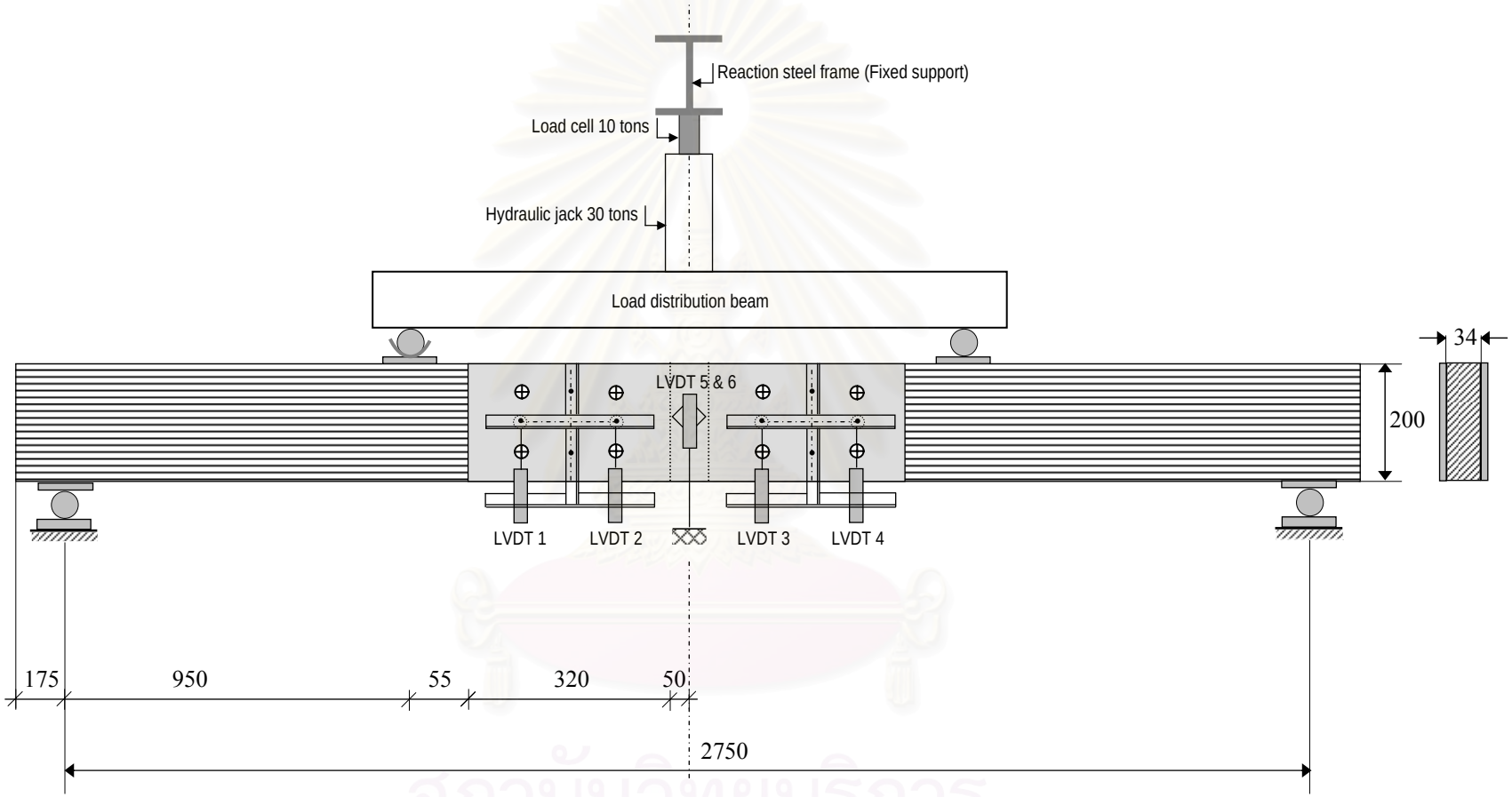

Figure 3.4 Test set-up of moment resisting connection

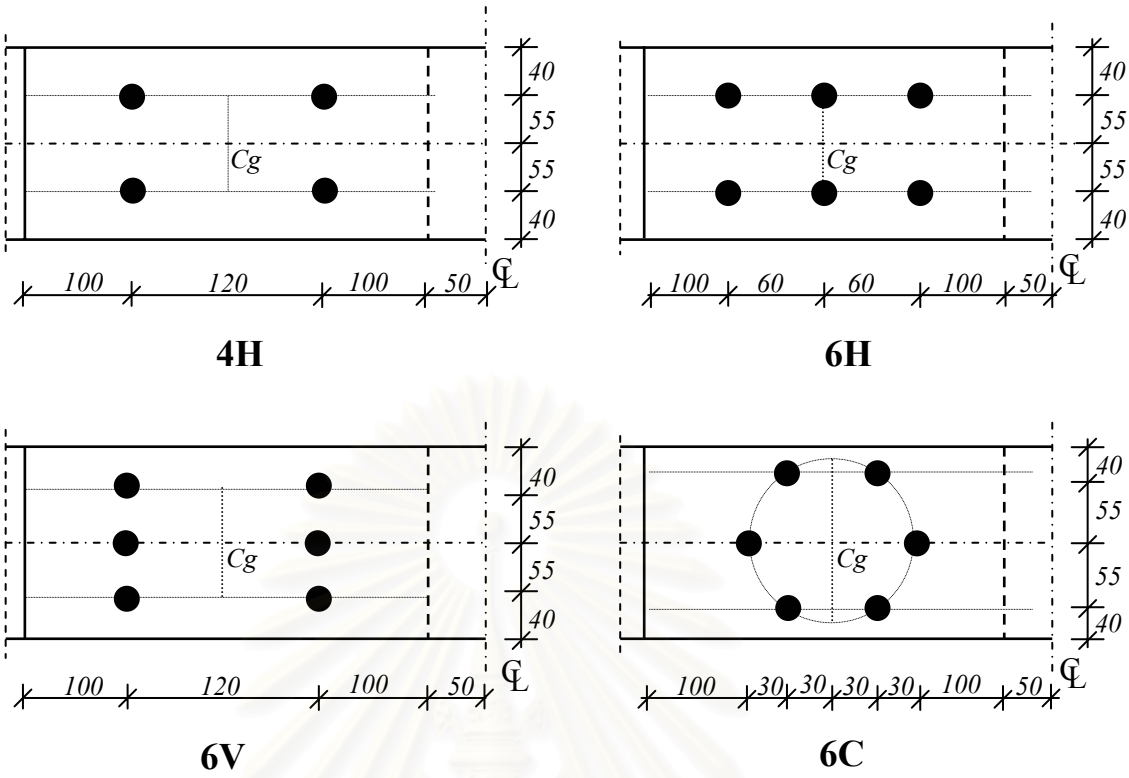

Figure 3.5 Multiple-fastener configurations (unit is in mm)

$$\theta \approx \frac{\delta_1 + \delta_2}{2d} \quad \text{..... (3.8)}$$

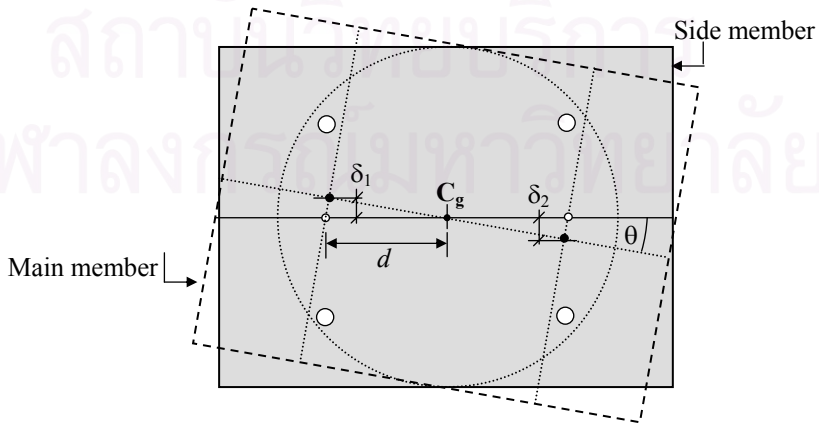

Figure 3.6 Joint rotation measurement

3.6 Theoretical Prediction of Moment-Rotation Curve

Theoretical moment-rotation curve of multiple-bolt connection subjected to pure bending moment can be evaluated based on the test results of single bolt connection. The overall steps of determining the Moment-rotation curve of prediction are as follows:

1) Read displacement δ_1 and δ_2 from experiment.

2) Calculate joint rotation using Equation (3.8).

3) Determine slip of each fastener using Equation (3.9). In further analysis, the initial slip will be assumed to be zero because of its small value.

$$s_i = r_i\theta \qquad \text{..... (3.9)}$$

4) Define the elastic and maximum fastener slips according to test results of single bolt connections.

5) Find out the elastic slip modulus of each fastener using Equation (3.10). $k_{e//}$ and $k_{e\perp}$ are elastic slip modulus obtained from single bolt connection for directions of parallel and perpendicular, respectively.

$$k_{e\alpha} = \frac{k_{e//}k_{e\perp}}{k_{e//}\sin^m\alpha + k_{e\perp}\cos^m\alpha} \qquad \text{..... (3.10)}$$

6) Find out the plastic slip modulus of each fastener using Equation (3.11). $k_{p//}$ and $k_{p\perp}$ are plastic slip modulus obtained from single bolt connection for directions of parallel and perpendicular, respectively

$$k_{p\alpha} = \frac{k_{p//} + k_{p\perp}}{2} \qquad \text{..... (3.11)}$$

7) Calculate the internal moment resistance using Equation (3.12).

$$M = \sum_{i=1}^{n} F_i r_i = \sum_{i=1}^{n} k_i s_i r_i = \frac{\delta_1 + \delta_2}{2d}\sum_{i=1}^{n} k_i r_i^2 \qquad \text{..... (3.12)}$$

CHAPTER 4

RESULTS AND DISCUSSION

In this research, wood specimens of shorea obtusa species were chosen for the study since this wood species is widely used in structural application in Thailand. Experiments were conducted according to the procedures as stated in Chapter 3. Results from the experiments and theoretical prediction are shown in the following sections.

4.1 Moisture Content and Specific Gravity

The moisture content and specific gravity were measured for wood specimens taken from the same pieces with those used in single bolt connection test. Twenty-one specimens were kept in an oven for almost forty-eight hours to get the oven-dry condition. Making use of Equation (3.2), the average moisture content was found as 14.17%. This result has shown that the water content of wood is in equilibrium moisture content, so that drying treatment was not a necessity to do. Specific gravity of wood specimen obtained from Equation (3.3) is 0.86 with coefficient of variance 0.1% (see Appendix 1). This value is smaller than that commonly found in market as stated by Chovichien (1999).

4.2 Bending Yield Stress of Bolt

A three-point bending test with span length of 147 mm was conducted on two bolts. The nominal diameter of bolt was 12.4 mm, and the length of the unthreaded part was 160 mm. Flexural deflection at mid-span was recorded up to 20 mm. A

typical flexural load versus flexural deflection curve can be seen in Figure 4.1. The maximum applied load was formed at flexural deflection between 10 mm and 15 mm, and after that the load was constant until the flexural deflection reached 20 mm (experiment limitation). Significant ductility of the bolt can be observed from load-deflection curve. The yield load of EUROCODE 5 is taken as the maximum load of experiment. An offset line of 5% of bolt diameter was also plotted on Figure 4.1 to obtain the yield load of NDS of U.S. (1997). The bending yield stress of bolt at maximum applied load is calculated by Equation (3.1). The average bending yield stress of bolt both of NDS (1997) and EUROCODE 5 (1995) are 463.41 N/mm^2 and 606.75 N/mm^2, respectively.

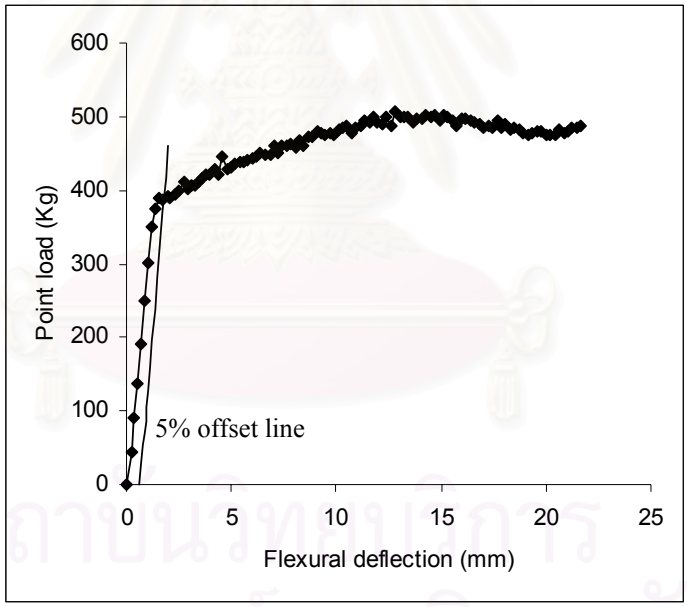

Figure 4.1 Load-slip curve of three-point bending test of fastener

4.3 Dowel Bearing Strength

Specimens under loading parallel to wood grain failed when their maximum load were reached. The failure mode was sudden splitting of wood parallel to the

grain. On the other hand, specimens under loading perpendicular to grain can attained more load after wood splitting. However, further load after wood splitting was not reflected the uniform bearing stress of wood under the bolt any more because more and more bending was observed in the bolt. The maximum load of specimens loaded perpendicular to grain was taken as the load at first wood splitting was formed. Before wood splitting, wood fiber deformation was localized around a half bolt hole as shown in Figure 4.2.

Figure 4.2 Wood crushing around the fastener hole

Average dowel bearing strength parallel and perpendicular to wood grain were found as 57.3 N/mm^2 and 34.37 N/mm^2, respectively. The comparison of these test results with values estimated by NDS (1997) and EUROCODE 5 (1995) are shown in Table 4.1. The estimated values by NDS and EUROCODE 5 are higher than the experiment results, especially for dowel bearing strength perpendicular to wood grain. These differences are due to some different factors such as the size of wood specimen and test configuration (half-hole test or full-hole test). NDS uses a half-hole test to obtain the dowel bearing strength parallel to wood grain which gives higher result than that of a full-hole test (Hirai 1998).

Table 4.1 Comparison study of dowel bearing strength

Loading orientation to wood grain	Dowel Bearing Strength (N/mm^2)		
	NDS	EUROCODE 5	Experiment
Parallel	66.44	60.60	57.30
Perpendicular	48.38	55.80	34.37

4.4 Lateral Load Resistance of Single Bolt Connection

Experimental results have been confirmed to previous research on some hardwood species conducted by Leijten *et al* (2004). Test results (see Figure 4.3 and Figure 4.4) have shown that loading angle drastically affects the lateral load resistance of connections. (The lateral load resistance was normalized with the thickness of main member due to the non-uniform wood thickness.) Lateral load resistance decreases as the loading angle increases. Hankinson formula (Equation 2.1) is chosen to fit the test results. Hankinson formula with m equal to 1.7 and m equal to 1.9 was found appropriate to explain the lateral load resistance for various loading orientations of steel to wood and wood to wood connections, respectively.

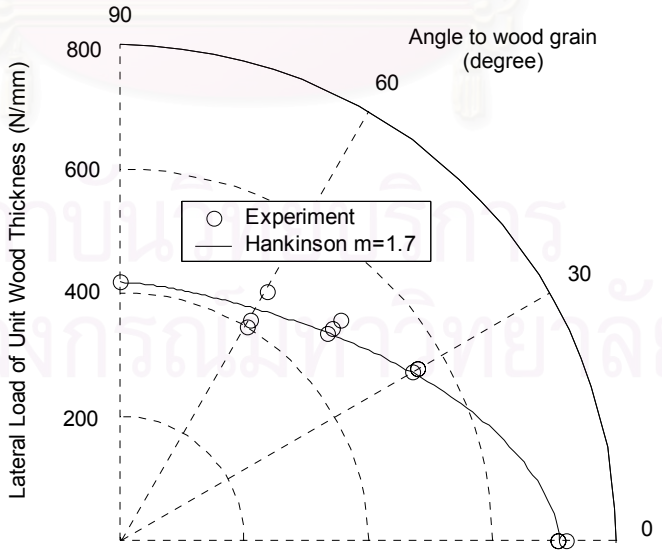

Figure 4.3 Lateral load of unit wood thickness of steel to wood connection

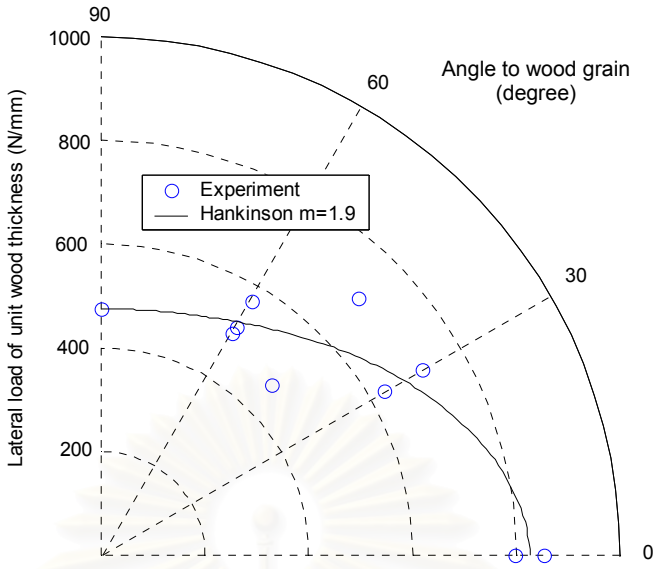

Figure 4.4 Lateral load of unit wood thickness of wood to wood connection

All specimens both wood to wood and steel to wood connections failed in I_m yield mode (wood crushing of main member) as expected. However, specimens under loading parallel to the grain showed small bending in the bolt. All of the specimens failed by wood splitting parallel to grain and followed by sudden load drop. Maximum lateral load was formed at slip less than 4 mm for all the loading orientations except specimens loaded parallel to grain, which showed a large slip before failure.

Load-slip curve from experiment was simplified with bilinear load-slip curve as shown in Figure 4.5 and Figure 4.6. The slope of the first line was called the elastic slip modulus (k_e). In this region, wood is assumed to be a perfectly elastic material. The slope of the second line is called plastic slip modulus (k_p). In all of the specimens, the plastic slip modulus is not equal to zero (not perfectly plastic) but with certain strain hardening. The elastic slip and maximum slip of fastener are presented in Table 4.2. Steel to wood connection tends to have smaller slip than that of wood to wood

connection. That is, the steel plates as side members are much stiffer than wooden plate, and hence deformation in the steel plate is negligible.

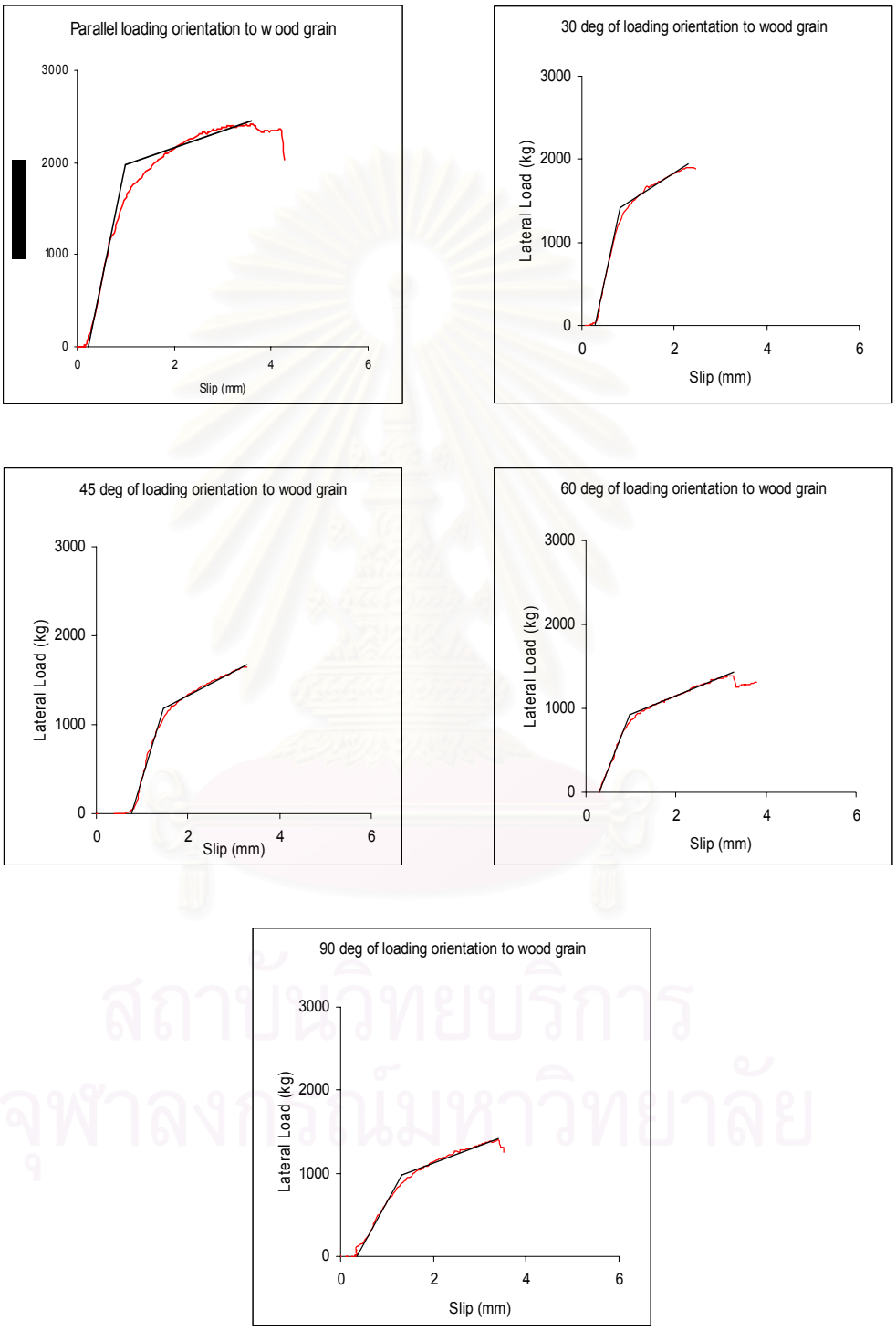

Figure 4.5 Bilinear load-slip curve of steel to wood connections

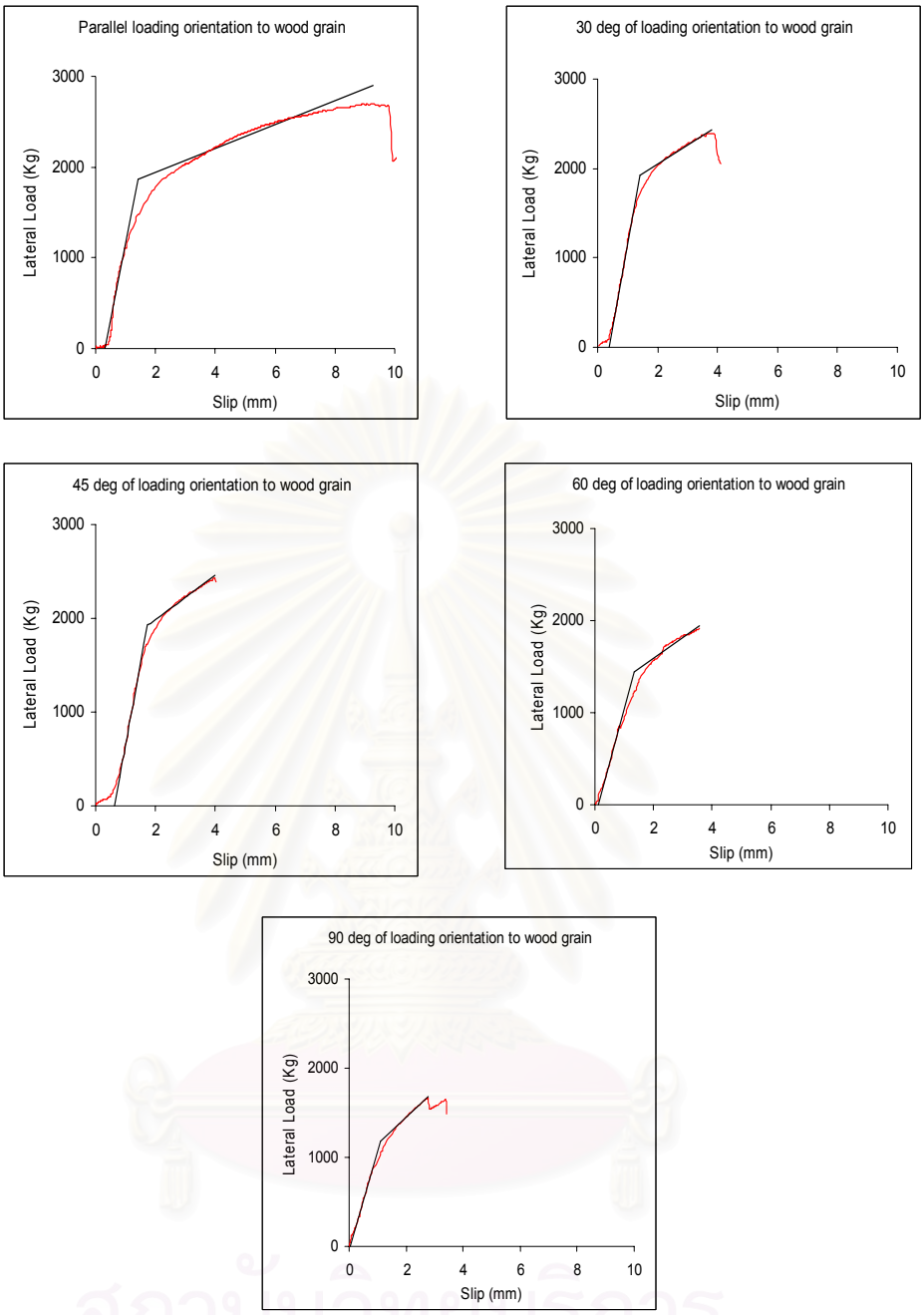

Figure 4.6 Bilinear load-slip curve of wood to wood connections

Table 4.2 Fastener slip of single bolt connection

Loading orientation (deg)	Wood to wood connection		Steel to wood connection	
	Elastic slip (mm)	Maximum slip (mm)	Elastic slip (mm)	Maximum slip (mm)
0	1.07	7.99[1]	0.52	2.74
30	1.20	3.31	0.77	2.28
45	1.28	3.20	0.70	2.46
60	1.35	3.44	0.67	2.91
90	1.18	2.91	0.97	2.72
average	**1.22**	**3.22**	**0.73**	**2.62**

[1]excluded in computing the average value

Similar to the lateral load resistance, polar coordinate system was used to describe the loading orientation effect on elastic slip-modulus (k_e) as shown in Figure 4.7 and Figure 4.8. (The elastic slip modulus was normalized with thickness of main member.) Hankinson formula with m equal to 1.9 and m equal to 2.2 is found appropriate to describe the effect of loading orientation on elastic slip modulus of steel to wood and wood to wood connections, respectively.

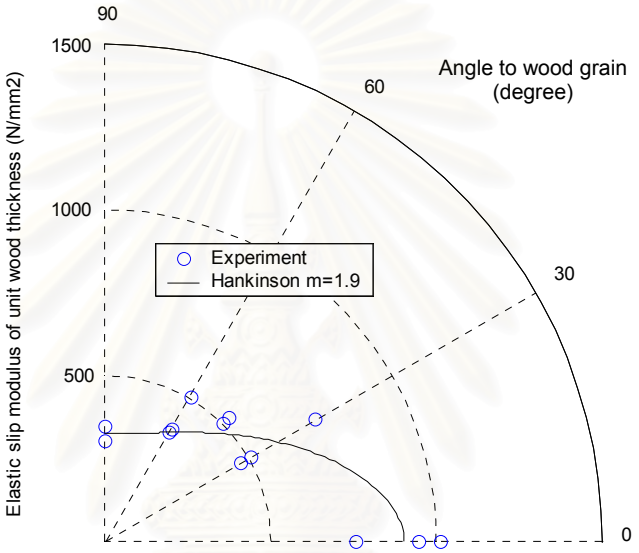

Figure 4.7 Elastic slip modulus of steel to wood connection

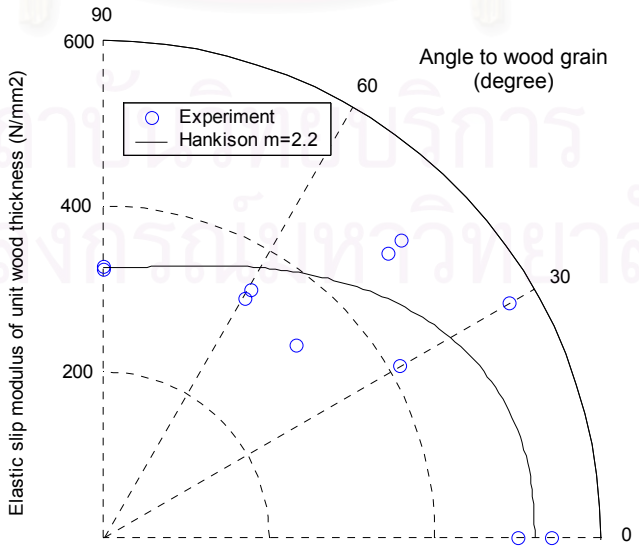

Figure 4.8 Elastic slip modulus of wood to wood connection

Test results of plastic slip modulus both wood to wood and steel to wood connections were scattered as shown in Figure 4.9, therefore Hankinson formula was not used as trial function. The test results have shown that, a constant line of average value between parallel loading and perpendicular loading is found appropriate to fit the data of both steel to wood and wood to wood connections.

The failure of wood main member both wood to wood and steel to wood connection was initiated by crushing failure around the bolt then followed by wood splitting parallel to wood grain regardless of loading direction. This result verified that shear strength parallel to grain is the weakest mechanical property of wood.

Figure 4.10 compares the slip modulus between experimental results and recommended by EUROCODE 5 (1995). EUROCODE 5 uses constant lines calculated from directions parallel and perpendicular to wood grain. We note here that plastic slip modulus recommended by EUROCODE 5 is higher than the experimental results for all loading angles.

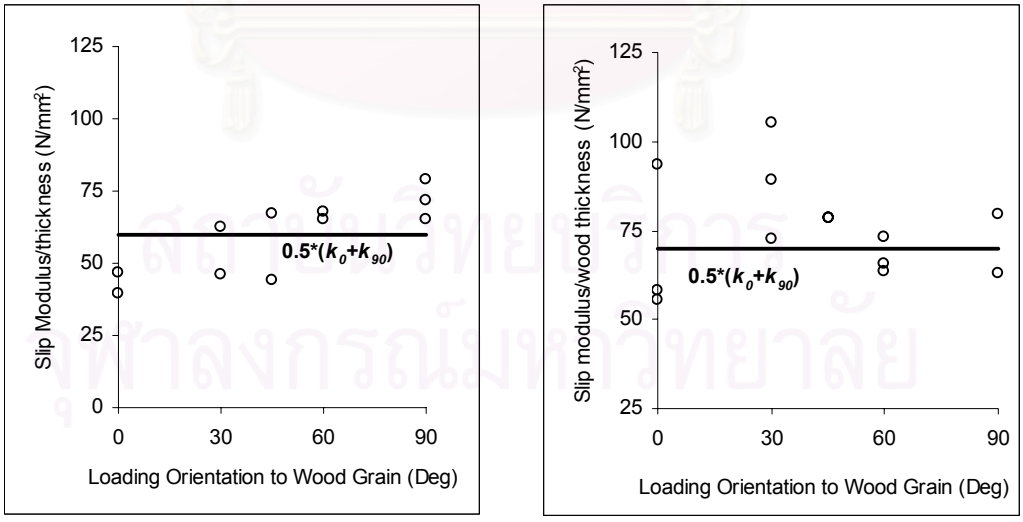

Figure 4.9 Plastic slip modulus of experiment: (a) steel to wood connection, (b) wood to wood connection

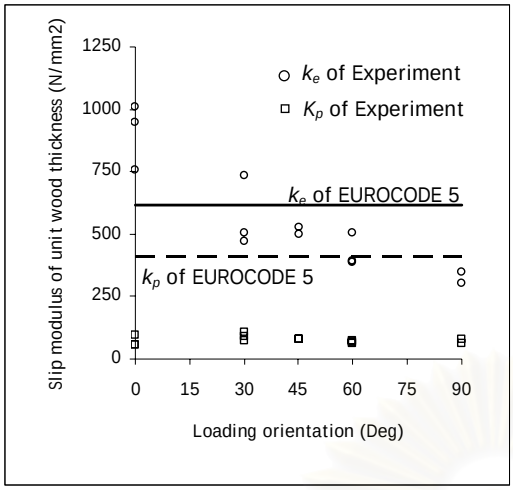

(a)

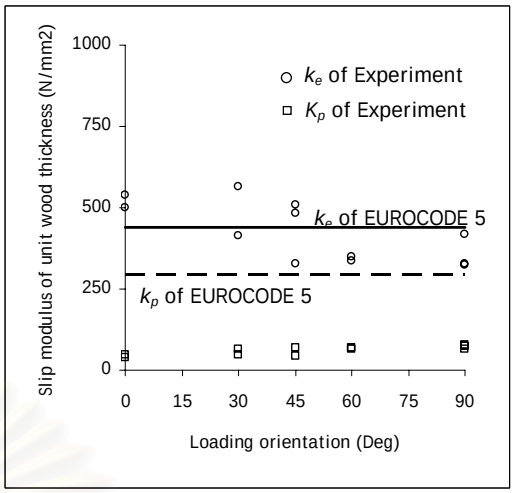

(b)

Figure 4.10 Slip modulus of experiment and calculated by EUROCODE 5: (a) steel to wood connection, (b) wood to wood connection

4.5 Moment Resistance of Multiple-Bolt Connection

Multiple-bolt connections were tested as shown in Figure 4.11. The behavior of connection was observed and recorded up to the failure condition. After the test for moment resistance, single bolt connection tests for the ultimate lateral load resistance in the directions parallel and perpendicular to wood grain ($F_{u//}$ and $F_{u\perp}$) were also carried out. The specimens for single bolt connection tests were actually taken from the wood lumbers which have been used in multiple-bolt connection test. The test results of single bolt connection are shown in Table 4.3. The ultimate lateral load resistance for intermediate angle to wood grain was calculated by Hankinson formula with the values of m equal to 1.7 and 1.9 for steel to wood connection and for wood to wood connection, respectively.

Table 4.3 Test results of single bolt connection

Specimen	Parallel to wood grain			Perpendicular to wood grain		
	$k_{e//}$ N/mm	$k_{p//}$ N/mm	$F_{u//}$ kN	$k_{e\perp}$ N/mm	$k_{p\perp}$ N/mm	$F_{u\perp}$ kN
SW4H	25594	4266	24.99	9185	3062	19.47
SW6H	20128	1496	24.77	7797	2243	16.56
SW6C	20128	1496	24.60	7797	2243	16.48
SW6V	20984	1617	22.61	9326	2366	12.96
WW4H	20069	1810	20.95	8242	1813	13.12
WW6H	15110	1965	23.90	9062	1664	18.88
WW6C	19953	2922	32.75	10008	1532	19.65
WW6V	17560	1537	32.88	8495	1870	16.17

Theoretical maximum moment resistance (M_{th}) by assuming that all bolts are capable to achieve their ultimate strength is obtained by applying Equation (2.2). Due to different lateral load resistances both direction parallel and perpendicular to wood grain of each specimen, experimental moment resistance is normalized with the average value of lateral load resistance in direction parallel and perpendicular to wood grain. Theoretical moment resistance (M_{th}), experimental moment resistance (M_{ex}), and normalized experimental moment resistance ($\overline{M}_{ex}$) of connection are presented in Table 4.4 and Table 4.5.

(a) (b)

Figure 4.11 Multiple-bolt connections under investigation: (a) steel to wood connection, (b) wood to wood connection

Bolt configuration affects the behavior of steel to wood connections and wood to wood connections in the same manner. Configuration 6V gives the highest normalized experimental moment resistance for both steel to wood and wood to wood connection. This is potentially caused by long distance along the grain between bolts that prevents connection splitting at low capacity. However, bolt configuration which yields the lowest moment resistance in steel to wood connection and wood to wood connection are different. Configurations 6H gives the lowest normalized experimental moment resistance in steel to wood connection, and configuration 6C gives the lowest normalized experimental moment resistance in wood to wood connection.

Test results of multiple-bolt connection have shown that all steel to wood connections yield less moment capacity than theoretical prediction; the highest ratio between experimental and theoretical maximum moment resistance (M_{ex}/M_{th}) is 0.77. In wood to wood connections, the ratio between experimental and theoretical maximum moment resistance varies from 0.80 to 1.23. Wood to wood connection shows more capacity than steel to wood connection significantly. Wooden plates as side members in wood to wood connection are more flexible than steel plates. This behavior allows more load redistribution among bolts.

Table 4.4 Maximum moment resistance of steel to wood connection

Multiple-bolt configuration	Lateral load resistance (kN)		Maximum moment resistance (kNm)		
	$F_{u//}$	$F_{u\perp}$	M_{th}	$M_{ex}(\overline{M}_{ex})$*	M_{ex}/M_{th}
SW4H	24.99	19.47	6.37	4.93 (0.22)	0.77
SW6H	24.77	16.56	8.48	3.61 (0.17)	0.43
SW6C	24.66	16.48	7.01	4.11 (0.20)	0.59
SW6V	22.61	12.96	6.30	4.40 (0.25)	0.70

* $\overline{M}_{ex} = \dfrac{M_{ex}}{0.5\left(F_{u//} + F_{u\perp}\right)}$

Table 4.5 Maximum moment resistance of wood to wood connection

Multiple-bolt configuration	Lateral load resistance (kN)		Maximum moment resistance (kNm)		
	$F_{u//}$	$F_{u\perp}$	M_{th}	$M_{ex}(\overline{M}_{ex})^1$	M_{ex}/M_{th}
SW4H	20.95	13.12	4.98	6.15 (0.36)	1.23
SW6H	23.90	18.88	9.20	7.40 (0.35)	0.80
SW6C	32.75	19.65	9.24	8.08 (0.31)	0.87
SW6V	32.88	16.17	8.57	9.62 (0.39)	1.12

[1] $\overline{M}_{ex}$ is as previously defined

4.6 Moment-Rotation Curve of Multiple-Bolt Connection

In the tests of multiple-bolt connections, joint rotation was measured by two LVDTs as illustrated in Figure 4.12. Experimental moment-rotation curves of steel to wood connection and wood to wood connection are shown in Figure 4.13 and Figure 4.14. Experimental data are represented with bilinear curve which consists elastic and plastic ranges. Connection ductility is obtained by dividing the maximum rotation (rotation at maximum moment resistance) with yield rotation, rotation at intersection point between elastic line and plastic line (Racher 1995b).

Some important flexural parameters of connection from these moment-rotation curves are summarized in Table 4.6 and Table 4.7 for steel to wood and wood to wood connection, respectively. In both steel to wood connections and wood to wood connections, bolt configuration 6V has the highest stiffness, the highest ductility, and the highest maximum joint rotation among the four configurations. Connection ductility of bolt configuration 6V is around four, while the ductility of the other configurations is less than two. Brittle failure such as wood splitting occurs in bolt configuration 6H at low joint rotation, before reaching the plastic range, so that this configuration gives very poor ductility. For the same bolt configuration, both steel to wood connections and wood to wood connections have almost equal ductility because of the same failure mode which is wood crushing of main member. Wood to wood

connections has higher maximum joint rotation than steel to wood connections because wood to wood connection behaves with lower degree of restraints.

Table 4.6 Experimental flexural parameters of steel to wood connections

Connection	Elastic slope (kNm/Rad)	Plastic slope (kNm/Rad)	Yield rotation (Rad)	Maximum rotation (Rad)	Ductility
SW4H	373	121	0.011	0.017	1.5
SW6H	369	-	0.009	0.009	1.0
SW6C	299	26	0.012	0.021	1.7
SW6V	419	68	0.007	0.029	4.1

Table 4.7 Experimental flexural parameters of wood to wood connections

Connection	Elastic slope (kNm/Rad)	Plastic slope (kNm/Rad)	Elastic rotation (Rad)	Maximum rotation (Rad)	Ductility
WW4H	426	56	0.014	0.017	1.2
WW6H	454	160	0.015	0.017	1.1
WW6C	450	122	0.015	0.025	1.7
WW6V	485	133	0.011	0.043	3.9

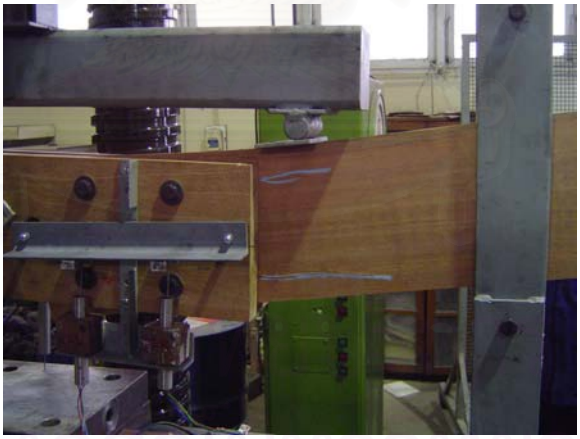

Figure 4.12 Joint rotation of experiment (specimen WW6V)

Moment resistance of connection can be predicted by Equation (3.12). Analysis of theoretical moment-rotation curve of steel to wood connection and wood to wood connection can be seen in Appendix 4 and Appendix 5, respectively.

Experimental and prediction moment-rotation curves are presented in Figure 4.15 and 4.16. For small angle of joint rotation, elastic range, predicted moment-rotation curves show a good agreement with the experimental curves for all bolt configurations. However, for large of joint rotation, moment-rotation curves of prediction show some differences with the experimental results. Intersection point between elastic and plastic lines, yield point, in moment-rotation curve of prediction and experiment are not located in the same place. Predicted moment-rotation curves have higher maximum joint rotation than experimental results. These differences are mostly caused by inappropriate assumptions used in the analysis as follows: 1) Elastic and maximum fastener slips used in the analysis were the average values from test results of single bolt connection for five different loading angles to wood grain, and 2) wood splitting behavior which occurs due to a large number of bolts (more than one bolt) in a row was not considered in the analysis.

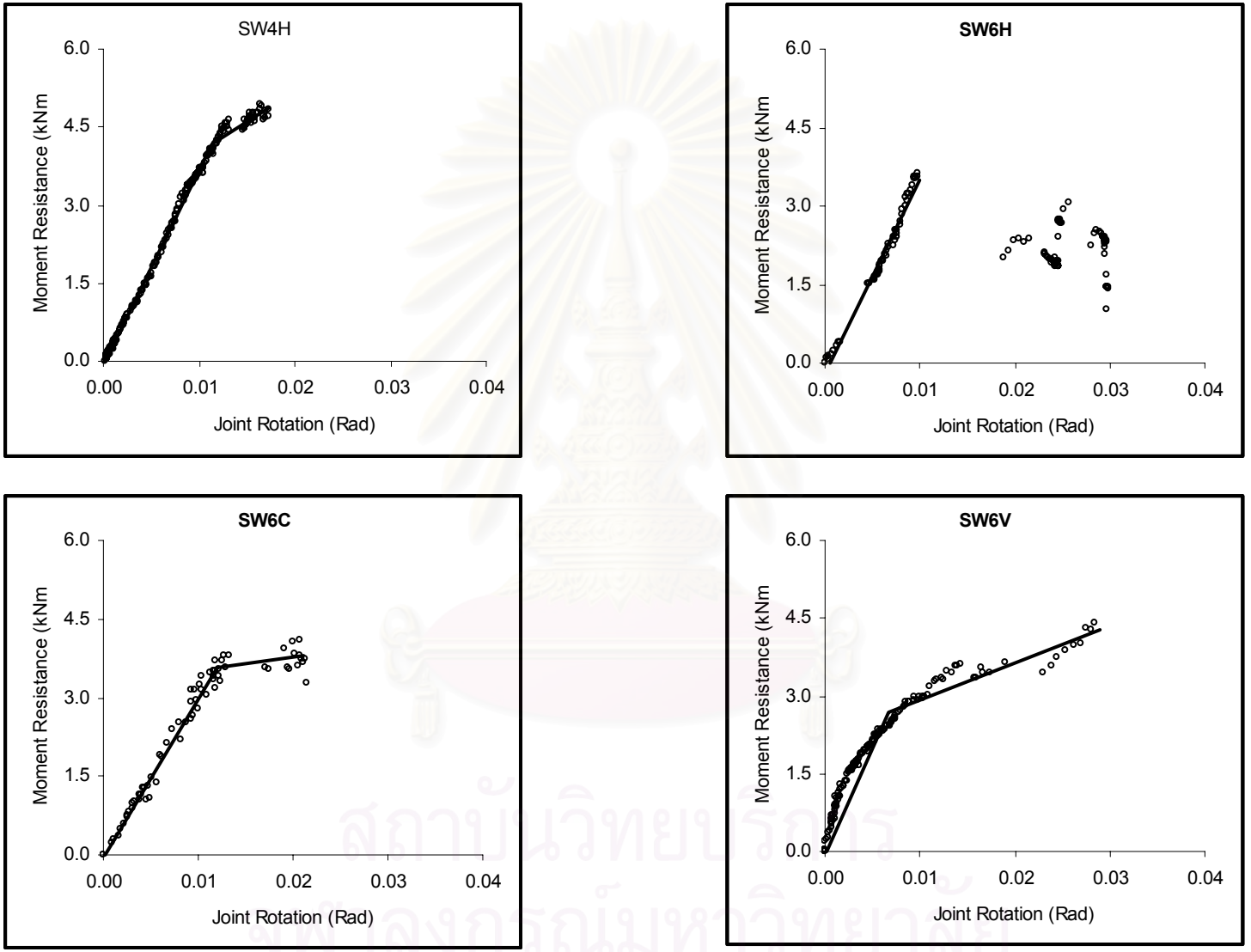

Figure 4.12 Experimental moment-rotation curve of steel to wood connection

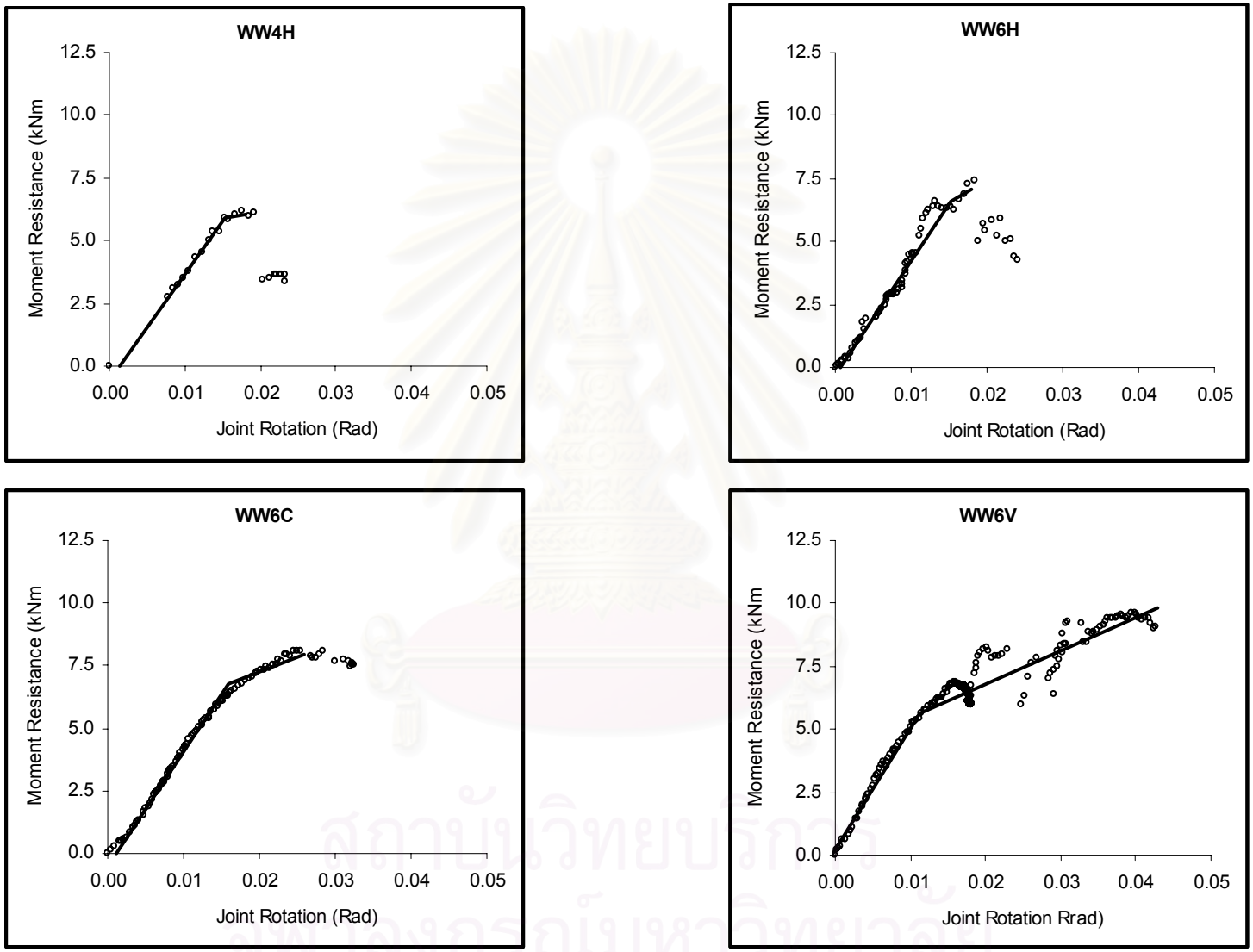

Figure 4.13 Experimental moment-rotation curve of wood to wood connection

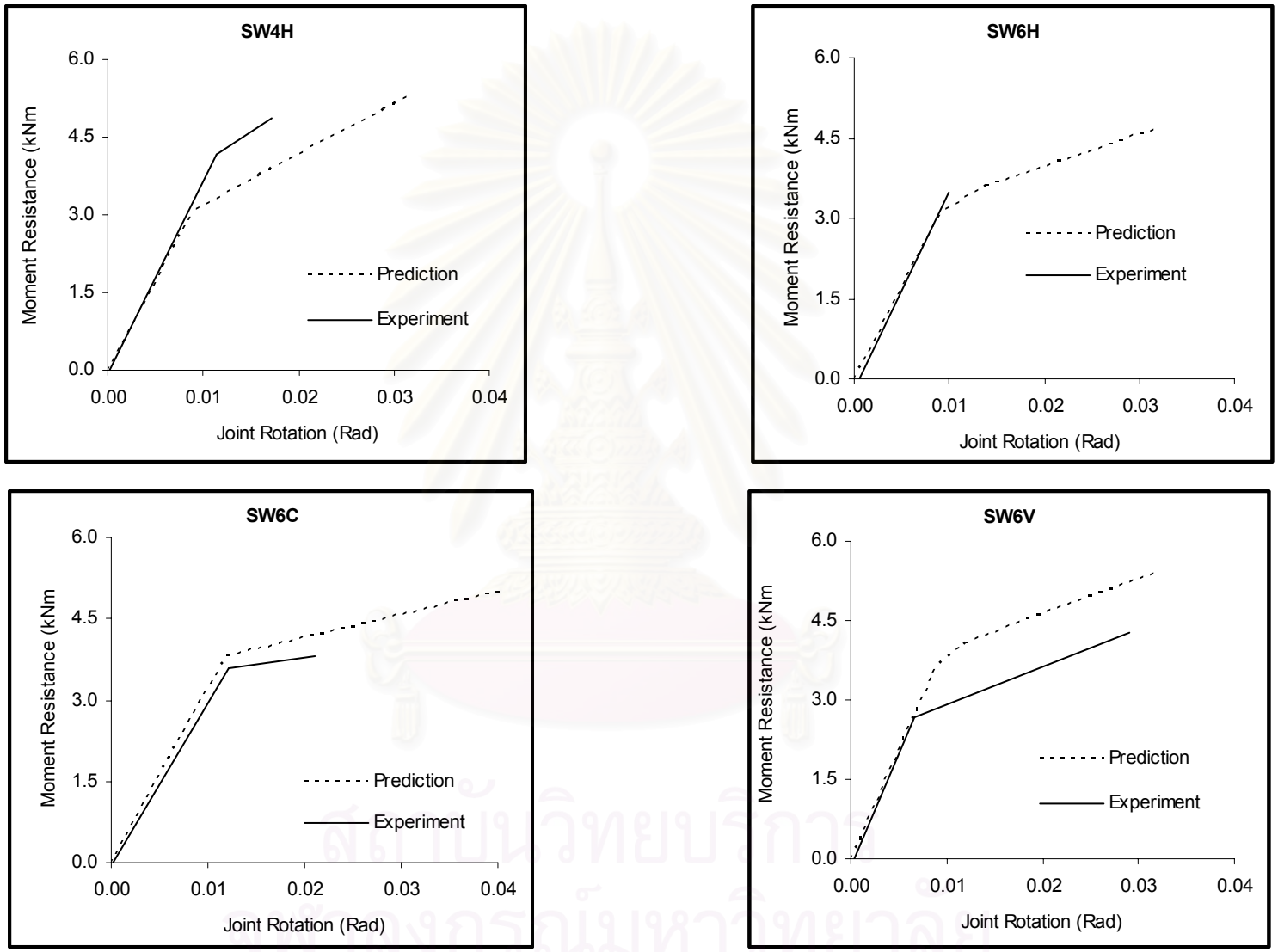

Figure 4.14 Analysis moment-rotation curve of steel to wood connection

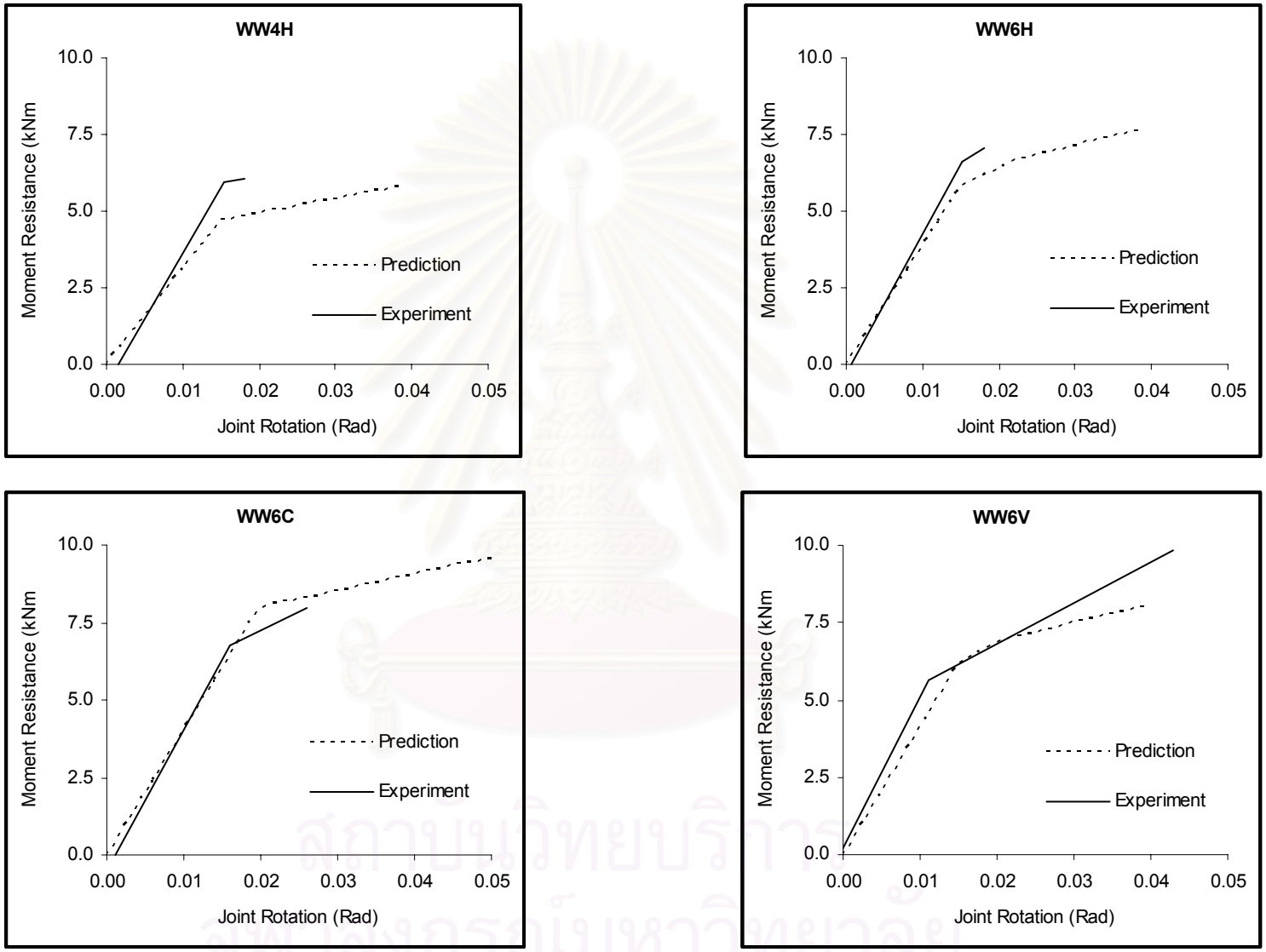

Figure 4.15 Analysis moment-rotation curve of wood to wood connection

4.7 Failure Mode of Multiple-Bolt Connection

Consider the deformed configuration of multiple-bolt connection as shown in Figure 4.17. Each lateral load resistance of fasteners, which equals to product of slip modulus and fastener slip, can be projected into parallel axis and perpendicular axis of wood grain of main member. Using rigid plate assumption and symmetrical arrangement of specimen, one may assume that the slip of fastener at side member is restricted but fastener slip at main member is permitted. The direction of fastener slips is assumed to be tangent with the radial direction from the center of fastener group.

After rotating with angle θ, compression zone (upper part from neutral axis) of right main member will be displaced to the left and push fasteners *i* and *j*. On the other hand, the tension zone (bottom part from neutral axis) of right main member will be displaced to the right and push the fasteners *k* and *l*. This main member rotation yields critical splitting lines as shown in Figure 4.17. These critical lines will initiate the connection to fail in row tear-out mode in the bottom part, and wood splitting in the upper part as shown in Figure 4.18. The failure mode of experiment both steel to wood and wood to wood connection shows a good agreement with the theoretical failure mode as can be seen in Figure 4.19 and Figure 4.20.

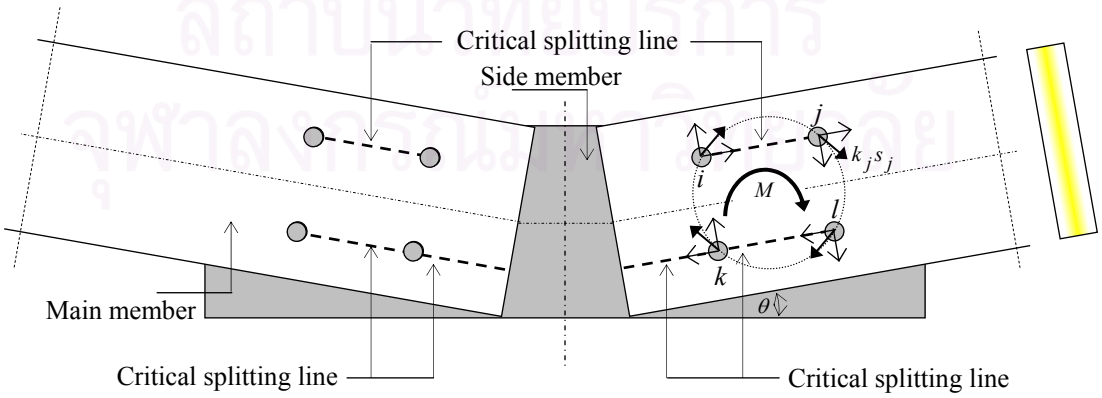

Figure 4.17 Critical splitting lines

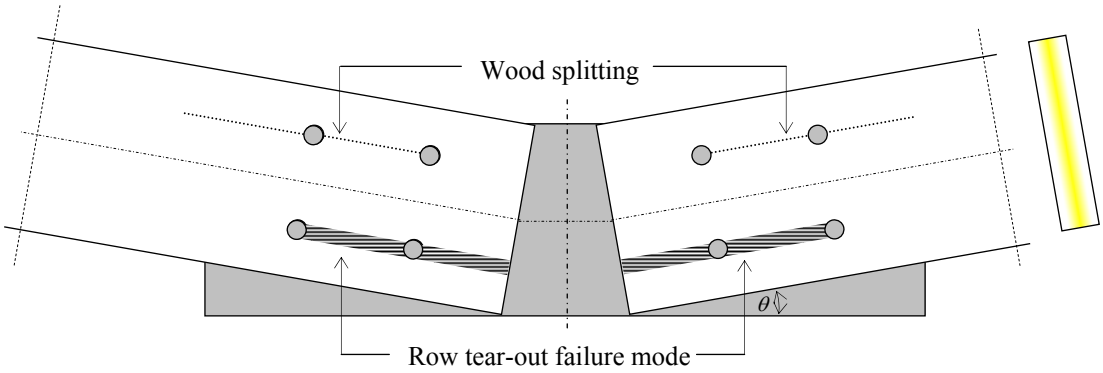

Figure 4.18 Theoretical failure mode of multiple-bolt connection

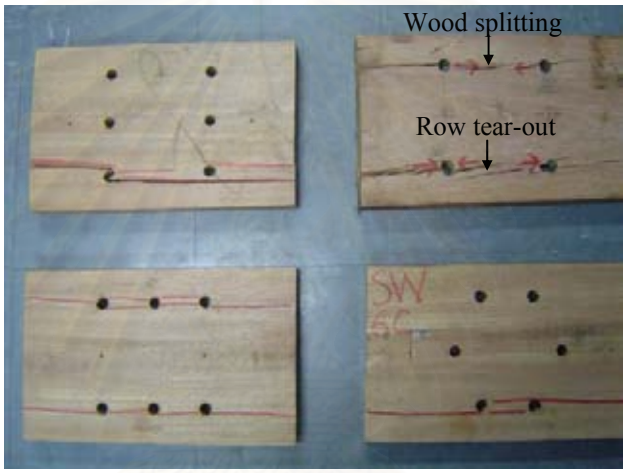

Figure 4.19 Failure mode of main member of steel to wood connection

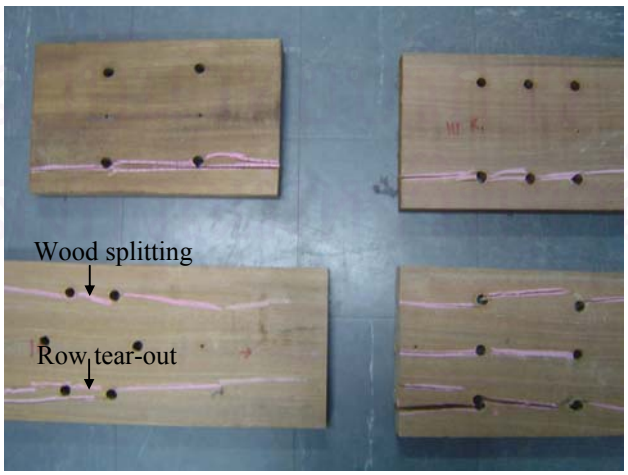

Figure 4.20 Failure mode of main member of wood to wood connection

CHAPTER 5

CONCLUSIONS

Moment-resisting connections are the most crucial parts in several types of wood structures, for example, arches and rigid frames. In multiple-bolt connection, the bending moment is counter-balanced by the product of the lateral load in each fastener and its distance to the center of the group. In most cases, fasteners in the group resist lateral load in different angles to wood grain, upon which resistance varies greatly. Therefore, the moment capacity of connection is greatly affected by the multiple-bolt configuration**.**

The strength of bolted connection is determined by parameters such as the bending yield strength of bolt, the bearing or shear strength of wood member, and the geometry of connection. Depending on these parameters, failure mode and strength of connection can be analyzed. In a multiple-fastener connection, however, the connection failure is often caused by wood splitting rather than by fastener yield or wood crushing of single fastener connection. This failure mode is caused by the low shear strength of wood and local stresses around fasteners. As a result, the strength of connection is reduced.

In this research, four steel to wood connections and four wood to wood connections, with different bolt arrangement, were tested under bending moment. Flexural behavior of connection such as moment resistance, moment-rotation curve, and failure mode were investigated. Wood specimens of shorea obtusa species were chosen. Theoretical prediction was also performed in this study. Based on the test results of single bolt connection, the effect of loading angle to wood grain on ultimate

lateral load resistance and slip modulus can be obtained. Applying the rigid plate assumption to multiple-bolt connection, maximum moment capacity of multiple-bolt connection can be obtained from the test results of single bolt connection. The results of analysis are compared with the experimental results.

Experimental results of single bolt connection tests have shown that load-slip curve of bolted connection is well represented by bilinear load-slip curve which consist of elastic and plastic ranges. In both steel to wood and wood to wood connections, loading angle drastically affects the elastic slip modulus. Elastic slip modulus decreases as the loading angle increases. Hankinson formula with m equal to 1.9 and m equal to 2.2 is found appropriate to fit the experimental results of elastic slip modulus for steel to wood and wood to wood connection, respectively. A constant line of average value between parallel loading and perpendicular loading is found appropriate to fit the plastic slip modulus of experimental results.

In both steel to wood and wood to wood connections, lateral load resistance decreases as the loading angle increases. Hankinson formula with m equal to 1.7 and m equal to 1.9 is found appropriate to fit the experimental results of ultimate lateral load resistance of steel to wood and wood to wood connection, respectively. Specimen loaded parallel to grain shows large slip before failure. Steel to wood connections have smaller fastener slip than wood to wood connection.

Test results of multiple-bolt connection have shown that all steel to wood connections yield less moment capacity than theoretical prediction; the highest ratio between experimental and theoretical maximum moment resistance is 0.77. In wood to wood connections, the ratio between experimental and theoretical maximum moment resistance varies from 0.80 to 1.23. Bolt configuration affects the behavior of steel to wood and wood to wood connections in the same manner. Bolt configuration

6V, which has long distance along the grain between bolts, gives the highest moment resistance among the four configurations. Wooden plates as side members in wood to wood connection are more flexible than steel plates. This behavior allows more load redistribution among bolts. As a result, wood to wood connection shows more capacity than steel to wood connection significantly.

In multiple-bolt configuration, both steel to wood and wood to wood connections, bolt configuration 6V has the highest stiffness, the highest ductility, and the highest maximum joint rotation among the four configurations. Connection ductility of bolt configuration 6V is around four, while the ductility of the other configurations is less than two. Bolt configuration which has short distance along the grain between bolts, for example configuration 6H, fails before reaching the plastic range. Brittle failure such as wood splitting occurs in this configuration at low joint rotation.

In case of using different side members, steel to wood and wood to wood connections with the same bolt configuration have almost equal ductility because of the same failure mode which is wood crushing of main member. However, wood to wood connection has higher maximum joint rotation than steel to wood connection because wood to wood connection behaves with lower degree of restraints.

Finally, the proposed theoretical prediction of moment-rotation curves using the rigid plate assumption show good agreements with the experimental results only in elastic range for both steel to wood and wood to wood connections. In plastic range, predicted moment-rotation curves show some differences. These differences are mostly caused by inappropriate assumptions used in the analysis. Therefore, an advanced analysis which considers the actual slip of each fastener as well as wood splitting behavior might be more appropriate.

REFERENCES

American Society of Civil Engineer. 1997. National Design and Specification for Timber Construction of U.S. New York: ASCE.

American Standard of Testing and Materials. 2002. Standard Test Method for Evaluating Dowel-Bearing Strength of Wood and Wood-Base Products: ASTM D5764-97a. ASTM. Philadelphia.

American Standard of Testing and Materials. 2002. Standard Test Methods for Specific Gravity of Wood and Wood-Based Materials: ASTM D2395-02. ASTM. Philadelphia.

American Standard of Testing and Materials. 2003. Standard Test Methods for Direct Moisture Content Measurement of Wood and Wood-Base Materials: ASTM D4442-92. ASTM. Philadelphia.

American Standard of Testing and Materials. 2003. Standard Test Methods for Determining Bending Yield Moment of Nails: ASTM F1575-03. ASTM. Philadelphia.

American Standard of Testing and Materials. 2002. Standard Test Method of Static Test of Lumber in Structural Size: ASTM D198-02. ASTM. Philadelphia.

Blass, H.J. 1995. Multiple Fastener Joints. Timber Engineering STEP I: C15/1-C15/8.

Blass, H.J., Schmid, M., Litze, H. and Wagner, B., ----. Nail Plate Reinforced Joint with Dowel-Type Fastener. PTEC 99 International Conference on Timber Engineering.

Ceceotti, A. 1993. Structural Timber: Characteristic and Testing. Journal of Structural Engineering (2): 95-98.

Chovichien, V. 1999. Timber Engineering and Design. Bangkok.

EUROCODE 5. 1995. Final Draft Design of Timber Structures. Part 1.1

Faherty, K.F. and Williamson, T.G. 1999. Wood Engineering and Construction. New York: Mc. Graw-Hill.

Frangi, A. and Fontana, M., 2003. Elasto-Plastic Model for Timber-Concrete Composite Beam with Ductile Connection. Journal of Structural Engineering (1): 47-57.

Gattesco, N., 1998. Strength and Local Deformability of Wood beneath Bolted-Connectors. Journal of Structural Engineering 124(2): 195-202.

Hilson, B.O. and Whale, L.R.J. 1990. Developments in the Design of Timber Joints. Journal of Structural Engineering 68(17): 148-150.

Hirai, T. 1983. Nonlinear Load-Slip Relationship of Bolted Wood-Joints with Steel Side-Members. Mokuzai Gakkaishi 29(12): 839-844.

Hirai, T. 1984. Effect of Loading Direction on the Bearing Characteristic of Wood Under A Bolt. --- (in Japanese Language).

Hirai, T. 1990a. Load-Slip Relationship of Mechanical Wood-Joints with Steel Web. Research Bulletin of the College Experiment Forests Faculty of Agriculture Hokkaido University 47(1): 215-248.

Hirai, T. 1990b. Some Considerations on Lateral Resistance of Mechanical Wood-Joints. Proceeding of the International Timber Engineering Conference: 241 - 247.

Hirai, T., Ohtomo, T., Wakashima, Y. 1998. Effective Resistance of Joints with Multiple-Fastenings. Proceeding of the 5th World Conference on Timber Engineering 4: 145 – 152.

Hoffmeyer, P. 1995. Wood as a Building Material. Timber Engineering STEP I: A4/1-C4/21.

Leijten, A.J.M. 1988. Steel Reinforced Joint with Dowels and Bolts. Proceeding of the International Timber Engineering Conference.

Leijten, A.J.M. and Kohler, J. 2004. Evaluation of Embedment Strength. Final Report on Short Scientific Mission: Cost Action E24.

McLain, T.E. and Thangjitham, S. 1983. Bolted Wood-Joint Yield Model. Journal of Structural Engineering 109(8): 1820 – 1835.

Racher, P. 1995a. Moment-Resisting Connection. Timber Engineering STEP I: C16/1-C16/10.

Racher, P. 1995b. Mechanical Timber Joints - General. Timber Engineering STEP I: C1/1-C1/10.

Smith, I. and Foliente, G. 2002. Load and Resistance Factor Design of Timber Joint: International Practice and Future Design. Journal of Structural Engineering 128(1): 48-59.

Soltis, L.A. and Hubbard, F.K. 1986. Bearing Strength of Bolted Timber Joints. Journal of Structural Engineering 112(9): 2141-2154.

Somayaji, S. 1995. Civil Engineering Materials. New Jersey: Prentice Hall.

Taylor, R.J., (2002). Is Your Wood Connection Stressed Out? It Needn't Be!.Washington DC: American Wood Council.

Tucker, B.J., Pollock, D.G., Fridley, K.J. and Peters, J.J. 2000. Governing Yield Modes for Common Bolted and Nailed Wood Connection. Practice Periodical on Structural Design and Construction 5(1): 14-26.

Wilkinson, T.L. 1986. Load Distribution among Bolts Parallel to Load. Journal of Structural Engineering 112(4): 835-852.

Zahn, J.J. 1992. Design Equation for Multiple-Fastener Wood Connection. Journal of Structural Engineering 117(11): 3477-3486.

APPENDICES

A. MOISTURE CONTENT AND SPECIFIC GRAVITY MEASUREMENT

(Taken from wood specimen of dowel bearing test)

Specimen	Green weight (gr)	Oven-dry weight (gr)	Volume (Oven-dry specimen) (cm^3)	Moisture content (%)	Specific Gravity (Oven-dry condition)
1	2.92	2.54	2.88	14.96	0.88
2	2.70	2.34	2.64	15.38	0.89
3	2.67	2.34	2.84	14.10	0.82
4	3.14	2.79	3.18	12.54	0.88
5	2.98	2.63	3.18	13.31	0.83
6	2.85	2.51	3.03	13.55	0.83
7	3.07	2.73	3.18	12.45	0.86
8	2.82	2.51	3.33	12.35	0.75
9	3.09	2.73	3.05	13.19	0.89
10	2.80	2.45	2.95	14.29	0.83
11	2.92	2.51	2.92	16.33	0.86
12	2.99	2.59	2.91	15.44	0.89
13	2.88	2.55	3.09	12.94	0.83
14	2.77	2.45	2.90	13.06	0.85
15	2.92	2.56	3.08	14.06	0.83
16	3.02	2.57	2.87	17.51	0.90
17	3.06	2.68	2.98	14.18	0.90
18	2.98	2.60	2.88	14.62	0.90
19	2.89	2.50	2.97	15.60	0.84
20	2.98	2.60	3.10	14.62	0.84
21	3.12	2.76	3.07	13.04	0.90
Max				17.51	0.90
Min				12.35	0.75
Mean				14.17	0.86
STD				1.36	0.04
COV				1.85	0.001

B. Lateral Load Resistance and Failure Mode of Single Bolt Connection

A. Wood to Wood Connection

Data:

Thickness of main member (t_2)	33.90	mm
Thickness of side member (t_1)	33.90	mm
Diameter of bolt	12.40	mm
Bending yield moment of bolt (M_{yk})	182858	N/mm^2

α 0 Degree

F_{e0}	Z/I_s	Z/I_m	Z/III_s	Z/IV	Z	Yield mode
(N/mm^2)	(N)	(N)	(N)	(N)	(N)	
57.30	48173	24087	27503	44491	24087	**I_m**

α 30 Degree

F_{e30}	Z/I_s	Z/I_m	Z/III_s	Z/IV	Z	Yield mode
(N/mm^2)	(N)	(N)	(N)	(N)	(N)	
56.10	47160	23580	27134	44020	23580	**I_m**

α 45 Degree

F_{e45}	Z/I_s	Z/I_m	Z/III_s	Z/IV	Z	Yield mode
(N/mm^2)	(N)	(N)	(N)	(N)	(N)	
54.94	46189	23094	26778	43565	**23094**	**I_m**

α 60 Degree

F_{e60}	Z/I_s	Z/I_m	Z/III_s	Z/IV	Z	Yield mode
(N/mm^2)	(N)	(N)	(N)	(N)	(N)	
53.83	45256	22628	26435	43123	22628	**I_m**

α 90 Degree

F_{e90}	Z/I_s	Z/I_m	Z/III_s	Z/IV	Z	Yield mode
(N/mm^2)	(N)	(N)	(N)	(N)	(N)	
52.76	44358	22179	26105	42693	22179	**I_m**

Lateral Load Resistance and Failure Mode of Single Bolt Connection

B. Steel to Wood Connection

Data:

Thickness of main member (t_2)	33.80	mm
Diameter of bolt	12.40	mm
Bending yield moment of bolt (M_{yk})	182858	N/mm^2

α 0 Degree

F_{e0}	Z/I_m	Z/III_s	Z	Yield mode
(N/mm^2)	(N)	(N)	(N)	
57.30	24016	44491	24016	**I_m**

α 30 Degree

F_{e30}	Z/I_m	Z/III_s	Z	Yield mode
(N/mm^2)	(N)	(N)	(N)	
56.10	23511	44020	23511	**I_m**

α 45 Degree

F_{e45}	Z/I_m	Z/III_s	Z	Yield mode
(N/mm^2)	(N)	(N)	(N)	
54.94	23026	43565	23026	**I_m**

α 60 Degree

F_{e60}	Z/I_m	Z/III_s	Z	Yield mode
(N/mm^2)	(N)	(N)	(N)	
53.83	22561	43123	22561	**I_m**

α 90 Degree

F_{e90}	Z/I_m	Z/III_s	Z	Yield mode
(N/mm^2)	(N)	(N)	(N)	
52.76	22114	42693	**22114**	**I_m**

C. Test Results of Single Bolt Connection with Various Loading Orientation

A. Steel to wood connection

Specimen*	Ultimate lateral load resistance (N/mm)		Slip modulus (N/mm^2)	
	Experiment	EUROCODE 5	Elastic	Plastic
sw001	720	711	755	56
sw002	705	711	1010	93
sw003	706	711	945	58
sw301	553	696	734	105
sw302	546	696	471	89
sw303	555	696	507	73
sw451	484	681	501	78
sw452	473	681	572	63
sw453	502	681	528	79
sw601	402	667	384	63
sw602	413	667	507	65
sw603	467	668	395	73
sw901	417	654	303	63
sw902	435	654	347	79

B. Wood to wood connection

Specimen**	Ultimate lateral load resistance (N/mm)		Slip modulus (N/mm^2)	
	Experiment	EUROCODE 5	Elastic	Plastic
ww001	798	711	500	47
ww002	854	711	541	39
ww301	716	696	565	63
ww302	406	696	216	65
ww303	630	696	413	46
ww451	702	681	507	67
ww452	463	681	485	44
ww453	837	681	328	106
ww601	569	667	348	68
ww602	512	667	336	65
ww603	498	667	224	63
ww901	476	654	324	79
ww902	701	654	327	65
ww903	604	654	654	72

* sw451: sw (steel to wood connection), 45 (loading orientation), 1(specimen number)

** ww902: ww (wood to wood connection), 90 (loading orientation), 2(specimen number)

D. ANALYSIS MAXIMUM MOMENT RESISTANCE OF STEEL TO WOOD CONNECTION

SW4H

Bolt	Wood Thickness	Position from C_g			Load to grain	Ultimate Lateral Load Resistance			M_{th}
		x	y	r	(α)	$F_{u0,1}$	$F_{u90,1}$	$F_{u\alpha,1}$	$F_{ui}*r_i*t$
	mm	mm	mm	mm	degree	N/mm	N/mm	N/mm	kNm
1	35	60	55	81.39	47	714	556	559	1.59
2	35	60	-55	81.39	47	714	556	559	1.59
3	35	-60	-55	81.39	47	714	556	559	1.59
4	35	-60	55	81.39	47	714	556	559	1.59
								M_u	6.37

SW6H

Bolt	Wood Thickness	Position from C_g			Load to grain	Ultimate Lateral Load Resistance			M_{id}
		x	y	r	(α)	$F_{u0,1}$	$F_{u90,1}$	$F_{u\alpha,1}$	$F_{ui}*r_i*t$
	mm	mm	mm	mm	degree	N/mm	N/mm	N/mm	kNm
1	34.3	60	55	81.39	47	723	483	515	1.44
2	34.3	60	-55	81.39	47	723	483	515	1.44
3	34.3	0	-55	55.00	0	723	483	723	1.36
4	34.3	-60	-55	81.39	47	723	483	515	1.44
5	34.3	-60	55	81.39	47	723	483	515	1.44
6	34.3	0	55	55.00	0	723	483	723	1.36
								M_u	8.48

ANALYSIS MAXIMUM MOMENT RESISTANCE OF STEEL TO WOOD CONNECTION

SW6V

Bolt	Wood Thickness	Position from C_g			Load to grain	Ultimate Lateral Load Resistance			M_{id}
		x	y	r	(α)	$F_{u0,1}$	$F_{u90,1}$	$F_{u\alpha,1}$	$F_{ui}*r_i*t$
	mm	mm	mm	mm	degree	N/mm	N/mm	N/mm	kNm
1	34.4	60	55	81.39	47	657	377	423	1.19
2	34.4	60	0	60.00	90	657	377	377	0.78
3	34.4	60	-55	81.39	47	657	377	423	1.19
4	34.4	-60	-55	81.39	47	657	377	423	1.19
5	34.4	-60	0	60.00	90	657	377	377	0.78
6	34.4	-60	55	81.39	47	657	377	423	1.19
								M_u	6.30

SW6C

Bolt	Wood Thickness	Position from C_g			Load to grain	Ultimate Lateral Load Resistance			M_{id}
		x	y	r	(α)	$F_{u0,1}$	$F_{u90,1}$	$F_{u\alpha,1}$	$F_{ui}*r_i*t$
	mm	mm	mm	mm	degree	N/mm	N/mm	N/mm	kNm
1	34.1	30	55	62.65	29	723	483	588	1.26
2	34.1	60	0	60.00	90	723	483	483	0.99
3	34.1	30	-55	62.65	29	723	483	588	1.26
4	34.1	-30	-55	62.65	29	723	483	588	1.26
5	34.1	-60	0	60.00	90	723	483	483	0.99
6	34.1	-30	55	62.65	29	723	483	588	1.26
								M_u	7.01

ANALYSIS MAXIMUM MOMENT RESISTANCE OF WOOD TO WOOD CONNECTION

WW4H

Bolt	Wood Thickness	Position from C_g			Load to grain	Ultimate Lateral Load Resistance			M_{id}
		x	y	r	(α)	$F_{u0,1}$	$F_{u90,1}$	$F_{u\alpha,1}$	$F_{ui}*r_i*t$
	mm	mm	mm	mm	degree	N/mm	N/mm	N/mm	kNm
1	33	60	55	81.39	47	635	398	464	1.25
2	33	60	-55	81.39	47	635	398	464	1.25
3	33	-60	-55	81.39	47	635	398	464	1.25
4	33	-60	55	81.39	47	635	398	464	1.25
								M_u	4.98

WW6H

Bolt	Wood Thickness	Position from C_g			Load to grain	Ultimate Lateral Load Resistance			M_{id}
		x	y	r	(α)	$F_{u0,1}$	$F_{u90,1}$	$F_{u\alpha,1}$	$F_{ui}*r_i*t$
	mm	mm	mm	mm	degree	N/mm	N/mm	N/mm	kNm
1	34.8	60	55	81.39	47	687	543	580	1.64
2	34.8	60	-55	81.39	47	687	543	580	1.64
3	34.8	0	-55	55.00	0	687	543	687	1.31
4	34.8	-60	-55	81.39	47	687	543	580	1.64
5	34.8	-60	55	81.39	47	687	543	580	1.64
6	34.8	0	55	55.00	0	687	543	687	1.31
								M_u	9.20

ANALYSIS MAXIMUM MOMENT RESISTANCE OF WOOD TO WOOD CONNECTION

WW6V

Bolt	Wood Thickness	Position from C_g			Load to grain	Ultimate Lateral Load Resistance			M_{id}
		x	y	r	(α)	$F_{u0,1}$	$F_{u90,1}$	$F_{u\alpha,1}$	$F_{ui}*r_i*t$
	mm	mm	mm	mm	degree	N/mm	N/mm	N/mm	kNm
1	33.7	60	55	81.39	47	976	480	605	1.66
2	33.7	60	0	60.00	90	976	480	480	0.97
3	33.7	60	-55	81.39	47	976	480	605	1.66
4	33.7	-60	-55	81.39	47	976	480	605	1.66
5	33.7	-60	0	60.00	90	976	480	480	0.97
6	33.7	-60	55	81.39	47	976	480	605	1.66
								M_u	8.57

WW6C

Bolt	Wood Thickness	Position from C_g			Load to grain	Ultimate Lateral Load Resistance			M_{id}
		x	y	r	(α)	$F_{u0,1}$	$F_{u90,1}$	$F_{u\alpha,1}$	$F_{ui}*r_i*t$
	mm	mm	mm	mm	degree	N/mm	N/mm	N/mm	kNm
1	33.6	30	55	62.65	29	975	585	818	1.72
2	33.6	60	0	60.00	90	975	585	585	1.18
3	33.6	30	-55	62.65	29	975	585	818	1.72
4	33.6	-30	-55	62.65	29	975	585	818	1.72
5	33.6	-60	0	60.00	90	975	585	585	1.18
6	33.6	-30	55	62.65	29	975	585	818	1.72
								M_u	9.24

E. Moment-Rotation Curve Analysis of SW4H

Joint Data

$k_{e0,1}$	744	N/mm
$k_{e90,1}$	267	N/mm
$k_{p,1}$	106	N/mm
s_y	0.73	mm
s_u	2.62	mm
t	35	mm

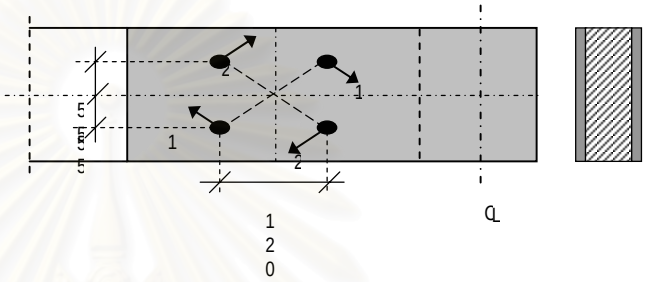

Joint rotation (rad)	Couple 1			Couple 2			Moment of Joint
	Actual slip mm	Lateral load (N)	Moment (kNm)	Actual slip mm	Lateral load (N)	Moment (kNm)	(kNm)
0							0
0.010	0.814	9732	1.58	0.814	9732	1.58	3.17
0.011	0.895	10035	1.63	0.895	10035	1.63	3.27
0.012	0.977	10338	1.68	0.977	10338	1.68	3.37
0.013	1.058	10641	1.73	1.058	10641	1.73	3.46
0.014	1.139	10945	1.78	1.139	10945	1.78	3.56
0.015	1.221	11248	1.83	1.221	11248	1.83	3.66
0.016	1.302	11551	1.88	1.302	11551	1.88	3.76
0.017	1.384	11854	1.93	1.384	11854	1.93	3.86
0.018	1.465	12157	1.98	1.465	12157	1.98	3.96
0.019	1.546	12461	2.03	1.546	12461	2.03	4.06
0.020	1.628	12764	2.08	1.628	12764	2.08	4.16
0.021	1.709	13067	2.13	1.709	13067	2.13	4.25

Joint rotation (rad)	Couple 1			Couple 2			Moment of Joint (kNm)
	Actual slip mm	Lateral load (N)	Moment (kNm)	Actual slip mm	Lateral load (N)	Moment (kNm)	
0.022	1.791	13370	2.18	1.791	13370	2.18	4.35
0.023	1.872	13673	2.23	1.872	13673	2.23	4.45
0.024	1.953	13977	2.28	1.953	13977	2.28	4.55
0.025	2.035	14280	2.32	2.035	14280	2.32	4.65
0.026	2.116	14583	2.37	2.116	14583	2.37	4.75
0.027	2.198	14886	2.42	2.198	14886	2.42	4.85
0.028	2.279	15189	2.47	2.279	15189	2.47	4.95
0.029	2.360	15493	2.52	2.360	15493	2.52	5.04
0.030	2.442	15796	2.57	2.442	15796	2.57	5.14
0.031	2.523	16099	2.62	2.523	16099	2.62	5.24
0.032	2.604	16402	2.67	2.604	16402	2.67	**5.34**
0.033	2.686	0	0.00	2.686	0	0.00	**0.00**

Moment-Rotation Curve Analysis of SW6H

Joint Data

$k_{e0,1}$	592	N/mm
$k_{e90,1}$	226	N/mm
$k_{p,1}$	54	N/mm
s_y	0.73	mm
s_u	2.62	mm
t	34.3	mm

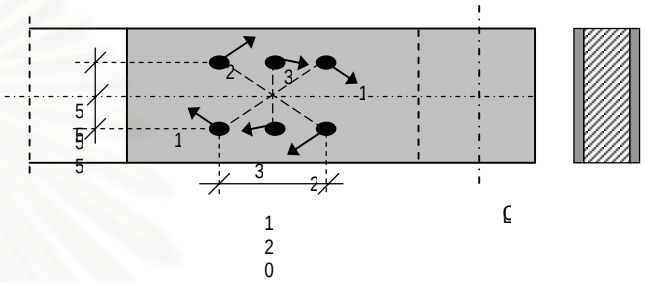

Joint rotation (rad)	Couple 1			Couple 2			Couple 3			Moment of Joint (kNm)
	Actual slip mm	Lateral load (N)	Moment (kNm)	Actual slip mm	Lateral load (N)	Moment (kNm)	Actual slip mm	Lateral load (N)	Moment (kNm)	
0										0
0.001	0.081	856	0.14	0.081	856	0.14	0.055	579	0.06	0.34
0.002	0.163	1713	0.28	0.163	1713	0.28	0.110	1157	0.13	0.68
0.003	0.244	2569	0.42	0.244	2569	0.42	0.165	1736	0.19	1.03
0.004	0.326	3425	0.56	0.326	3425	0.56	0.220	2315	0.25	1.37
0.005	0.407	4282	0.70	0.407	4282	0.70	0.275	2893	0.32	1.71
0.006	0.488	5138	0.84	0.488	5138	0.84	0.330	3472	0.38	2.05
0.007	0.570	5995	0.98	0.570	5995	0.98	0.385	4051	0.45	2.40
0.008	0.651	6851	1.12	0.651	6851	1.12	0.440	4630	0.51	2.74
0.009	0.733	7685	1.25	0.733	7685	1.25	0.495	5208	0.57	3.07
0.010	0.814	7837	1.28	0.814	7837	1.28	0.550	5787	0.64	3.19
0.011	0.895	7988	1.30	0.895	7988	1.30	0.605	6366	0.70	3.30
0.012	0.977	8139	1.32	0.977	8139	1.32	0.660	6944	0.76	3.41

Joint	Couple 1			Couple 2			Couple 3			Moment
rotation (rad)	Actual slip mm	Lateral load (N)	Moment (kNm)	Actual slip mm	Lateral load (N)	Moment (kNm)	Actual slip mm	Lateral load (N)	Moment (kNm)	of Joint (kNm)
0.013	1.058	8290	1.35	1.058	8290	1.35	0.715	7523	0.83	3.53
0.014	1.139	8441	1.37	1.139	8441	1.37	0.770	7755	0.85	3.60
0.015	1.221	8592	1.40	1.221	8592	1.40	0.825	7857	0.86	3.66
0.016	1.302	8743	1.42	1.302	8743	1.42	0.880	7959	0.88	3.72
0.017	1.384	8894	1.45	1.384	8894	1.45	0.935	8061	0.89	3.78
0.018	1.465	9046	1.47	1.465	9046	1.47	0.990	8164	0.90	3.84
0.019	1.546	9197	1.50	1.546	9197	1.50	1.045	8266	0.91	3.90
0.020	1.628	9348	1.52	1.628	9348	1.52	1.100	8368	0.92	3.96
0.021	1.709	9499	1.55	1.709	9499	1.55	1.155	8470	0.93	4.02
0.022	1.791	9650	1.57	1.791	9650	1.57	1.210	8572	0.94	4.08
0.023	1.872	9801	1.60	1.872	9801	1.60	1.265	8674	0.95	4.15
0.024	1.953	9952	1.62	1.953	9952	1.62	1.320	8776	0.97	4.21
0.025	2.035	10103	1.64	2.035	10103	1.64	1.375	8878	0.98	4.27
0.026	2.116	10254	1.67	2.116	10254	1.67	1.430	8981	0.99	4.33
0.027	2.198	10406	1.69	2.198	10406	1.69	1.485	9083	1.00	4.39
0.028	2.279	10557	1.72	2.279	10557	1.72	1.540	9185	1.01	4.45
0.029	2.360	10708	1.74	2.360	10708	1.74	1.595	9287	1.02	4.51
0.030	2.442	10859	1.77	2.442	10859	1.77	1.650	9389	1.03	4.57
0.031	2.523	11010	1.79	2.523	11010	1.79	1.705	9491	1.04	4.63
0.032	2.604	11161	1.82	2.604	11161	1.82	1.760	9593	1.06	**4.69**
0.033	2.686	0	0.00	2.686	0	0.00	1.815	9695	1.07	**1.07**

Moment-Rotation Curve Analysis of SW6C

Joint Data

$k_{e0,1}$	592	N/mm
$k_{e90,1}$	226	N/mm
$k_{p,1}$	54	N/mm
s_y	0.73	mm
s_u	2.62	mm
t	34.1	mm

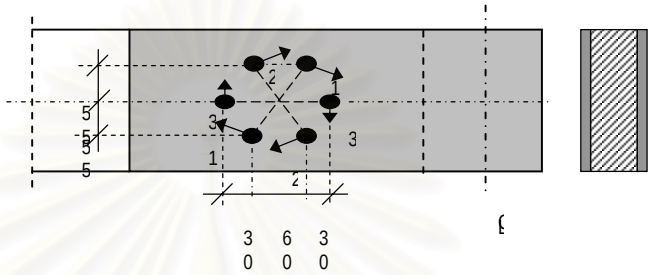

Joint rotation (rad)	Couple 1			Couple 2			Couple 3			Moment of Joint (kNm)
	Actual slip mm	Lateral load (N)	Moment (kNm)	Actual slip mm	Lateral load (N)	Moment (kNm)	Actual slip mm	Lateral load (N)	Moment (kNm)	
0										0
0.001	0.063	881	0.11	0.063	881	0.11	0.060	844	0.10	0.32
0.002	0.125	1762	0.22	0.125	1762	0.22	0.120	1687	0.20	0.64
0.003	0.188	2642	0.33	0.188	2642	0.33	0.180	2531	0.30	0.97
0.004	0.251	3523	0.44	0.251	3523	0.44	0.240	3374	0.40	1.29
0.005	0.313	4404	0.55	0.313	4404	0.55	0.300	4218	0.51	1.61
0.006	0.376	5285	0.66	0.376	5285	0.66	0.360	5061	0.61	1.93
0.007	0.439	6166	0.77	0.439	6166	0.77	0.420	5905	0.71	2.25
0.008	0.501	7046	0.88	0.501	7046	0.88	0.480	6748	0.81	2.58
0.009	0.564	7927	0.99	0.564	7927	0.99	0.540	7592	0.91	2.90
0.010	0.627	8808	1.10	0.627	8808	1.10	0.600	8435	1.01	3.22
0.011	0.689	9689	1.21	0.689	9689	1.21	0.660	9279	1.11	3.54
0.012	0.752	10303	1.29	0.752	10303	1.29	0.720	10122	1.21	3.80

Joint rotation (rad)	Couple 1			Couple 2			Couple 3			Moment of Joint (kNm)
	Actual slip mm	Lateral load (N)	Moment (kNm)	Actual slip mm	Lateral load (N)	Moment (kNm)	Actual slip mm	Lateral load (N)	Moment (kNm)	
0.013	0.814	10419	1.31	0.814	10419	1.31	0.780	10355	1.24	3.85
0.014	0.877	10535	1.32	0.877	10535	1.32	0.840	10466	1.26	3.90
0.015	0.940	10651	1.33	0.940	10651	1.33	0.900	10577	1.27	3.94
0.016	1.002	10767	1.35	1.002	10767	1.35	0.960	10688	1.28	3.98
0.017	1.065	10882	1.36	1.065	10882	1.36	1.020	10799	1.30	4.02
0.018	1.128	10998	1.38	1.128	10998	1.38	1.080	10910	1.31	4.07
0.019	1.190	11114	1.39	1.190	11114	1.39	1.140	11021	1.32	4.11
0.020	1.253	11230	1.41	1.253	11230	1.41	1.200	11132	1.34	4.15
0.021	1.316	11346	1.42	1.316	11346	1.42	1.260	11243	1.35	4.19
0.022	1.378	11461	1.44	1.378	11461	1.44	1.320	11354	1.36	4.23
0.023	1.441	11577	1.45	1.441	11577	1.45	1.380	11465	1.38	4.28
0.024	1.504	11693	1.47	1.504	11693	1.47	1.440	11576	1.39	4.32
0.025	1.566	11809	1.48	1.566	11809	1.48	1.500	11686	1.40	4.36
0.026	1.629	11925	1.49	1.629	11925	1.49	1.560	11797	1.42	4.40
0.027	1.692	12041	1.51	1.692	12041	1.51	1.620	11908	1.43	4.45
0.028	1.754	12156	1.52	1.754	12156	1.52	1.680	12019	1.44	4.49
0.029	1.817	12272	1.54	1.817	12272	1.54	1.740	12130	1.46	4.53
0.030	1.880	12388	1.55	1.880	12388	1.55	1.800	12241	1.47	4.57
0.031	1.942	12504	1.57	1.942	12504	1.57	1.860	12352	1.48	4.62
0.032	2.005	12620	1.58	2.005	12620	1.58	1.920	12463	1.50	4.66
0.033	2.067	12735	1.60	2.067	12735	1.60	1.980	12574	1.51	4.70
0.034	2.130	12851	1.61	2.130	12851	1.61	2.040	12685	1.52	4.74
0.035	2.193	12967	1.62	2.193	12967	1.62	2.100	12796	1.54	4.79

Joint rotation (rad)	Couple 1			Couple 2			Couple 3			Moment of Joint (kNm)
	Actual slip mm	Lateral load (N)	Moment (kNm)	Actual slip mm	Lateral load (N)	Moment (kNm)	Actual slip mm	Lateral load (N)	Moment (kNm)	
0.036	2.255	13083	1.64	2.255	13083	1.64	2.160	12907	1.55	4.83
0.037	2.318	13199	1.65	2.318	13199	1.65	2.220	13017	1.56	4.87
0.038	2.381	13315	1.67	2.381	13315	1.67	2.280	13128	1.58	4.91
0.039	2.443	13430	1.68	2.443	13430	1.68	2.340	13239	1.59	4.95
0.040	2.506	13546	1.70	2.506	13546	1.70	2.400	13350	1.60	5.00
0.041	2.569	13662	1.71	2.569	13662	1.71	2.460	13461	1.62	**5.04**
0.042	2.631	0	0.00	2.631	0	0.00	2.520	13572	1.63	1.63

Joint Data

$k_{e0,1}$	610	N/mm
$k_{e90,1}$	268	N/mm
$k_{p,1}$	57.8	N/mm
s_y	0.73	mm
s_u	2.62	mm
t	34.4	mm

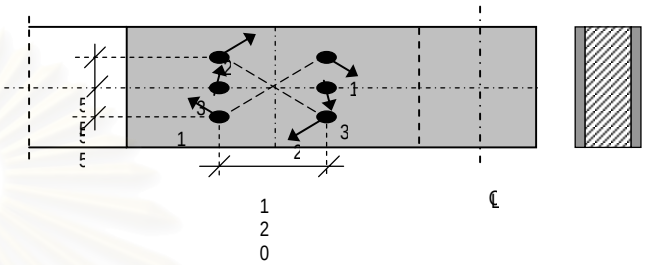

Joint rotation (rad)	Couple 1			Couple 2			Couple 3			Moment of Joint (kNm)
	Actual slip mm	Lateral load (N)	Moment (kNm)	Actual slip mm	Lateral load (N)	Moment (kNm)	Actual slip mm	Lateral load (N)	Moment (kNm)	
0										0
0.001	0.081	983	0.16	0.081	983	0.16	0.060	724	0.09	0.41
0.002	0.163	1965	0.32	0.163	1965	0.32	0.120	1449	0.17	0.81
0.003	0.244	2948	0.48	0.244	2948	0.48	0.180	2173	0.26	1.22
0.004	0.326	3930	0.64	0.326	3930	0.64	0.240	2897	0.35	1.63
0.005	0.407	4913	0.80	0.407	4913	0.80	0.300	3622	0.43	2.03
0.006	0.488	5895	0.96	0.488	5895	0.96	0.360	4346	0.52	2.44
0.007	0.570	6878	1.12	0.570	6878	1.12	0.420	5070	0.61	2.85
0.008	0.651	7860	1.28	0.651	7860	1.28	0.480	5795	0.70	3.25
0.009	0.733	8818	1.44	0.733	8818	1.44	0.540	6519	0.78	3.65
0.010	0.814	8980	1.46	0.814	8980	1.46	0.600	7243	0.87	3.79
0.011	0.895	9141	1.49	0.895	9141	1.49	0.660	7968	0.96	3.93
0.012	0.977	9303	1.51	0.977	9303	1.51	0.720	8692	1.04	4.07

Joint rotation (rad)	Couple 1			Couple 2			Couple 3			Moment of Joint (kNm)
	Actual slip mm	Lateral load (N)	Moment (kNm)	Actual slip mm	Lateral load (N)	Moment (kNm)	Actual slip mm	Lateral load (N)	Moment (kNm)	
0.013	1.058	9465	1.54	1.058	9465	1.54	0.780	8912	1.07	4.15
0.014	1.139	9627	1.57	1.139	9627	1.57	0.840	9031	1.08	4.22
0.015	1.221	9789	1.59	1.221	9789	1.59	0.900	9151	1.10	4.28
0.016	1.302	9951	1.62	1.302	9951	1.62	0.960	9270	1.11	4.35
0.017	1.384	10112	1.65	1.384	10112	1.65	1.020	9389	1.13	4.42
0.018	1.465	10274	1.67	1.465	10274	1.67	1.080	9509	1.14	4.49
0.019	1.546	10436	1.70	1.546	10436	1.70	1.140	9628	1.16	4.55
0.020	1.628	10598	1.73	1.628	10598	1.73	1.200	9747	1.17	4.62
0.021	1.709	10760	1.75	1.709	10760	1.75	1.260	9867	1.18	4.69
0.022	1.791	10921	1.78	1.791	10921	1.78	1.320	9986	1.20	4.75
0.023	1.872	11083	1.80	1.872	11083	1.80	1.380	10105	1.21	4.82
0.024	1.953	11245	1.83	1.953	11245	1.83	1.440	10224	1.23	4.89
0.025	2.035	11407	1.86	2.035	11407	1.86	1.500	10344	1.24	4.95
0.026	2.116	11569	1.88	2.116	11569	1.88	1.560	10463	1.26	5.02
0.027	2.198	11731	1.91	2.198	11731	1.91	1.620	10582	1.27	5.09
0.028	2.279	11892	1.94	2.279	11892	1.94	1.680	10702	1.28	5.16
0.029	2.360	12054	1.96	2.360	12054	1.96	1.740	10821	1.30	5.22
0.030	2.442	12216	1.99	2.442	12216	1.99	1.800	10940	1.31	5.29
0.031	2.523	12378	2.01	2.523	12378	2.01	1.860	11060	1.33	5.36
0.032	2.604	12540	2.04	2.604	12540	2.04	1.920	11179	1.34	**5.42**
0.033	2.686	0	0.00	2.686	0	0.00	1.980	11298	1.36	**1.36**

F. Moment-Rotation Curve Analysis of WW4H

Joint Data

$k_{e0,1}$	610	N/mm
$k_{e90,1}$	241	N/mm
$k_{p,1}$	54	N/mm
s_y	1.22	mm
s_u	3.22	mm
t	33	mm

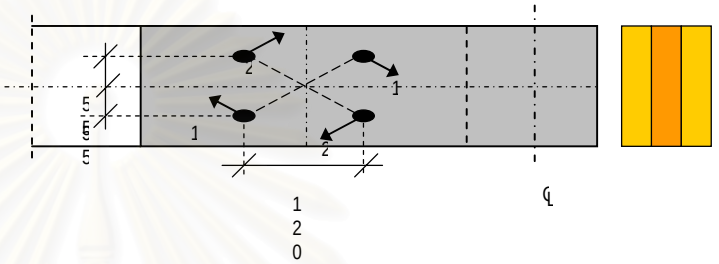

Joint rotation (rad)	Couple 1			Couple 2			Moment of Joint
	Actual slip mm	Lateral load (N)	Moment (kNm)	Actual slip mm	Lateral load (N)	Moment (kNm)	(kNm)
0							0
0.001	0.081	963	0.16	0.081	963	0.16	0.31
0.002	0.163	1925	0.31	0.163	1925	0.31	0.63
0.003	0.244	2888	0.47	0.244	2888	0.47	0.94
0.004	0.326	3851	0.63	0.326	3851	0.63	1.25
0.005	0.407	4813	0.78	0.407	4813	0.78	1.57
0.006	0.488	5776	0.94	0.488	5776	0.94	1.88
0.007	0.570	6739	1.10	0.570	6739	1.10	2.19
0.008	0.651	7701	1.25	0.651	7701	1.25	2.51
0.009	0.733	8664	1.41	0.733	8664	1.41	2.82
0.010	0.814	9627	1.57	0.814	9627	1.57	3.13
0.011	0.895	10589	1.72	0.895	10589	1.72	3.45
0.012	0.977	11552	1.88	0.977	11552	1.88	3.76

Joint rotation (rad)	Couple 1			Couple 2			Moment of Joint (kNm)
	Actual slip mm	Lateral load (N)	Moment (kNm)	Actual slip mm	Lateral load (N)	Moment (kNm)	
0.013	1.058	12515	2.04	1.058	12515	2.04	4.07
0.014	1.139	13477	2.19	1.139	13477	2.19	4.39
0.015	1.221	14432	2.35	1.221	14432	2.35	4.70
0.016	1.302	14577	2.37	1.302	14577	2.37	4.75
0.017	1.384	14722	2.40	1.384	14722	2.40	4.79
0.018	1.465	14867	2.42	1.465	14867	2.42	4.84
0.019	1.546	15012	2.44	1.546	15012	2.44	4.89
0.020	1.628	15157	2.47	1.628	15157	2.47	4.93
0.021	1.709	15302	2.49	1.709	15302	2.49	4.98
0.022	1.791	15447	2.51	1.791	15447	2.51	5.03
0.023	1.872	15592	2.54	1.872	15592	2.54	5.08
0.024	1.953	15737	2.56	1.953	15737	2.56	5.12
0.025	2.035	15882	2.59	2.035	15882	2.59	5.17
0.026	2.116	16027	2.61	2.116	16027	2.61	5.22
0.027	2.198	16172	2.63	2.198	16172	2.63	5.26
0.028	2.279	16317	2.66	2.279	16317	2.66	5.31
0.029	2.360	16462	2.68	2.360	16462	2.68	5.36
0.030	2.442	16607	2.70	2.442	16607	2.70	5.41
0.031	2.523	16752	2.73	2.523	16752	2.73	5.45
0.032	2.604	16897	2.75	2.604	16897	2.75	5.50
0.033	2.686	17042	2.77	2.686	17042	2.77	5.55
0.034	2.767	17187	2.80	2.767	17187	2.80	5.60
0.035	2.849	17332	2.82	2.849	17332	2.82	5.64

Joint rotation (rad)	Couple 1			Couple 2			Moment of Joint (kNm)
	Actual slip mm	Lateral load (N)	Moment (kNm)	Actual slip mm	Lateral load (N)	Moment (kNm)	
0.036	2.930	17477	2.84	2.930	17477	2.84	5.69
0.037	3.011	17622	2.87	3.011	17622	2.87	5.74
0.038	3.093	17767	2.89	3.093	17767	2.89	5.78
0.039	3.174	17912	2.92	3.174	17912	2.92	**5.83**
0.040	3.256	0	0.00	3.256	0	0.00	0.00

Moment-Rotation Curve Analysis of WW6H

Joint Data

$k_{e0,1}$	446	N/mm
$k_{e90,1}$	256	N/mm
$k_{p,1}$	53	N/mm
s_y	1.22	mm
s_u	3.22	mm
t	34.8	mm

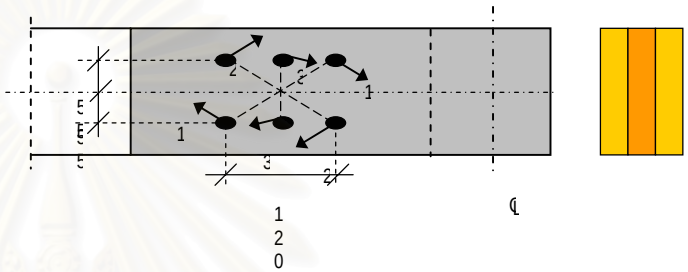

Joint rotation (rad)	Couple 1			Couple 2			Couple 3			Moment of Joint (kNm)
	Actual slip mm	Lateral load (N)	Moment (kNm)	Actual slip mm	Lateral load (N)	Moment (kNm)	Actual slip mm	Lateral load (N)	Moment (kNm)	
0										0
0.0010	0.081	967	0.16	0.081	967	0.16	0.055	654	0.07	0.39
0.0020	0.163	1935	0.31	0.163	1935	0.31	0.110	1307	0.14	0.77
0.0030	0.244	2902	0.47	0.244	2902	0.47	0.165	1961	0.22	1.16
0.0040	0.326	3869	0.63	0.326	3869	0.63	0.220	2615	0.29	1.55
0.0050	0.407	4837	0.79	0.407	4837	0.79	0.275	3269	0.36	1.93
0.0060	0.488	5804	0.94	0.488	5804	0.94	0.330	3922	0.43	2.32
0.0070	0.570	6772	1.10	0.570	6772	1.10	0.385	4576	0.50	2.71
0.0080	0.651	7739	1.26	0.651	7739	1.26	0.440	5230	0.58	3.09
0.0090	0.733	8706	1.42	0.733	8706	1.42	0.495	5883	0.65	3.48
0.0100	0.814	9674	1.57	0.814	9674	1.57	0.550	6537	0.72	3.87
0.0110	0.895	10641	1.73	0.895	10641	1.73	0.605	7191	0.79	4.26

Joint rotation (rad)	Couple 1			Couple 2			Couple 3			Moment of Joint (kNm)
	Actual slip mm	Lateral load (N)	Moment (kNm)	Actual slip mm	Lateral load (N)	Moment (kNm)	Actual slip mm	Lateral load (N)	Moment (kNm)	
0.0120	0.977	11608	1.89	0.977	11608	1.89	0.660	7844	0.86	4.64
0.0130	1.058	12576	2.05	1.058	12576	2.05	0.715	8498	0.93	5.03
0.0140	1.139	13543	2.20	1.139	13543	2.20	0.770	9152	1.01	5.42
0.0150	1.221	14502	2.36	1.221	14502	2.36	0.825	9806	1.08	5.80
0.0160	1.302	14652	2.39	1.302	14652	2.39	0.880	10459	1.15	5.92
0.0170	1.384	14802	2.41	1.384	14802	2.41	0.935	11113	1.22	6.04
0.0180	1.465	14952	2.43	1.465	14952	2.43	0.990	11767	1.29	6.16
0.0190	1.546	15102	2.46	1.546	15102	2.46	1.045	12420	1.37	6.28
0.0200	1.628	15252	2.48	1.628	15252	2.48	1.100	13074	1.44	6.40
0.0210	1.709	15403	2.51	1.709	15403	2.51	1.155	13728	1.51	6.52
0.0220	1.791	15553	2.53	1.791	15553	2.53	1.210	14381	1.58	6.65
0.0230	1.872	15703	2.56	1.872	15703	2.56	1.265	14583	1.60	6.72
0.0240	1.953	15853	2.58	1.953	15853	2.58	1.320	14685	1.62	6.78
0.0250	2.035	16003	2.60	2.035	16003	2.60	1.375	14786	1.63	6.84
0.0260	2.116	16153	2.63	2.116	16153	2.63	1.430	14888	1.64	6.90
0.0270	2.198	16303	2.65	2.198	16303	2.65	1.485	14989	1.65	6.96
0.0280	2.279	16453	2.68	2.279	16453	2.68	1.540	15091	1.66	7.02
0.0290	2.360	16603	2.70	2.360	16603	2.70	1.595	15192	1.67	7.08
0.0300	2.442	16754	2.73	2.442	16754	2.73	1.650	15293	1.68	7.14
0.0310	2.523	16904	2.75	2.523	16904	2.75	1.705	15395	1.69	7.20
0.0320	2.604	17054	2.78	2.604	17054	2.78	1.760	15496	1.70	7.26
0.0330	2.686	17204	2.80	2.686	17204	2.80	1.815	15598	1.72	7.32

Joint rotation (rad)	Couple 1			Couple 2			Couple 3			Moment of Joint (kNm)
	Actual slip mm	Lateral load (N)	Moment (kNm)	Actual slip mm	Lateral load (N)	Moment (kNm)	Actual slip mm	Lateral load (N)	Moment (kNm)	
0.0340	2.767	17354	2.82	2.767	17354	2.82	1.870	15699	1.73	7.38
0.0350	2.849	17504	2.85	2.849	17504	2.85	1.925	15801	1.74	7.44
0.0360	2.930	17654	2.87	2.930	17654	2.87	1.980	15902	1.75	7.50
0.0370	3.011	17804	2.90	3.011	17804	2.90	2.035	16003	1.76	7.56
0.0380	3.093	17955	2.92	3.093	17955	2.92	2.090	16105	1.77	7.62
0.0390	3.174	18105	2.95	3.174	18105	2.95	2.145	16206	1.78	**7.68**
0.0400	3.256	0	0.00	3.256	0	0.00	2.200	16308	1.79	1.79

Moment-Rotation Curve Analysis of WW6C

Joint Data

$k_{e0,1}$	601	N/mm
$k_{e90,1}$	307	N/mm
$k_{p,1}$	68	N/mm
s_y	1.22	mm
s_u	3.22	mm
t	33.6	mm

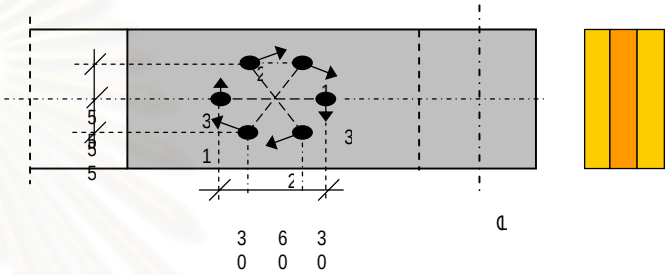

Joint rotation (rad)	Couple 1			Couple 2			Couple 3			Moment of Joint (kNm)
	Actual slip mm	Lateral load (N)	Moment (kNm)	Actual slip mm	Lateral load (N)	Moment (kNm)	Actual slip mm	Lateral load (N)	Moment (kNm)	
0										0
0.001	0.063	1107	0.14	0.063	1107	0.14	0.060	1060	0.13	0.40
0.002	0.125	2214	0.28	0.125	2214	0.28	0.120	2121	0.25	0.81
0.003	0.188	3322	0.42	0.188	3322	0.42	0.180	3181	0.38	1.21
0.004	0.251	4429	0.55	0.251	4429	0.55	0.240	4241	0.51	1.62
0.005	0.313	5536	0.69	0.313	5536	0.69	0.300	5302	0.64	2.02
0.006	0.376	6643	0.83	0.376	6643	0.83	0.360	6362	0.76	2.43
0.007	0.439	7750	0.97	0.439	7750	0.97	0.420	7422	0.89	2.83
0.008	0.501	8857	1.11	0.501	8857	1.11	0.480	8483	1.02	3.24
0.009	0.564	9965	1.25	0.564	9965	1.25	0.540	9543	1.15	3.64
0.010	0.627	11072	1.39	0.627	11072	1.39	0.600	10603	1.27	4.05
0.011	0.689	12179	1.53	0.689	12179	1.53	0.660	11664	1.40	4.45

Joint	Couple 1			Couple 2			Couple 3			Moment
rotation (rad)	Actual slip mm	Lateral load (N)	Moment (kNm)	Actual slip mm	Lateral load (N)	Moment (kNm)	Actual slip mm	Lateral load (N)	Moment (kNm)	of Joint (kNm)
0.012	0.752	13286	1.66	0.752	13286	1.66	0.720	12724	1.53	4.86
0.013	0.814	14393	1.80	0.814	14393	1.80	0.780	13784	1.65	5.26
0.014	0.877	15500	1.94	0.877	15500	1.94	0.840	14845	1.78	5.67
0.015	0.940	16608	2.08	0.940	16608	2.08	0.900	15905	1.91	6.07
0.016	1.002	17715	2.22	1.002	17715	2.22	0.960	16965	2.04	6.48
0.017	1.065	18822	2.36	1.065	18822	2.36	1.020	18026	2.16	6.88
0.018	1.128	19929	2.50	1.128	19929	2.50	1.080	19086	2.29	7.28
0.019	1.190	21036	2.64	1.190	21036	2.64	1.140	20147	2.42	7.69
0.020	1.253	21636	2.71	1.253	21636	2.71	1.200	21207	2.54	7.97
0.021	1.316	21779	2.73	1.316	21779	2.73	1.260	21652	2.60	8.06
0.022	1.378	21922	2.75	1.378	21922	2.75	1.320	21789	2.61	8.11
0.023	1.441	22065	2.76	1.441	22065	2.76	1.380	21926	2.63	8.16
0.024	1.504	22208	2.78	1.504	22208	2.78	1.440	22063	2.65	8.21
0.025	1.566	22351	2.80	1.566	22351	2.80	1.500	22200	2.66	8.27
0.026	1.629	22495	2.82	1.629	22495	2.82	1.560	22337	2.68	8.32
0.027	1.692	22638	2.84	1.692	22638	2.84	1.620	22474	2.70	8.37
0.028	1.754	22781	2.85	1.754	22781	2.85	1.680	22611	2.71	8.42
0.029	1.817	22924	2.87	1.817	22924	2.87	1.740	22748	2.73	8.47
0.030	1.880	23067	2.89	1.880	23067	2.89	1.800	22885	2.75	8.53
0.031	1.942	23210	2.91	1.942	23210	2.91	1.860	23023	2.76	8.58
0.032	2.005	23353	2.93	2.005	23353	2.93	1.920	23160	2.78	8.63
0.033	2.067	23497	2.94	2.067	23497	2.94	1.980	23297	2.80	8.68

Joint	Couple 1			Couple 2			Couple 3			Moment
rotation	Actual slip	Lateral load	Moment	Actual slip	Lateral load	Moment	Actual slip	Lateral load	Moment	of Joint
(rad)	mm	(N)	(kNm)	mm	(N)	(kNm)	mm	(N)	(kNm)	(kNm)
0.034	2.130	23640	2.96	2.130	23640	2.96	2.040	23434	2.81	8.74
0.035	2.193	23783	2.98	2.193	23783	2.98	2.100	23571	2.83	8.79
0.036	2.255	23926	3.00	2.255	23926	3.00	2.160	23708	2.84	8.84
0.037	2.318	24069	3.02	2.318	24069	3.02	2.220	23845	2.86	8.89
0.038	2.381	24212	3.03	2.381	24212	3.03	2.280	23982	2.88	8.95
0.039	2.443	24355	3.05	2.443	24355	3.05	2.340	24119	2.89	9.00
0.040	2.506	24499	3.07	2.506	24499	3.07	2.400	24256	2.91	9.05
0.041	2.569	24642	3.09	2.569	24642	3.09	2.460	24393	2.93	9.10
0.042	2.631	24785	3.11	2.631	24785	3.11	2.520	24531	2.94	9.15
0.043	2.694	24928	3.12	2.694	24928	3.12	2.580	24668	2.96	9.21
0.044	2.757	25071	3.14	2.757	25071	3.14	2.640	24805	2.98	9.26
0.045	2.819	25214	3.16	2.819	25214	3.16	2.700	24942	2.99	9.31
0.046	2.882	25357	3.18	2.882	25357	3.18	2.760	25079	3.01	9.36
0.047	2.945	25501	3.20	2.945	25501	3.20	2.820	25216	3.03	9.42
0.048	3.007	25644	3.21	3.007	25644	3.21	2.880	25353	3.04	9.47
0.049	3.070	25787	3.23	3.070	25787	3.23	2.940	25490	3.06	9.52
0.050	3.133	25930	3.25	3.133	25930	3.25	3.000	25627	3.08	9.57
0.051	3.195	26073	3.27	3.195	26073	3.27	3.060	25764	3.09	**9.63**
0.052	3.258	0	0.00	3.258	0	0.00	3.120	25901	3.11	3.11

Moment-Rotation Curve Analysis of WW6V

Joint Data

$k_{e0,1}$	537	N/mm
$k_{e90,1}$	259	N/mm
$k_{p,1}$	52	N/mm
s_y	1.22	mm
s_u	3.22	mm
t	33.7	mm

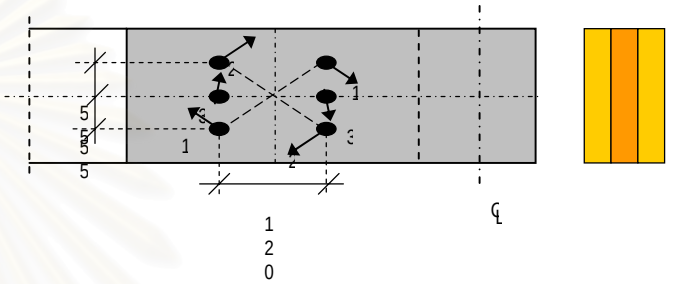

Joint rotation (rad)	Couple 1			Couple 2			Couple 3			Moment of Joint (kNm)
	Actual slip mm	Lateral load (N)	Moment (kNm)	Actual slip mm	Lateral load (N)	Moment (kNm)	Actual slip mm	Lateral load (N)	Moment (kNm)	
0										0
0.0010	0.081	1001	0.16	0.081	1001	0.16	0.060	738	0.09	0.41
0.0020	0.163	2001	0.33	0.163	2001	0.33	0.120	1475	0.18	0.83
0.0030	0.244	3002	0.49	0.244	3002	0.49	0.180	2213	0.27	1.24
0.0040	0.326	4002	0.65	0.326	4002	0.65	0.240	2950	0.35	1.66
0.0050	0.407	5003	0.81	0.407	5003	0.81	0.300	3688	0.44	2.07
0.0060	0.488	6003	0.98	0.488	6003	0.98	0.360	4426	0.53	2.49
0.0070	0.570	7004	1.14	0.570	7004	1.14	0.420	5163	0.62	2.90
0.0080	0.651	8004	1.30	0.651	8004	1.30	0.480	5901	0.71	3.31
0.0090	0.733	9005	1.47	0.733	9005	1.47	0.540	6638	0.80	3.73
0.0100	0.814	10005	1.63	0.814	10005	1.63	0.600	7376	0.89	4.14
0.0110	0.895	11006	1.79	0.895	11006	1.79	0.660	8113	0.97	4.56

Joint rotation (rad)	Couple 1			Couple 2			Couple 3			Moment of Joint (kNm)
	Actual slip mm	Lateral load (N)	Moment (kNm)	Actual slip mm	Lateral load (N)	Moment (kNm)	Actual slip mm	Lateral load (N)	Moment (kNm)	
0.0120	0.977	12006	1.95	0.977	12006	1.95	0.720	8851	1.06	4.97
0.0130	1.058	13007	2.12	1.058	13007	2.12	0.780	9589	1.15	5.39
0.0140	1.139	14008	2.28	1.139	14008	2.28	0.840	10326	1.24	5.80
0.0150	1.221	14999	2.44	1.221	14999	2.44	0.900	11064	1.33	6.21
0.0160	1.302	15142	2.46	1.302	15142	2.46	0.960	11801	1.42	6.35
0.0170	1.384	15284	2.49	1.384	15284	2.49	1.020	12539	1.50	6.48
0.0180	1.465	15427	2.51	1.465	15427	2.51	1.080	13277	1.59	6.62
0.0190	1.546	15570	2.53	1.546	15570	2.53	1.140	14014	1.68	6.75
0.0200	1.628	15712	2.56	1.628	15712	2.56	1.200	14752	1.77	6.89
0.0210	1.709	15855	2.58	1.709	15855	2.58	1.260	15068	1.81	6.97
0.0220	1.791	15998	2.60	1.791	15998	2.60	1.320	15173	1.82	7.03
0.0230	1.872	16140	2.63	1.872	16140	2.63	1.380	15278	1.83	7.09
0.0240	1.953	16283	2.65	1.953	16283	2.65	1.440	15383	1.85	7.15
0.0250	2.035	16425	2.67	2.035	16425	2.67	1.500	15488	1.86	7.21
0.0260	2.116	16568	2.70	2.116	16568	2.70	1.560	15593	1.87	7.27
0.0270	2.198	16711	2.72	2.198	16711	2.72	1.620	15699	1.88	7.32
0.0280	2.279	16853	2.74	2.279	16853	2.74	1.680	15804	1.90	7.38
0.0290	2.360	16996	2.77	2.360	16996	2.77	1.740	15909	1.91	7.44
0.0300	2.442	17139	2.79	2.442	17139	2.79	1.800	16014	1.92	7.50
0.0310	2.523	17281	2.81	2.523	17281	2.81	1.860	16119	1.93	7.56
0.0320	2.604	17424	2.84	2.604	17424	2.84	1.920	16224	1.95	7.62
0.0330	2.686	17566	2.86	2.686	17566	2.86	1.980	16329	1.96	7.68

Joint rotation (rad)	Couple 1			Couple 2			Couple 3			Moment of Joint (kNm)
	Actual slip mm	Lateral load (N)	Moment (kNm)	Actual slip mm	Lateral load (N)	Moment (kNm)	Actual slip mm	Lateral load (N)	Moment (kNm)	
0.0340	2.767	17709	2.88	2.767	17709	2.88	2.040	16435	1.97	7.74
0.0350	2.849	17852	2.91	2.849	17852	2.91	2.100	16540	1.98	7.80
0.0360	2.930	17994	2.93	2.930	17994	2.93	2.160	16645	2.00	7.86
0.0370	3.011	18137	2.95	3.011	18137	2.95	2.220	16750	2.01	7.91
0.0380	3.093	18280	2.98	3.093	18280	2.98	2.280	16855	2.02	7.97
0.0390	3.174	18422	3.00	3.174	18422	3.00	2.340	16960	2.04	**8.03**
0.0400	3.256	0	0.00	3.256	0	0.00	2.400	17065	2.05	2.05

G. Moment Resisting Connection Test

Specimen: **SW4H**

Applied load kN	Moment kNm	Rotation rad	Applied load kN	Moment kNm	Rotation rad
0.00	0.00	0.000	0.68	0.32	0.001
0.18	0.08	0.000	0.84	0.40	0.001
0.09	0.04	0.000	1.05	0.50	0.002
0.12	0.06	0.000	1.13	0.54	0.002
0.05	0.02	0.000	1.12	0.53	0.002
0.09	0.04	0.000	1.25	0.59	0.002
0.16	0.07	0.000	1.28	0.61	0.002
0.25	0.12	0.000	1.35	0.64	0.002
0.26	0.12	0.000	1.49	0.71	0.002
0.19	0.09	0.000	1.42	0.68	0.002
0.43	0.21	0.000	1.55	0.74	0.002
0.39	0.19	0.000	1.45	0.69	0.002
0.28	0.14	0.001	1.57	0.75	0.002
0.29	0.14	0.001	1.62	0.77	0.002
0.44	0.21	0.001	1.78	0.84	0.002
0.45	0.21	0.001	1.78	0.84	0.002
0.51	0.24	0.001	1.89	0.90	0.003
0.58	0.27	0.001	1.73	0.82	0.003
0.57	0.27	0.001	1.91	0.91	0.003
0.62	0.29	0.001	2.03	0.96	0.003
0.61	0.29	0.001	2.24	1.06	0.003
0.73	0.34	0.001	2.14	1.02	0.003
0.51	0.24	0.001	2.26	1.07	0.003
0.63	0.30	0.001	2.39	1.14	0.003
0.50	0.24	0.001	2.41	1.15	0.004
0.73	0.34	0.001	2.37	1.13	0.004
0.69	0.33	0.001	2.45	1.16	0.004
0.77	0.37	0.001	2.64	1.25	0.004
0.77	0.37	0.001	2.84	1.35	0.004
0.72	0.34	0.001	2.73	1.30	0.004
0.75	0.35	0.001	2.87	1.37	0.004
0.84	0.40	0.001	3.15	1.50	0.004
0.91	0.43	0.001	3.11	1.48	0.004
0.83	0.40	0.001	3.09	1.47	0.005

Specimen: SW4H (Cont.)

Applied load kN	Moment kNm	Rotation rad	Applied load kN	Moment kNm	Rotation rad
3.10	1.47	0.005	6.78	3.22	0.009
3.36	1.60	0.005	6.94	3.29	0.009
3.45	1.64	0.005	6.73	3.20	0.009
3.57	1.70	0.005	7.11	3.38	0.009
3.43	1.63	0.005	6.91	3.28	0.009
3.84	1.82	0.005	7.13	3.39	0.009
3.97	1.89	0.005	7.09	3.37	0.009
3.86	1.83	0.005	7.02	3.34	0.009
3.99	1.90	0.006	7.21	3.42	0.009
4.21	2.00	0.006	7.15	3.40	0.009
4.17	1.98	0.006	7.28	3.46	0.009
4.28	2.03	0.006	7.26	3.45	0.009
4.40	2.09	0.006	7.19	3.42	0.009
4.61	2.19	0.006	7.36	3.49	0.009
4.57	2.17	0.006	7.32	3.48	0.010
4.76	2.26	0.006	7.40	3.51	0.010
4.91	2.33	0.007	7.51	3.57	0.010
4.94	2.35	0.007	7.38	3.50	0.010
5.13	2.44	0.007	7.55	3.59	0.010
5.30	2.52	0.007	7.51	3.57	0.010
5.12	2.43	0.007	7.60	3.61	0.010
5.40	2.56	0.007	7.63	3.63	0.010
5.61	2.67	0.007	7.51	3.57	0.010
5.49	2.61	0.007	7.68	3.65	0.010
5.37	2.55	0.007	7.61	3.62	0.010
5.65	2.68	0.007	7.79	3.70	0.010
5.91	2.81	0.008	7.80	3.70	0.010
5.68	2.70	0.008	7.62	3.62	0.010
5.86	2.78	0.008	7.61	3.62	0.010
6.12	2.91	0.008	7.80	3.70	0.010
6.06	2.88	0.008	7.80	3.70	0.011
6.32	3.00	0.008	7.92	3.76	0.011
6.64	3.15	0.008	8.03	3.82	0.011
6.75	3.21	0.008	8.29	3.94	0.011
6.60	3.14	0.008	8.11	3.85	0.011
6.52	3.10	0.009	8.37	3.97	0.011

Specimen: SW4H (Cont.)

Applied load kN	Moment kNm	Rotation rad	Applied load kN	Moment kNm	Rotation rad
8.31	3.95	0.011	9.50	4.51	0.015
8.43	4.00	0.011	9.41	4.47	0.015
8.57	4.07	0.011	9.34	4.44	0.015
8.50	4.04	0.011	8.92	4.24	0.015
8.57	4.07	0.011	9.22	4.38	0.015
8.45	4.01	0.011	9.23	4.38	0.015
8.54	4.06	0.011	9.40	4.46	0.015
8.42	4.00	0.011	9.76	4.64	0.015
8.55	4.06	0.012	9.54	4.53	0.015
8.36	3.97	0.012	9.60	4.56	0.015
8.65	4.11	0.012	9.59	4.56	0.015
8.81	4.18	0.012	9.61	4.57	0.015
8.80	4.18	0.012	9.73	4.62	0.015
8.94	4.25	0.012	9.78	4.65	0.015
8.96	4.25	0.012	10.03	4.76	0.015
9.07	4.31	0.012	9.89	4.70	0.015
9.13	4.34	0.012	9.79	4.65	0.015
9.22	4.38	0.012	9.83	4.67	0.016
9.37	4.45	0.012	9.65	4.59	0.016
9.47	4.50	0.013	10.02	4.76	0.016
9.40	4.46	0.013	9.71	4.61	0.016
9.28	4.41	0.013	9.84	4.67	0.016
9.60	4.56	0.013	10.04	4.77	0.016
9.46	4.49	0.013	10.07	4.79	0.016
9.63	4.58	0.013	10.38	**4.93**	0.016
9.76	4.64	0.013	10.17	4.83	0.016
9.36	4.45	0.013	10.34	4.91	0.017
8.65	4.11	0.014	9.92	4.71	0.017
8.53	4.05	0.014	9.80	4.66	0.017
8.78	4.17	0.014	10.12	4.81	0.017
8.67	4.12	0.014	9.86	4.68	0.017
9.00	4.27	0.014	10.17	4.83	0.017
9.16	4.35	0.015	9.89	4.70	0.017
9.04	4.30	0.015			
9.32	4.43	0.015			
9.25	4.39	0.015			

Moment Resisting Connection Test

Specimen: **SW6H**

Applied load kN	Moment kNm	Rotation rad	Applied load kN	Moment kNm	Rotation rad
0.00	0.00	0.000	5.22	2.48	0.008
0.20	0.09	0.000	5.36	2.54	0.007
0.16	0.07	0.000	5.36	2.54	0.008
0.29	0.14	0.000	5.57	2.65	0.008
0.37	0.18	0.001	5.72	2.72	0.008
0.52	0.25	0.001	5.94	2.82	0.008
0.67	0.32	0.001	6.15	2.92	0.008
0.81	0.39	0.001	6.31	3.00	0.009
0.81	0.39	0.002	6.49	3.08	0.009
3.17	1.51	0.004	6.68	3.17	0.009
3.22	1.53	0.005	6.78	3.22	0.009
3.32	1.57	0.005	6.78	3.22	0.009
3.34	1.58	0.005	6.94	3.29	0.009
3.43	1.63	0.005	7.17	3.41	0.009
3.46	1.64	0.005	7.48	3.55	0.009
3.53	1.68	0.006	7.43	3.53	0.009
3.60	1.71	0.006	7.42	3.52	0.010
3.71	1.76	0.006	7.51	3.57	0.010
3.68	1.75	0.006	7.60	**3.61**	0.010
3.72	1.77	0.006	4.27	2.03	0.019
3.87	1.84	0.006	4.49	2.13	0.019
3.96	1.88	0.006	4.91	2.33	0.020
4.08	1.94	0.006	5.02	2.39	0.020
4.06	1.93	0.006	4.85	2.30	0.021
4.20	1.99	0.006	4.97	2.36	0.022
4.38	2.08	0.006	4.41	2.10	0.023
4.33	2.05	0.007	4.39	2.08	0.023
4.49	2.13	0.007	4.30	2.04	0.023
4.65	2.21	0.007	4.22	2.00	0.024
4.77	2.26	0.007	4.17	1.98	0.024
4.72	2.24	0.007	4.13	1.96	0.024
5.08	2.41	0.007	4.08	1.94	0.024
4.95	2.35	0.007	4.23	2.01	0.024
5.10	2.42	0.008	4.02	1.91	0.024

Specimen: SW6H (Cont.)

Applied load kN	Moment kNm	Rotation rad	Applied load kN	Moment kNm	Rotation rad
4.03	1.92	0.024	4.97	2.36	0.030
4.05	1.92	0.024	4.91	2.33	0.030
4.02	1.91	0.024	4.95	2.35	0.030
4.04	1.92	0.024	4.91	2.33	0.030
4.00	1.90	0.024	4.91	2.33	0.030
3.92	1.86	0.024	4.91	2.33	0.030
3.90	1.85	0.024	4.85	2.30	0.030
3.99	1.90	0.024	4.68	2.22	0.030
3.94	1.87	0.024	4.83	2.29	0.030
3.94	1.87	0.024	4.76	2.26	0.030
4.12	1.96	0.024	4.35	2.06	0.030
3.88	1.85	0.025	3.54	1.68	0.030
3.98	1.89	0.025	2.18	1.03	0.030
3.89	1.85	0.025	3.03	1.44	0.030
3.87	1.84	0.025	3.03	1.44	0.030
4.06	1.93	0.025	3.01	1.43	0.030
5.10	2.42	0.025	3.05	1.45	0.030
5.76	2.74	0.025			
5.75	2.73	0.025			
5.67	2.69	0.025			
5.66	2.69	0.025			
5.62	2.67	0.025			
5.63	2.67	0.025			
6.18	2.94	0.025			
6.48	3.08	0.026			
4.74	2.25	0.028			
5.20	2.47	0.029			
5.36	2.54	0.029			
5.26	2.50	0.029			
5.23	2.48	0.029			
5.07	2.41	0.029			
5.05	2.40	0.029			
5.00	2.38	0.029			
5.03	2.39	0.029			
4.96	2.36	0.030			
4.93	2.34	0.030			

Moment Resisting Connection Test

Specimen: **SW6C**

Applied load kN	Moment kNm	Rotation rad	Applied load kN	Moment kNm	Rotation rad
0.00	0.00	0.000	6.19	2.94	0.010
0.50	0.24	0.001	5.90	2.80	0.010
0.61	0.29	0.001	6.85	3.25	0.010
0.78	0.37	0.002	7.16	3.40	0.010
1.02	0.48	0.002	6.64	3.15	0.010
1.27	0.60	0.002	6.43	3.05	0.011
1.55	0.74	0.002	7.35	3.49	0.011
1.62	0.77	0.002	7.20	3.42	0.012
1.71	0.81	0.003	7.37	3.50	0.012
1.87	0.89	0.003	7.05	3.35	0.012
2.05	0.97	0.003	6.73	3.20	0.012
2.15	1.02	0.003	7.39	3.51	0.012
2.23	1.06	0.004	7.77	3.69	0.012
2.38	1.13	0.004	7.49	3.56	0.012
2.42	1.15	0.004	7.19	3.42	0.012
2.70	1.28	0.004	6.98	3.32	0.012
2.71	1.29	0.004	7.77	3.69	0.012
2.79	1.32	0.005	8.02	3.81	0.013
2.21	1.05	0.005	7.52	3.57	0.013
2.31	1.10	0.005	6.89	3.27	0.013
3.12	1.48	0.005	7.99	3.79	0.013
2.89	1.37	0.006	7.25	3.44	0.013
4.01	1.91	0.006	6.73	3.20	0.014
3.95	1.88	0.006	7.00	3.33	0.014
4.49	2.13	0.007	7.31	3.47	0.014
5.04	2.40	0.007	6.57	3.12	0.014
5.30	2.52	0.008	6.83	3.24	0.014
4.64	2.20	0.008	6.67	3.17	0.014
5.33	2.53	0.009	6.41	3.04	0.014
6.16	2.93	0.009	6.63	3.15	0.014
5.42	2.58	0.009	5.79	2.75	0.015
5.58	2.65	0.009	6.51	3.09	0.015
6.59	3.13	0.009	5.50	2.61	0.015
6.59	3.13	0.010	6.53	3.10	0.015

Specimen: SW6C (Cont.)

Applied load kN	Moment kNm	Rotation rad
5.68	2.70	0.015
6.35	3.01	0.015
6.33	3.01	0.016
7.13	3.39	0.016
7.24	3.44	0.017
7.55	3.59	0.017
7.49	3.56	0.017
6.97	3.31	0.018
7.05	3.35	0.018
6.99	3.32	0.019
8.31	3.95	0.019
7.55	3.59	0.019
7.43	3.53	0.020
8.52	4.05	0.020
8.07	3.83	0.020
7.61	3.62	0.020
8.64	**4.11**	0.021
8.03	3.82	0.021
7.90	3.75	0.021
7.73	3.67	0.021
7.87	3.74	0.021
6.91	3.28	0.0214

Moment Resisting Connection Test

Specimen: **SW6V**

Applied load kN	Moment kNm	Rotation rad	Applied load kN	Moment kNm	Rotation rad
0.00	0.00	0.000	2.61	1.24	0.002
0.03	0.01	0.000	2.63	1.25	0.002
0.05	0.02	0.000	2.63	1.25	0.002
0.09	0.04	0.000	2.84	1.35	0.002
0.34	0.16	0.000	2.89	1.37	0.002
0.41	0.20	0.000	3.11	1.48	0.002
0.47	0.22	0.000	3.27	1.55	0.003
0.57	0.27	0.000	3.23	1.53	0.003
0.74	0.35	0.000	3.29	1.56	0.003
0.83	0.40	0.001	3.32	1.57	0.003
0.96	0.46	0.001	3.35	1.59	0.003
1.21	0.57	0.001	3.36	1.60	0.003
1.09	0.52	0.001	3.41	1.62	0.003
1.29	0.62	0.001	3.44	1.64	0.003
1.22	0.58	0.001	3.50	1.66	0.003
1.43	0.68	0.001	3.53	1.68	0.003
1.33	0.63	0.001	3.57	1.70	0.003
1.28	0.61	0.001	3.61	1.71	0.003
1.46	0.69	0.001	3.53	1.68	0.003
1.31	0.62	0.001	3.50	1.66	0.003
1.51	0.72	0.001	3.72	1.77	0.003
1.68	0.80	0.001	3.63	1.72	0.003
1.81	0.86	0.001	3.63	1.72	0.004
1.89	0.90	0.001	3.47	1.65	0.004
1.80	0.85	0.001	3.92	1.86	0.004
1.97	0.94	0.001	3.78	1.79	0.004
2.18	1.03	0.001	3.95	1.88	0.004
2.27	1.08	0.001	3.97	1.89	0.004
2.07	0.98	0.001	4.01	1.91	0.004
2.23	1.06	0.001	4.15	1.97	0.004
2.37	1.13	0.002	4.13	1.96	0.004
2.23	1.06	0.002	4.26	2.02	0.005
2.54	1.21	0.002	4.25	2.02	0.005
2.69	1.28	0.002	4.02	1.91	0.005

Specimen: SW6V (Cont.)

Applied load kN	Moment kNm	Rotation rad	Applied load kN	Moment kNm	Rotation rad
4.33	2.05	0.005	6.15	2.92	0.010
4.25	2.02	0.005	6.25	2.97	0.010
4.34	2.06	0.005	6.22	2.95	0.010
4.36	2.07	0.005	6.28	2.98	0.010
4.51	2.14	0.005	6.28	2.98	0.011
4.48	2.13	0.005	6.38	3.03	0.011
4.77	2.26	0.005	6.73	3.20	0.011
4.45	2.12	0.005	6.94	3.29	0.012
4.73	2.25	0.005	6.99	3.32	0.012
4.66	2.21	0.006	7.01	3.33	0.012
4.77	2.26	0.006	6.97	3.31	0.013
4.96	2.36	0.006	7.32	3.48	0.013
4.78	2.27	0.006	7.23	3.43	0.013
4.91	2.33	0.006	7.51	3.57	0.014
4.92	2.34	0.006	7.50	3.56	0.014
4.88	2.32	0.006	7.59	3.61	0.014
4.97	2.36	0.006	7.07	3.36	0.016
5.08	2.41	0.007	7.06	3.36	0.016
5.09	2.42	0.006	7.48	3.55	0.016
5.09	2.42	0.007	7.25	3.44	0.017
5.15	2.45	0.007	7.29	3.46	0.017
5.26	2.50	0.007	7.68	3.65	0.019
5.29	2.51	0.007	7.23	3.43	0.023
5.35	2.54	0.007	7.51	3.57	0.024
5.38	2.55	0.007	7.87	3.74	0.024
5.46	2.60	0.008	8.15	3.87	0.025
5.53	2.63	0.008	8.38	3.98	0.026
5.63	2.67	0.008	8.46	4.02	0.027
5.72	2.72	0.008	9.08	4.31	0.028
5.89	2.80	0.008	9.00	4.27	0.028
5.92	2.81	0.008	9.26	4.40	0.029
6.06	2.88	0.009			
6.09	2.89	0.009			
6.10	2.90	0.009			
6.15	2.92	0.009			
6.25	2.97	0.009			

Moment Resisting Connection Test

Specimen: **SW6C**

Applied load kN	Moment kNm	Rotation rad	Applied load kN	Moment kNm	Rotation rad
0.00	0.00	0.000	6.19	2.94	0.010
0.50	0.24	0.001	5.90	2.80	0.010
0.61	0.29	0.001	6.85	3.25	0.010
0.78	0.37	0.002	7.16	3.40	0.010
1.02	0.48	0.002	6.64	3.15	0.010
1.27	0.60	0.002	6.43	3.05	0.011
1.55	0.74	0.002	7.35	3.49	0.011
1.62	0.77	0.002	7.20	3.42	0.012
1.71	0.81	0.003	7.37	3.50	0.012
1.87	0.89	0.003	7.05	3.35	0.012
2.05	0.97	0.003	6.73	3.20	0.012
2.15	1.02	0.003	7.39	3.51	0.012
2.23	1.06	0.004	7.77	3.69	0.012
2.38	1.13	0.004	7.49	3.56	0.012
2.42	1.15	0.004	7.19	3.42	0.012
2.70	1.28	0.004	6.98	3.32	0.012
2.71	1.29	0.004	7.77	3.69	0.012
2.79	1.32	0.005	8.02	3.81	0.013
2.21	1.05	0.005	7.52	3.57	0.013
2.31	1.10	0.005	6.89	3.27	0.013
3.12	1.48	0.005	7.99	3.79	0.013
2.89	1.37	0.006	7.25	3.44	0.013
4.01	1.91	0.006	6.73	3.20	0.014
3.95	1.88	0.006	7.00	3.33	0.014
4.49	2.13	0.007	7.31	3.47	0.014
5.04	2.40	0.007	6.57	3.12	0.014
5.30	2.52	0.008	6.83	3.24	0.014
4.64	2.20	0.008	6.67	3.17	0.014
5.33	2.53	0.009	6.41	3.04	0.014
6.16	2.93	0.009	6.63	3.15	0.014
5.42	2.58	0.009	5.79	2.75	0.015
5.58	2.65	0.009	6.51	3.09	0.015
6.59	3.13	0.009	5.50	2.61	0.015
6.59	3.13	0.010	6.53	3.10	0.015

Specimen: SW6C (Cont.)

Applied load kN	Moment kNm	Rotation rad
5.68	2.70	0.015
6.35	3.01	0.015
6.33	3.01	0.016
7.13	3.39	0.016
7.24	3.44	0.017
7.55	3.59	0.017
7.49	3.56	0.017
6.97	3.31	0.018
7.05	3.35	0.018
6.99	3.32	0.019
8.31	3.95	0.019
7.55	3.59	0.019
7.43	3.53	0.020
8.52	4.05	0.020
8.07	3.83	0.020
7.61	3.62	0.020
8.64	**4.11**	0.021
8.03	3.82	0.021
7.90	3.75	0.021
7.73	3.67	0.021
7.87	3.74	0.021
6.91	3.28	0.0214

Moment Resisting Connection Test

Specimen: **SW6V**

Applied load kN	Moment kNm	Rotation rad	Applied load kN	Moment kNm	Rotation rad
0.00	0.00	0.000	2.61	1.24	0.002
0.03	0.01	0.000	2.63	1.25	0.002
0.05	0.02	0.000	2.63	1.25	0.002
0.09	0.04	0.000	2.84	1.35	0.002
0.34	0.16	0.000	2.89	1.37	0.002
0.41	0.20	0.000	3.11	1.48	0.002
0.47	0.22	0.000	3.27	1.55	0.003
0.57	0.27	0.000	3.23	1.53	0.003
0.74	0.35	0.000	3.29	1.56	0.003
0.83	0.40	0.001	3.32	1.57	0.003
0.96	0.46	0.001	3.35	1.59	0.003
1.21	0.57	0.001	3.36	1.60	0.003
1.09	0.52	0.001	3.41	1.62	0.003
1.29	0.62	0.001	3.44	1.64	0.003
1.22	0.58	0.001	3.50	1.66	0.003
1.43	0.68	0.001	3.53	1.68	0.003
1.33	0.63	0.001	3.57	1.70	0.003
1.28	0.61	0.001	3.61	1.71	0.003
1.46	0.69	0.001	3.53	1.68	0.003
1.31	0.62	0.001	3.50	1.66	0.003
1.51	0.72	0.001	3.72	1.77	0.003
1.68	0.80	0.001	3.63	1.72	0.003
1.81	0.86	0.001	3.63	1.72	0.004
1.89	0.90	0.001	3.47	1.65	0.004
1.80	0.85	0.001	3.92	1.86	0.004
1.97	0.94	0.001	3.78	1.79	0.004
2.18	1.03	0.001	3.95	1.88	0.004
2.27	1.08	0.001	3.97	1.89	0.004
2.07	0.98	0.001	4.01	1.91	0.004
2.23	1.06	0.001	4.15	1.97	0.004
2.37	1.13	0.002	4.13	1.96	0.004
2.23	1.06	0.002	4.26	2.02	0.005
2.54	1.21	0.002	4.25	2.02	0.005
2.69	1.28	0.002	4.02	1.91	0.005

Specimen: SW6V (Cont.)

Applied load kN	Moment kNm	Rotation rad	Applied load kN	Moment kNm	Rotation rad
4.33	2.05	0.005	6.15	2.92	0.010
4.25	2.02	0.005	6.25	2.97	0.010
4.34	2.06	0.005	6.22	2.95	0.010
4.36	2.07	0.005	6.28	2.98	0.010
4.51	2.14	0.005	6.28	2.98	0.011
4.48	2.13	0.005	6.38	3.03	0.011
4.77	2.26	0.005	6.73	3.20	0.011
4.45	2.12	0.005	6.94	3.29	0.012
4.73	2.25	0.005	6.99	3.32	0.012
4.66	2.21	0.006	7.01	3.33	0.012
4.77	2.26	0.006	6.97	3.31	0.013
4.96	2.36	0.006	7.32	3.48	0.013
4.78	2.27	0.006	7.23	3.43	0.013
4.91	2.33	0.006	7.51	3.57	0.014
4.92	2.34	0.006	7.50	3.56	0.014
4.88	2.32	0.006	7.59	3.61	0.014
4.97	2.36	0.006	7.07	3.36	0.016
5.08	2.41	0.007	7.06	3.36	0.016
5.09	2.42	0.006	7.48	3.55	0.016
5.09	2.42	0.007	7.25	3.44	0.017
5.15	2.45	0.007	7.29	3.46	0.017
5.26	2.50	0.007	7.68	3.65	0.019
5.29	2.51	0.007	7.23	3.43	0.023
5.35	2.54	0.007	7.51	3.57	0.024
5.38	2.55	0.007	7.87	3.74	0.024
5.46	2.60	0.008	8.15	3.87	0.025
5.53	2.63	0.008	8.38	3.98	0.026
5.63	2.67	0.008	8.46	4.02	0.027
5.72	2.72	0.008	9.08	4.31	0.028
5.89	2.80	0.008	9.00	4.27	0.028
5.92	2.81	0.008	9.26	4.40	0.029
6.06	2.88	0.009			
6.09	2.89	0.009			
6.10	2.90	0.009			
6.15	2.92	0.009			
6.25	2.97	0.009			

Moment Resisting Connection Test

Specimen: **SW6H**

Applied load kN	Moment kNm	Rotation rad	Applied load kN	Moment kNm	Rotation rad
0.00	0.00	0.000	5.22	2.48	0.008
0.20	0.09	0.000	5.36	2.54	0.007
0.16	0.07	0.000	5.36	2.54	0.008
0.29	0.14	0.000	5.57	2.65	0.008
0.37	0.18	0.001	5.72	2.72	0.008
0.52	0.25	0.001	5.94	2.82	0.008
0.67	0.32	0.001	6.15	2.92	0.008
0.81	0.39	0.001	6.31	3.00	0.009
0.81	0.39	0.002	6.49	3.08	0.009
3.17	1.51	0.004	6.68	3.17	0.009
3.22	1.53	0.005	6.78	3.22	0.009
3.32	1.57	0.005	6.78	3.22	0.009
3.34	1.58	0.005	6.94	3.29	0.009
3.43	1.63	0.005	7.17	3.41	0.009
3.46	1.64	0.005	7.48	3.55	0.009
3.53	1.68	0.006	7.43	3.53	0.009
3.60	1.71	0.006	7.42	3.52	0.010
3.71	1.76	0.006	7.51	3.57	0.010
3.68	1.75	0.006	7.60	**3.61**	0.010
3.72	1.77	0.006	4.27	2.03	0.019
3.87	1.84	0.006	4.49	2.13	0.019
3.96	1.88	0.006	4.91	2.33	0.020
4.08	1.94	0.006	5.02	2.39	0.020
4.06	1.93	0.006	4.85	2.30	0.021
4.20	1.99	0.006	4.97	2.36	0.022
4.38	2.08	0.006	4.41	2.10	0.023
4.33	2.05	0.007	4.39	2.08	0.023
4.49	2.13	0.007	4.30	2.04	0.023
4.65	2.21	0.007	4.22	2.00	0.024
4.77	2.26	0.007	4.17	1.98	0.024
4.72	2.24	0.007	4.13	1.96	0.024
5.08	2.41	0.007	4.08	1.94	0.024
4.95	2.35	0.007	4.23	2.01	0.024
5.10	2.42	0.008	4.02	1.91	0.024

Specimen: SW6H (Cont.)

Applied load kN	Moment kNm	Rotation rad	Applied load kN	Moment kNm	Rotation rad
4.03	1.92	0.024	4.97	2.36	0.030
4.05	1.92	0.024	4.91	2.33	0.030
4.02	1.91	0.024	4.95	2.35	0.030
4.04	1.92	0.024	4.91	2.33	0.030
4.00	1.90	0.024	4.91	2.33	0.030
3.92	1.86	0.024	4.91	2.33	0.030
3.90	1.85	0.024	4.85	2.30	0.030
3.99	1.90	0.024	4.68	2.22	0.030
3.94	1.87	0.024	4.83	2.29	0.030
3.94	1.87	0.024	4.76	2.26	0.030
4.12	1.96	0.024	4.35	2.06	0.030
3.88	1.85	0.025	3.54	1.68	0.030
3.98	1.89	0.025	2.18	1.03	0.030
3.89	1.85	0.025	3.03	1.44	0.030
3.87	1.84	0.025	3.03	1.44	0.030
4.06	1.93	0.025	3.01	1.43	0.030
5.10	2.42	0.025	3.05	1.45	0.030
5.76	2.74	0.025			
5.75	2.73	0.025			
5.67	2.69	0.025			
5.66	2.69	0.025			
5.62	2.67	0.025			
5.63	2.67	0.025			
6.18	2.94	0.025			
6.48	3.08	0.026			
4.74	2.25	0.028			
5.20	2.47	0.029			
5.36	2.54	0.029			
5.26	2.50	0.029			
5.23	2.48	0.029			
5.07	2.41	0.029			
5.05	2.40	0.029			
5.00	2.38	0.029			
5.03	2.39	0.029			
4.96	2.36	0.030			
4.93	2.34	0.030			

Moment Resisting Connection Test

Specimen: **WW4H**

Applied load kN	Moment kNm	Rotation rad
0.00	0.00	0.000
5.71	2.71	0.008
6.46	3.07	0.009
6.80	3.23	0.009
7.40	3.51	0.010
8.01	3.80	0.011
9.15	4.35	0.011
9.53	4.53	0.012
10.54	5.01	0.013
11.35	5.39	0.014
11.30	5.37	0.015
12.50	5.94	0.015
12.32	5.85	0.016
12.78	6.07	0.017
12.96	**6.15**	0.018
12.65	6.01	0.018
12.88	6.12	0.019
7.21	3.42	0.020
7.43	3.53	0.021
7.70	3.66	0.022
7.71	3.66	0.022
7.60	3.61	0.023
7.60	3.61	0.023
7.64	3.63	0.023
7.09	3.37	0.023

Moment Resisting Connection Test

Specimen: **WW6H**

Applied load kN	Moment kNm	Rotation rad	Applied load kN	Moment kNm	Rotation rad
0.00	0.00	0.000	7.26	3.45	0.009
0.18	0.08	0.000	7.77	3.69	0.009
0.30	0.14	0.000	8.10	3.85	0.009
0.42	0.20	0.001	8.67	4.12	0.009
0.60	0.28	0.001	8.86	4.21	0.010
0.69	0.33	0.001	9.41	4.47	0.010
0.84	0.40	0.001	9.42	4.48	0.010
0.77	0.36	0.002	9.49	4.51	0.010
1.18	0.56	0.002	9.58	4.55	0.011
1.58	0.75	0.002	11.04	5.24	0.011
2.03	0.96	0.003	11.63	5.53	0.011
2.12	1.01	0.003	12.49	5.93	0.012
2.28	1.08	0.003	12.82	6.09	0.012
2.50	1.19	0.003	13.14	6.24	0.012
3.17	1.50	0.004	13.51	6.42	0.013
3.77	1.79	0.004	13.81	6.56	0.013
4.06	1.93	0.004	13.47	6.40	0.014
4.14	1.97	0.005	13.28	6.31	0.014
4.46	2.12	0.006	13.30	6.32	0.015
4.61	2.19	0.006	13.376	6.35	0.015
4.90	2.33	0.006	13.11	6.23	0.016
5.25	2.49	0.007	14.02	6.66	0.016
5.68	2.70	0.007	14.44	6.86	0.017
5.86	2.79	0.007	15.32	7.28	0.018
6.04	2.87	0.007	15.57	**7.40**	0.018
6.01	2.85	0.007	10.60	5.03	0.019
6.21	2.95	0.007	11.98	5.69	0.019
6.21	2.95	0.008	11.36	5.40	0.020
6.07	2.88	0.008	12.33	5.85	0.021
6.28	2.98	0.008	11.02	5.23	0.021
6.28	2.98	0.008	12.41	5.89	0.022
6.55	3.11	0.008	10.54	5.01	0.022
6.70	3.18	0.009	10.67	5.07	0.023
7.00	3.32	0.009	9.22	4.38	0.024

Moment Resisting Connection Test

Specimen: **WW6C**

Applied load kN	Moment kNm	Rotation rad	Applied load kN	Moment kNm	Rotation rad
0.00	0.00	0.000	7.76	3.69	0.009
0.27	0.13	0.000	8.02	3.81	0.009
0.63	0.30	0.001	8.07	3.83	0.009
0.95	0.45	0.002	8.40	3.99	0.010
1.04	0.49	0.002	8.70	4.13	0.010
1.21	0.57	0.002	8.93	4.24	0.010
1.34	0.64	0.003	9.04	4.29	0.010
1.74	0.82	0.003	9.16	4.35	0.010
2.14	1.02	0.003	9.53	4.53	0.011
2.32	1.10	0.004	9.90	4.70	0.011
2.55	1.21	0.004	10.03	4.76	0.011
2.73	1.30	0.004	10.19	4.84	0.012
3.19	1.51	0.005	10.33	4.91	0.012
3.51	1.67	0.005	10.59	5.03	0.012
3.71	1.76	0.005	10.81	5.14	0.012
3.93	1.87	0.005	11.08	5.26	0.012
4.20	2.00	0.006	11.20	5.32	0.013
4.54	2.16	0.006	11.28	5.36	0.013
4.89	2.33	0.006	11.38	5.41	0.013
5.07	2.41	0.006	11.54	5.48	0.013
5.09	2.42	0.006	11.93	5.67	0.014
5.29	2.51	0.007	12.01	5.70	0.014
5.36	2.54	0.007	12.14	5.77	0.014
5.74	2.73	0.007	12.54	5.96	0.014
5.81	2.76	0.007	12.39	5.88	0.015
5.91	2.81	0.007	12.59	5.98	0.015
6.02	2.86	0.007	12.84	6.10	0.015
6.16	2.93	0.008	12.74	6.05	0.015
6.40	3.04	0.008	13.22	6.28	0.016
6.62	3.15	0.008	13.17	6.26	0.016
6.83	3.25	0.008	13.28	6.31	0.016
6.98	3.31	0.008	13.50	6.41	0.016
7.06	3.35	0.008	13.65	6.48	0.016
7.34	3.49	0.009	13.88	6.59	0.017

Specimen: WW6C (Cont.)

Applied load kN	Moment kNm	Rotation rad
14.10	6.70	0.017
14.30	6.79	0.018
14.50	6.89	0.018
14.72	6.99	0.019
14.89	7.07	0.019
15.08	7.17	0.019
15.26	7.25	0.020
15.37	7.30	0.020
15.47	7.35	0.021
15.64	7.43	0.021
15.62	7.42	0.021
15.91	7.56	0.022
15.84	7.52	0.022
16.26	7.72	0.023
16.07	7.63	0.023
16.65	7.91	0.023
16.66	7.91	0.024
16.59	7.88	0.024
17.00	8.07	0.025
16.94	8.05	0.025
17.02	**8.08**	0.026
16.62	7.90	0.027
16.50	7.84	0.027
16.44	7.81	0.028
16.70	7.93	0.028
17.01	8.08	0.029
16.08	7.64	0.030
16.31	7.75	0.031
16.12	7.66	0.032
15.65	7.43	0.032
16.03	7.61	0.032
15.89	7.55	0.032
15.90	7.55	0.033

Moment Resisting Connection Test

Specimen: **WW6V**

Applied load kN	Moment kNm	Rotation rad	Applied load kN	Moment kNm	Rotation rad
0.00	0.00	0.000	9.38	4.46	0.009
0.43	0.20	0.000	9.66	4.59	0.009
0.64	0.30	0.001	10.07	4.79	0.009
0.72	0.34	0.001	10.27	4.88	0.010
1.30	0.62	0.001	10.28	4.88	0.010
1.36	0.65	0.001	10.69	5.08	0.010
1.75	0.83	0.002	11.07	5.26	0.010
1.98	0.94	0.002	11.16	5.30	0.011
2.38	1.13	0.002	11.27	5.35	0.011
3.01	1.43	0.003	11.40	5.42	0.011
3.11	1.48	0.003	11.86	5.64	0.012
3.60	1.71	0.003	12.17	5.78	0.012
4.06	1.93	0.004	12.17	5.78	0.012
4.24	2.01	0.004	12.46	5.92	0.012
4.71	2.24	0.004	12.54	5.96	0.013
4.69	2.23	0.004	12.75	6.06	0.013
5.03	2.39	0.004	12.72	6.04	0.013
5.53	2.63	0.005	13.04	6.19	0.014
5.80	2.76	0.005	13.15	6.25	0.014
6.35	3.01	0.005	13.13	6.24	0.014
6.62	3.15	0.006	13.22	6.28	0.014
6.86	3.26	0.006	13.14	6.24	0.014
7.20	3.42	0.006	13.42	6.37	0.014
7.47	3.55	0.006	13.89	6.60	0.015
7.76	3.69	0.007	13.62	6.47	0.015
7.56	3.59	0.007	14.03	6.66	0.015
7.43	3.53	0.007	14.15	6.72	0.015
7.87	3.74	0.007	14.35	6.81	0.015
8.05	3.83	0.007	14.42	6.85	0.016
8.34	3.96	0.007	14.43	6.85	0.016
8.67	4.12	0.008	14.37	6.83	0.016
8.78	4.17	0.008	14.30	6.79	0.016
8.78	4.17	0.008	14.34	6.81	0.016
9.09	4.32	0.008	14.29	6.79	0.016

Specimen:	WW6V	(Cont.)			
Applied load kN	**Moment kNm**	**Rotation rad**	**Applied load kN**	**Moment kNm**	**Rotation rad**
14.27	6.78	0.016	13.90	6.60	0.017
14.25	6.77	0.016	13.92	6.61	0.018
14.24	6.76	0.016	13.94	6.62	0.018
14.17	6.73	0.016	13.90	6.60	0.018
14.20	6.75	0.016	13.81	6.56	0.018
14.12	6.71	0.017	13.86	6.58	0.018
14.11	6.70	0.017	13.79	6.55	0.018
14.09	6.69	0.017	13.80	6.56	0.018
14.08	6.69	0.017	13.78	6.54	0.018
14.02	6.66	0.017	13.77	6.54	0.018
14.02	6.66	0.017	13.75	6.53	0.018
14.14	6.72	0.017	13.73	6.52	0.018
14.06	6.68	0.017	13.69	6.50	0.018
14.03	6.66	0.017	13.72	6.52	0.018
14.10	6.70	0.017	13.62	6.47	0.018
14.10	6.70	0.017	13.65	6.48	0.018
14.11	6.70	0.017	13.65	6.48	0.018
14.16	6.73	0.017	13.63	6.47	0.018
14.20	6.75	0.017	13.60	6.46	0.018
14.21	6.75	0.017	13.62	6.47	0.018
14.21	6.75	0.017	13.62	6.47	0.018
14.17	6.73	0.017	13.58	6.45	0.018
14.10	6.70	0.017	13.55	6.43	0.018
14.11	6.70	0.017	13.55	6.44	0.018
14.03	6.67	0.017	13.58	6.45	0.018
13.95	6.63	0.017	13.52	6.42	0.018
13.92	6.61	0.017	13.48	6.40	0.018
13.94	6.62	0.017	13.46	6.39	0.018
13.95	6.63	0.017	13.49	6.41	0.018
13.99	6.65	0.017	13.47	6.40	0.018
14.00	6.65	0.017	13.42	6.37	0.018
14.10	6.70	0.017	13.45	6.39	0.018
14.06	6.68	0.017	13.45	6.39	0.018
14.04	6.67	0.017	13.39	6.36	0.018
14.03	6.66	0.017	13.37	6.35	0.018
14.04	6.67	0.017	13.38	6.35	0.018

Specimen:	WW6V	(Cont.)			
Applied load kN	**Moment kNm**	**Rotation rad**	**Applied load kN**	**Moment kNm**	**Rotation rad**
14.00	6.65	0.017	13.37	6.35	0.018
13.95	6.62	0.017	13.39	6.36	0.018
13.30	6.32	0.018	12.98	6.16	0.018
13.35	6.34	0.018	12.98	6.17	0.018
13.31	6.32	0.018	12.98	6.17	0.018
13.29	6.31	0.018	13.00	6.18	0.018
13.39	6.36	0.018	13.02	6.18	0.018
13.28	6.31	0.018	12.95	6.15	0.018
13.26	6.30	0.018	12.92	6.14	0.018
13.24	6.29	0.018	12.93	6.14	0.018
13.29	6.31	0.018	12.91	6.13	0.018
13.22	6.28	0.018	12.93	6.14	0.018
13.20	6.27	0.018	12.92	6.14	0.018
13.21	6.27	0.018	12.91	6.13	0.018
13.41	6.37	0.018	12.88	6.12	0.018
13.03	6.19	0.018	12.94	6.15	0.018
13.19	6.26	0.018	12.88	6.12	0.018
13.20	6.27	0.018	12.91	6.13	0.018
13.14	6.24	0.018	12.86	6.11	0.018
13.16	6.25	0.018	12.88	6.12	0.018
13.17	6.26	0.018	12.84	6.10	0.018
13.19	6.26	0.018	12.84	6.10	0.018
13.17	6.26	0.018	12.82	6.09	0.018
13.17	6.26	0.018	12.82	6.09	0.018
13.14	6.24	0.018	12.77	6.07	0.018
13.13	6.24	0.018	12.66	6.02	0.018
13.14	6.24	0.018	12.74	6.05	0.018
13.10	6.22	0.018	12.75	6.06	0.018
13.06	6.21	0.018	12.75	6.06	0.018
13.08	6.21	0.018	12.74	6.05	0.018
13.06	6.21	0.018	12.79	6.07	0.018
13.11	6.23	0.018	12.75	6.06	0.018
13.09	6.22	0.018	12.77	6.07	0.018
13.09	6.22	0.018	12.74	6.05	0.018
13.11	6.23	0.018	12.72	6.04	0.018
13.08	6.21	0.018	12.68	6.02	0.018

Specimen:	**WW6V**	**(Cont.)**			
Applied load kN	**Moment kNm**	**Rotation rad**	**Applied load kN**	**Moment kNm**	**Rotation rad**
13.01	6.18	0.018	12.68	6.02	0.018
13.03	6.19	0.018	12.68	6.02	0.018
13.05	6.20	0.018	12.63	6.00	0.018
13.02	6.18	0.018	12.66	6.02	0.018
12.66	6.02	0.018	16.97	8.06	0.030
12.64	6.00	0.018	17.58	8.35	0.030
12.64	6.00	0.018	17.70	8.41	0.031
12.71	6.04	0.018	16.62	7.89	0.029
12.64	6.00	0.018	17.13	8.14	0.030
12.67	6.02	0.018	17.54	8.33	0.030
12.62	5.99	0.018	18.56	8.82	0.030
12.61	5.99	0.018	19.34	9.19	0.031
12.59	5.98	0.018	19.54	9.28	0.031
12.56	5.96	0.018	19.38	9.21	0.033
12.61	5.99	0.018	17.75	8.43	0.033
12.97	6.16	0.018	17.73	8.42	0.033
13.25	6.29	0.018	18.71	8.89	0.034
14.20	6.75	0.018	18.53	8.80	0.034
15.15	7.19	0.018	18.64	8.86	0.035
15.67	7.44	0.019	18.80	8.93	0.035
16.08	7.64	0.019	19.13	9.08	0.035
16.56	7.87	0.019	19.27	9.15	0.036
16.94	8.05	0.019	19.47	9.25	0.036
17.26	8.20	0.020	19.74	9.38	0.036
17.35	8.24	0.020	19.84	9.42	0.037
17.01	8.08	0.020	19.84	9.42	0.037
16.50	7.84	0.021	19.84	9.42	0.037
16.63	7.90	0.021	20.02	9.51	0.038
16.70	7.93	0.022	20.16	9.57	0.038
16.79	7.98	0.022	19.93	9.46	0.038
17.19	8.17	0.023	19.85	9.43	0.039
12.61	5.99	0.025	20.25	**9.62**	0.040
13.25	6.29	0.025	20.03	9.52	0.040
14.95	7.10	0.026	19.82	9.41	0.040
16.01	7.60	0.026	19.67	9.34	0.041
16.47	7.82	0.027	19.78	9.40	0.041

BIOGRAPHY

Mr. Ali Awaludin was born on 17th November 1977 in Bandung, Indonesia. He finished his undergraduate study in the field of civil engineering in 1999. After that, he worked as a lecturer in Civil Engineering Department of Gadjah Mada University, the same university where he graduated. His fields of interest are timber engineering, structural analysis, engineering mathematics, and engineering materials. In June 2003, he continues his further study in graduate school of Civil Engineering of Chulalongkorn University. He achieved his master's degree in January 2005.